The Design of a Flexible Damper For Passive Energy-Dissipation in Assistive Devices

Master's Thesis

Souri Venkata Shanmukha Sreeramagiri

TU Delft

ఓం భూర్భువస్వః ।
తత్స వితుర్వరేణ్యం ।
భర్గో దేవస్య ధీమహి ।
ధియో యోనఃప్రచోదయాత్ ॥

THE DESIGN OF A FLEXIBLE DAMPER FOR PASSIVE ENERGY-DISSIPATION IN ASSISTIVE DEVICES

ME51035

Souri Venkata Shanmukha Sreeramagiri

Master's Thesis report submitted in partial fulfillment of the requirements for the degree of

Master of Science
in Mechanical Engineering

at The Delft University of Technology,
To be defended publicly on:
Tuesday, September 26th at 9:00 AM

Student number:	5447844
Project Duration:	March, 2023 - September, 2023
Thesis committee:	
Chair and Supervisor:	Dr. Ir. G. Smit
Supervisor:	Prof. Dr. Ing. H. Vallery
Staff Member:	Dr. Ir. A.H.A. Stienen
External Member:	Dr. L. Peternel

An electronic version of this thesis is available at `http://repository.tudelft.nl/`.

Faculty of Mechanical, Maritime and Materials Engineering (3ME) · Delft University of Technology

Preface

This report is the outcome of the ME51035 Master's thesis, submitted in partial fulfillment of the M.Sc Mechanical Engineering, BioMechanical Design program at the Mechanical, Maritime and Materials Engineering (3mE) Faculty of TU Delft. The project was carried out at the Biorobotics lab under the supervision of Prof. Dr. Ing. Heike Vallery and Dr.Ir. Gerwin Smit from March 2023 to September 2023. The focal point of this work is the development of a flexible, passive viscous damper with a shear rate-dependent response, intended as the first step towards creating an implantable quadriceps assistive device.

The idea to develop implantable soft actuators or "artificial muscles" was first born during one of my lectures in Bio-inspired design. My aspiration was to contribute to the restoration of mobility for millions of disabled individuals worldwide. The quest to improve human-machine interaction and ergonomics has driven research towards soft actuators and flexible devices. The field of Assistive devices has seen such advancements with the development of soft exoskeletons, artificial muscle-based actuation, and compliant joints. They are cheaper, more comfortable to wear, and function synergistically with the human body. This begged the question; Can assistive devices one day be permanently integrated with and perhaps within the human body?

With this idea in mind, I conducted my literature study on the types of artificial muscles and their scope for implantation. Together with my supervisors, I decided to develop an implantable assistive device for the quadriceps muscle group in my thesis. However, I encountered a major roadblock while discussing the idea with medical professionals. Their concerns about the technical challenges, particularly long-term mechano-biological integration, brought into question the feasibility and even the need for such a device at this stage. I then decided to concentrate my efforts on designing a functional proof-of-concept, laying the groundwork for potential future implementation once extensive research on mechanical coupling with the skeletal system is conducted. Thus, I decided that the logical first step to developing such a prototype would be to design a soft, passive energy-dissipating device.

This thesis is the culmination of my efforts toward developing a passive flexible damper and my first true endeavor in conducting independent research. It reflects my earnest dedication towards developing assistive devices with a user-centric approach, driven by innovative mechanical design. I hope this document can provoke further research into the field of implanted assistive technologies and also open new avenues for deploying soft passive dampers.

Acknowledgements

Over the course of my master's program at TU Delft, I have been privileged to have the support and encouragement of an indispensable set of individuals. I owe a deep gratitude to everyone that has been a part of my life up to this point and hope you will continue to be a part of it for the years to come.

Above all, to my family. for providing me with the liberty to explore my interests and find my own way through life. For supporting me financially and emotionally. For instilling a strong sense of morals and work ethic in me, keeping me culturally rooted. For showing me through example, how to navigate the difficulties of academic life and keep my focus centered on the learning process above all.

To my supervisors, Heike Vallery and Gerwin Smit. For giving me the freedom to make mistakes and have agency over the direction to drive the project towards. Our conversations have been invaluable to me. I want to thank you for consistently taking time out of your schedules to meet with me, and keeping me from being overwhelmed with the task at hand. You have provided me with insightful perspectives and nurtured my interest in academic research, by being exemplary mentors.

This project could not have been completed without the following individuals: Jan van Frankenhuyzen, from the moment we began to collaborate, I knew the project would turn out great. Our mutual appreciation for well-designed mechanisms has led to some quality conversations. I truly hope we continue to work together in the future; Bob van-der Windt, right from the little road trip we took to Twente, I have thoroughly enjoyed our brainstorming sessions. The idea to use Non-Newtonian fluids first came up during one of our discussions at the lab; Bart Horstman, for the timely advice on the testing facilities at IDE and for the GoPro; Mascha Slingerland, for the immense help you provided with the experimental setups and your prompt response to all my queries. Finally, to Jacques Brenkman, Reinier van Antwerpen, and Damien De Nijs. You are the glue that holds 3me together with your assistance in every single one of our projects.

And finally, to my friends. I am fortunate to have been surrounded by an immensely talented, grounded, and driven group of people all my life. Through our shared tribulations, we have learned, and we have grown. It is a pleasure to watch all of you take on the world.

Abstract

Energy dissipation plays a crucial role in mitigating noise and vibration in a wide range of applications. In the field of assistive devices, energy dissipation is used to improve the stability of joint motion and protect the musculoskeletal system from excessive loads. It is not surprising that considerable effort has gone into developing effective energy dissipation mechanisms for this application. However conventional devices are bulky, expensive, and rigid. They are known to cause discomfort, and skin trauma to the patients. With the advances in soft robotics, novel soft exoskeletons that demonstrate bio-mimetic functionality, increased comfort, and cost-effective designs are being developed. This work proposes a novel soft, passive damper, intended for operation as an energy dissipator in assistive devices. The study begins with an overview of the state of the art in assistive devices, and energy dissipation mechanisms. A comparison is made of the various modes of energy dissipation for the intended application, and the most suitable one is selected. A proof-of-concept passive flexible damper is designed. A prototype is assembled and its working is experimentally verified. The study concludes with the successful demonstration of a novel soft damper, comments on the current limitations, and suggests future research directions to improve on this approach. This work is a contribution to the development of a new class of soft energy dissipators.

Contents

List of Figures

List of Tables

1 Introduction

1.1. Background

The field of assistive technologies has witnessed remarkable advancements in recent times, aiming to improve the quality of life of individuals with physical impairments. These technologies place a strong emphasis on user comfort, convenience, and seamless human-device interfaces as they operate in close proximity to and constantly interact with the users. The World Health Organisation (WHO) estimates that 10% of the population is currently in need of some kind of assistive device with an increasing number of cases globally, particularly in developing countries [1, 2]. Studies highlight a lack of access to appropriate medical care and limited or expensive choice of assistive technology solutions in developing nations [3, 4]. There is a need for affordable, simple, and durable assistive technologies that are accessible to everyone.

Among the physically challenged, those with lower limb impairments often struggle the most with performing Activities of Daily Living (ADL). They may find it difficult to stand upright, maintain balance, and walk. The quadriceps are a group of muscles in the thigh that are crucial to standing balance and gait. In addition to being the primary knee extensors, they also function as energy dissipators. Through eccentric contraction, the quadriceps actively resist knee flexion under the weight of the body. In this manner, the impact of heel strike or deceleration is absorbed and dissipated, protecting the knee joint from excessive forces and injury[5, 6]. Knee osteoarthritis,post-surgical complications Physical trauma, and stroke complications are a few conditions with no cure that can lead to lifelong impairment of this muscle group [6, 7, 8, 9]. In such instances, assistive devices can play a crucial role in restoring independence and mobility to the patients, significantly improving their quality of life and enabling them to carry out ADL [10]. Orthoses and prostheses are commonly used to support or correct gait and balance in such individuals[11, 12].

1.2. State of the Art

It follows that considerable research has been done on energy dissipation and knee joint stabilization for lower limb assistive devices. Some examples of the various approaches developed are classified on the power requirements, and presented in the following paragraph.

1.2.1. Passive Devices

The most basic knee joints are single-axis hinge joints that allow flexion and extension around a single point. However, they are inherently unstable and require the user to provide additional effort to maintain balance. Hence, many passive prosthetics incorporate a polycentric knee, utilizing a four-bar mechanism to stabilize motion kinematically [13, 14], or have a manual locking feature that can engage or disable free rotation of the knee joint [15]. Weight-activated stance control is another design that has the knee joint lock when weight is applied (during the stance phase) through the use of friction and mechanical slots. Finally, some prostheses employ a passive valve-controlled hydraulic damper, as seen in the Mauch knee [14, 16], to modulate movement. Similarly, passive Knee-Ankle-Foot-Orthoses (KAFO) typically feature rigid (locked) knee joints or hard end stops limiting the range of motion to prevent users from tipping over [17]. They use mechanical locks to allow or prevent joint rotation. Some orthoses have non-anthropomorphic knee joints positioned differently from the anatomical knee, thereby increasing its stability [18]. Stance-controlled orthoses have locking mechanisms that are synced to the gait cycle through cams or levers while friction-locking joints allow the user to adjust the amount of resistance offered to rotation. Some popular passive knee joint mechanisms are illustrated in Fig. 1.1

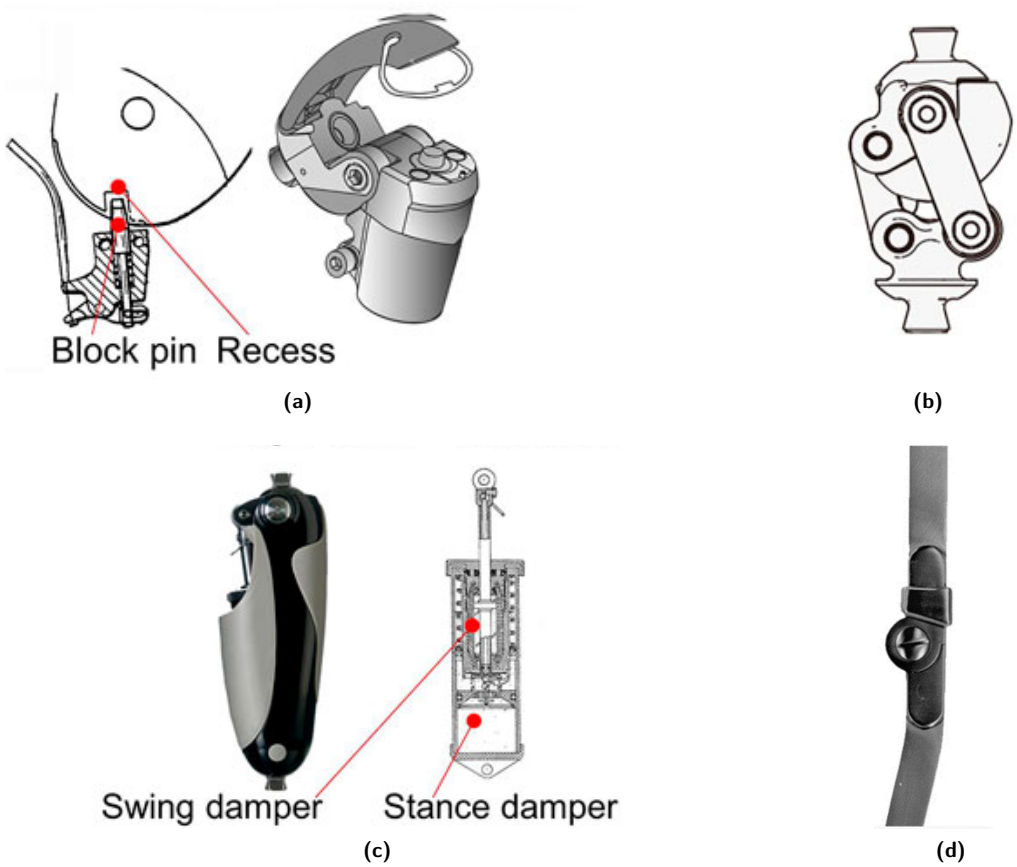

Figure 1.1: Examples of Passive Knee Joint Stabilizing Mechanisms : (a) Pin Locked Knee [15]. (b) Polycentric Knee: Four Bar Mechanism [15] (c) Mauch knee: Hydraulic Damper [14]. (d) Ring Locked Knee Joint [17].

1.2.2. Semi-Passive Devices

To provide better adaptability to varied terrains and walking speeds, some devices use control systems to detect and switch the amount of resistance offered at the joint (Fig. 1.2). The C-leg incorporates microprocessor-controlled hydraulic dampers that can adapt by varying the amount of resistance and hydraulic damping offered[19]. Devices such as the Rheo-knee [20, 21] utilize the controllable rheological properties of magnetorheological fluids to provide variable resistance to knee flexion. Such devices are used to ensure the knee joint is stiff during the stance phase and free to rotate during the swing phase of the gait cycle.

Semi-passive orthotic devices deploy controllable clutch-based mechanisms to either allow or prevent free rotation of the knee joint. Such systems are known as stance-controlled orthoses. The E-MAG KAFO [22] uses a magnetically controlled clutch mechanism to regulate the knee joint. Microprocessor-controlled [23] and MR damper-based semi-passive orthoses have also been developed, similar to their prosthetic counterparts.

1.2.3. Active Devices

Active orthoses and prostheses use motors or pneumatics to directly supply torque to counter gravitational torques or do so remotely through cables attached to the limbs [17, 24, 25]. They are usually bulky and have complex power and control systems to generate the necessary torques Fig. 1.3. Active systems often employ energy harvesting systems to bring down the overall power consumption and weight. Another unique class of devices that can be included in this group is based on functional electrode stimulation (FES). They use electrical stimulation to activate the user's muscles in case of weakness or paralysis and generate the additional required forces [26]. While they are not conventional active devices, they require power to supply electric signals, and complex control algorithms to synchronize excitation signals with the native muscle activity. Powered assistive devices tend to be the most expensive class due to their complexity.

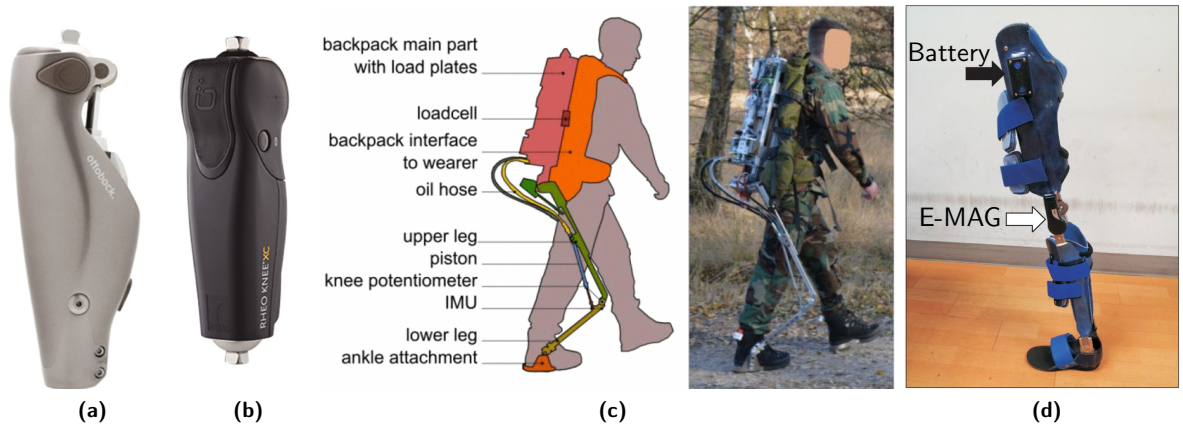

Figure 1.2: Examples of Semi-Passive Knee Joint Stabilizing Mechanisms: (a) C-leg: Microprocessor Controlled Knee [21] (b) Rheo-knee: Magnetorheological Fluid Damper [21] (c) Exobuddy: Non-Anthropomorphic Exoskeleton [23] (d) E-MAG: Magnetically controlled KAFO[22]

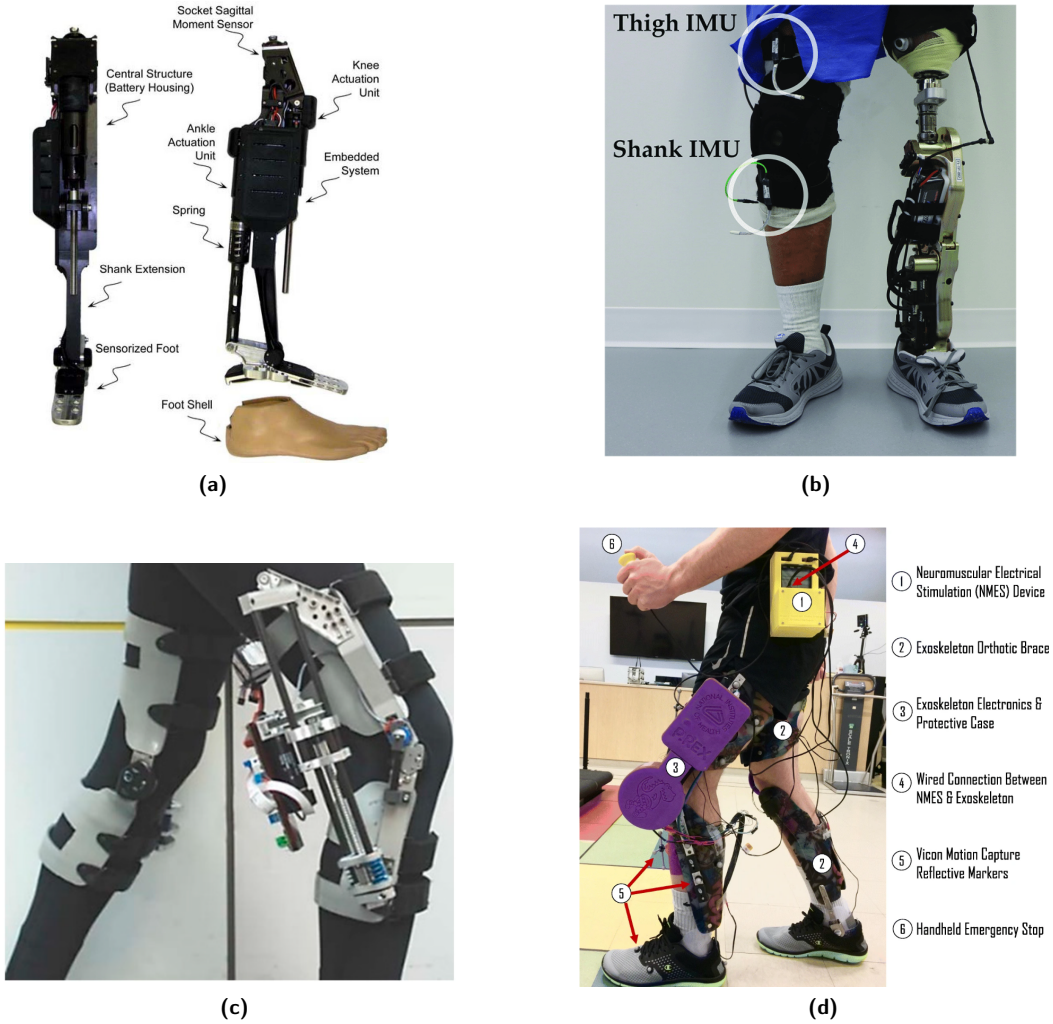

Figure 1.3: Examples of Active Knee Joint Stabilizing Mechanisms : (a) Active Self Contained Prosthesis [24] (b) Active Prosthesis Synchronized with Healthy Leg [25] (c) Electrically Powered KAFO [17](d) Active KAFO with FES Functionality [26]

1.3. Research Motivation

Conventional rigid assistive devices have been pivotal in restoring mobility and improving the quality of life for many individuals with limb impairments. However, they come with a set of limitations. Firstly, their rigid structure can lead to discomfort and skin trauma decreasing adherence, especially during prolonged use [12, 27]. This rigidity can also hinder natural movement, and force the body to conform to the device's motion profile, making it challenging for users to perform certain activities or adapt to varied terrains. Secondly, many of these devices are bulky when active, adding to the physical strain on the user and making them less aesthetically appealing [27, 28]. The bulkiness results from the materials used and the complex assemblies incorporated to provide stability, which also increases the cost of the devices. Additionally, the bulkiness increases the moment of inertia of the leg, requiring greater metabolic effort by the patients to lift their legs [28]. These issues make them unsuitable for a significant number of patients.

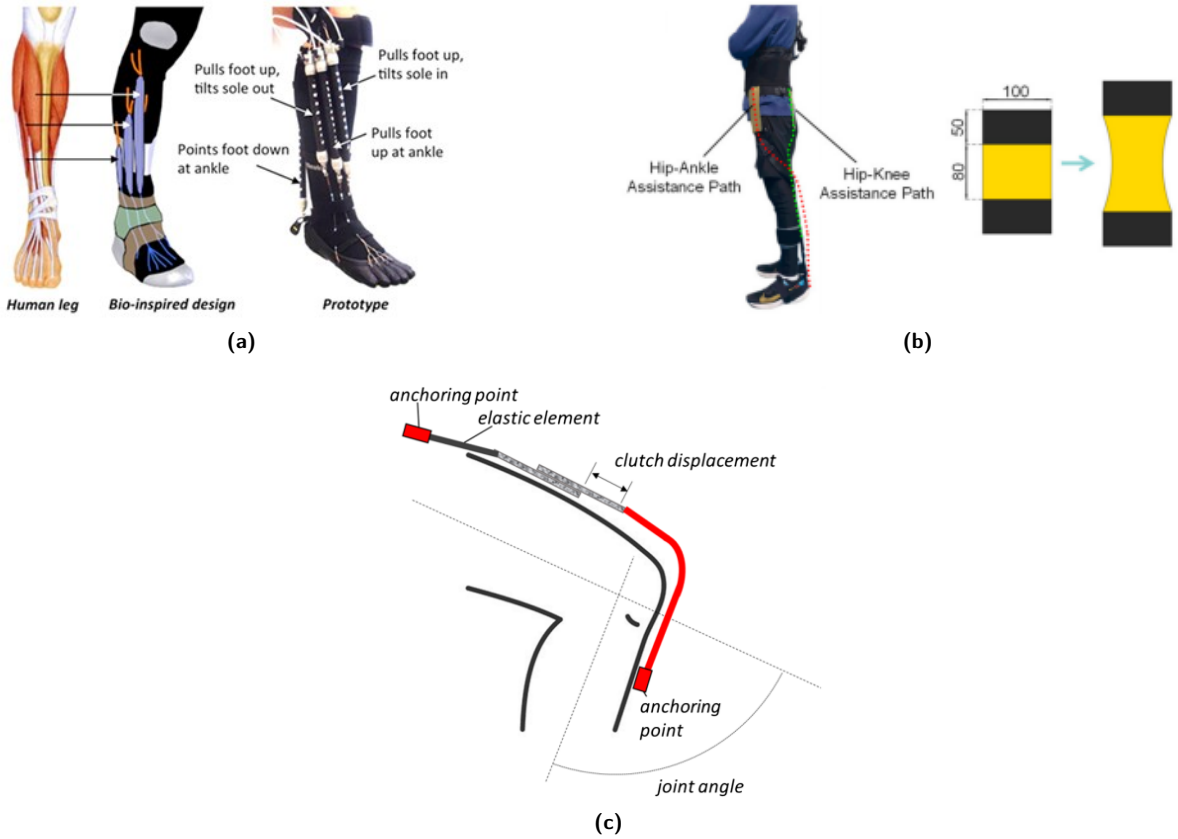

Figure 1.4: Examples of Soft Assistive Devices: (a) Biomimetic Orthosis with Pneumatic Artificial Muscles [29]. (b) Soft, Wearable Hip Assistive Brace [30]. (c) Flexible, Vacuum-Based Clutch for Knee-Joint Stabilization [31].

In light of these challenges, there is a growing interest in soft actuators and flexible exoskeletons as promising alternatives. Soft actuators, made from compliant materials, can mimic the natural flexibility of human muscles, providing a more comfortable and adaptive interface [29]. Flexible exoskeletons, on the other hand, can conform to the body's contours, reducing the risk of pressure points and enhancing wearability [31, 30]. They are simple in construction and generally do not require bulky, expensive components or manufacturing techniques. These innovations aim to combine functionality with comfort, potentially leading to more widespread adoption and improved user satisfaction. The improved wearability, ease of manufacturing, and low cost make them promising alternatives for developing countries. However, research has been focused on developing active devices like the pneumatic muscle-based exoskeletons[29], or semi-active clutch-based mechanisms[31]. They require sensitive electronics and power sources that can increase the cost, weight, and complexity of the system. Furthermore, these approaches rely on preventing knee buckling through the use of active force, or passive tension and do not address the issue of energy dissipation. These challenges point to the potential benefits of developing a soft,

passive energy dissipation device.

1.4. Research Objective

The goal of this thesis is to design and test a soft passive damping system that can be implemented in an assistive device. The system is to be designed to assist the knee extensors in resisting knee buckling under gravitational forces while allowing free movement during knee extension. This is the first step towards developing a soft, fully passive assistive device that can improve balance and absorb the impact of heel strike, in patients with knee extensor dysfunction or quadriceps weakness. The study aims to address the issues with current wearable assistive device technology, particularly in terms of comfort, complexity, and energy consumption, in light of their growing demand in developing countries.

Taking into consideration the time constraints, the scope of the project is limited to designing a proof of concept damper (See Appendix B), and experimental verification of its energy dissipation capacity. This exploratory study is intended to be the first step in designing a new class of lightweight, ergonomic, passive dampers.

1.5. Structure of The Thesis

This document is divided into three parts. The first part sets the context for the thesis project. Chapter 1 begins with an introduction to assistive device technology, the current state of the art of energy dissipation in assistive devices, and the motivation for undertaking this research topic. Chapter 2 provides a brief summary of the various energy dissipation mechanisms and the selection of the most suitable one for the design of a passive flexible energy dissipator.

The second part includes a scientific article on the design, prototyping, and experimental evaluation of a passive viscous damper Chapter 3. This article covers the majority of the thesis work.

The third part is a reflection (Chapter 4) on the thesis as a whole and an evaluation of the author's personal shortcomings, and growth over the course of the Masters course at TU Delft. Chapter 5 finally concludes this study and provides a summary of the whole document.

2

Energy Dissipation

2.1. What is Energy Dissipation

Energy dissipation is the irreversible loss of energy to the surroundings, achieved through the process of converting energy from one form to another. While often viewed as a detriment, due to the reduced efficiency from energy losses, it plays a crucial role in controlling noise and vibration and improving the stability of mechanical systems. In these applications, energy dissipation is used to transform mechanical energy into other forms such as heat and sound.

The dissipation of energy resulting from cyclic loading is commonly referred to as damping [32]. The most common examples of energy dissipators as dampers are vehicle suspension systems, earthquake-resistant structures and to reduce oscillations in tall buildings and bridges.

2.2. Modes of Energy Dissipation

There are various mechanisms that are responsible for energy dissipation, each with its own benefits and limitations. In this article, energy absorption is seen as analogous to energy dissipation, if the absorbed energy cannot be put back into the system. The working principles of dampers designed for mechanical energy dissipation are as follows (Fig. 2.1):

2.2.1. Dry Friction Damping

Coulomb or dry friction damping is a mechanism of energy dissipation where mechanical kinetic energy is converted to heat energy. It is achieved through the constant friction force that opposes relative motion between two surfaces in contact. Since friction always opposes relative motion, the damping acts in the direction opposite that of velocity. However it is a constant damping force, that does not depend on the magnitude of the relative motion of the sliding bodies, but rather only the magnitude of the normal forces between them [33]. Vehicle disc brakes and valve spring dampers are common examples of friction-based energy dissipation.

2.2.2. Viscous Damping

Viscous damping occurs in viscous fluids due to the resistance to relative motion between the layers of fluid flow. When fluids are forced through confined spaces, energy is absorbed to overcome viscous resistance to flow and is ultimately converted to heat. It always opposes the relative motion of fluid layers and depends on both the direction and magnitude of motion between the layers [34]. Vehicle suspension systems often use hydraulic dampers to minimize vibrations from the roads.

2.2.3. Electromagnetic Damping

Electromagnetic damping or magnetic eddy current damping is a phenomenon where a changing magnetic field or a conductor moving through a magnetic field or induces a current in the conductor. These currents, known as eddy currents, then generate their own magnetic field that opposes the original magnetic field, resulting in energy dissipation in the form of heat from the conductor. The induced field always opposes the change in the electromagnetic flux in the conductor and depends on the velocity of the conductor or the rate of change of the magnetic field [35]. Magnetic eddy current breaks used in elevators implement this principle of electromagnetic damping.

2.2.4. Hysteretic Damping

Material Yielding or Hysteretic damping involves the energy required to overcome strain energy and deform a material. Particularly, when a material is yielded beyond its elastic limit, it is deformed plastically, and the energy required to deform it cannot be recovered. The amount of energy absorbed or dissipated depends on the material properties, and the extent of plastic deformation [36]. Such energy dissipators are deployed as crash structures in automobiles.

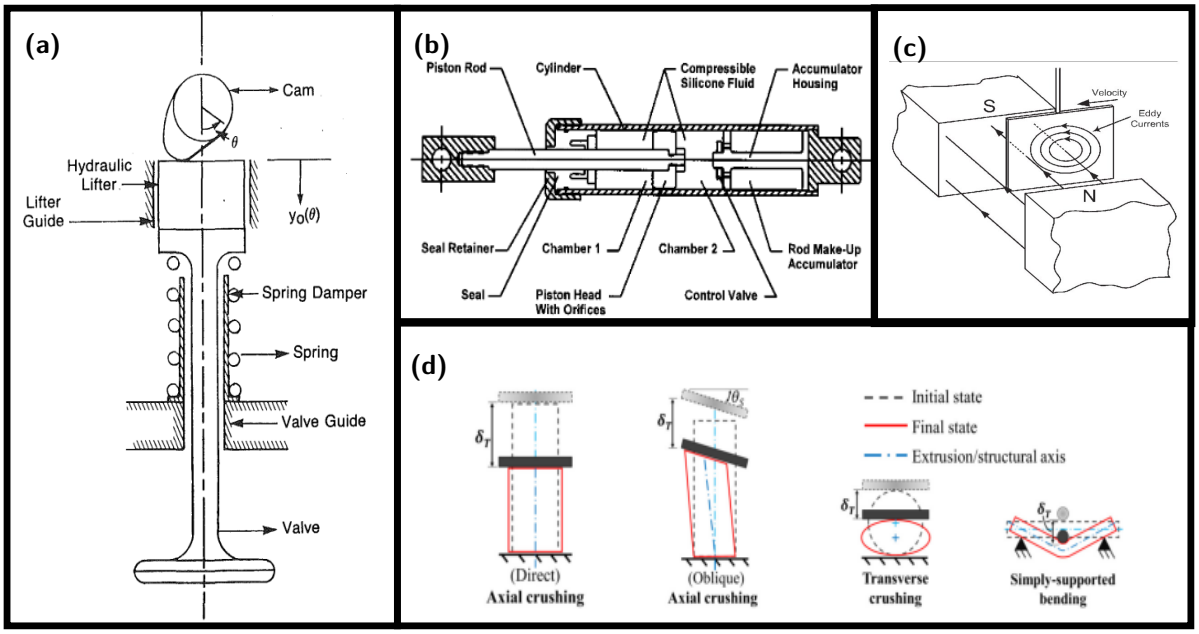

Figure 2.1: Principle Energy Dissipation Mechanisms: (a) Coulomb Friction Damper in Valve [37]. (b) Viscous Damper - Plunger style [34]. (c) Electromagnetic- Eddy Current Damper [35]. (d) Hysteretic Damper - Crash Structure[36]

2.2.5. Miscellaneous

In addition to the principles mentioned above, there are some other mechanisms that bear some similarities but do not fully fit within the stated classification. They are mentioned here:

Piezoelectric Damping

Piezoelectric dampers are a special class of coulomb friction dampers, that use piezoelectric materials as the contact surfaces. Mechanical energy is first converted into electrical energy through the piezoelectric effect and then lost as heat. Piezoelectric dampers can be used as energy harvesters and active vibration control dampers [38].

Viscoelastic Damping

Viscoelastic materials, work like hysteretic dampers, but they are capable of dissipating a significant amount of energy even in their elastic region due to internal friction between their molecular chains. They commonly comprise polymers, hydrogels, and biological tissue [39]. They are commonly used as seismic vibration dampers. Vehicle tires also offer some viscoelastic damping.

Aerodynamic Damping

Similar to viscous fluid dampers, aerodynamic dampers use air as the working fluid. Vortices generated by airflow around the body dissipate energy in the form of heat. As air is compressible, energy is absorbed in compressing air, which is also ultimately expelled as heat [40]. This principle is implemented in air dampers commonly in automobiles and cycles.

Thermoelastic Damping

Some materials when subjected to cyclic loads, undergo reversible temperature changes. When the heat generated from the increase in temperature is lost to the surroundings, energy is dissipated. Such devices are used in

microelectromechanical systems (MEMs) [41], as the small sizes of the devices limit the application of other damping mechanisms.

2.3. Requirements for Energy Dissipation in Assistive Devices

In the body, the viscoelasticity of connective tissue and eccentric contraction of the muscles together contribute to the damping of joints. Energy dissipation finds considerable use in assistive devices and wearables, contributing to both user comfort and performance. It serves to prevent excessive loading of joints and improve the stability of the joint motion. As highlighted in Chapter 1, dampers are of particular interest in lower limb assistive devices for stabilization of the knee joint, and preventing the buckling of the knee. Given the challenges associated with developing effective assistive solutions for lower limb deficiencies, particularly when considering individuals in developing nations, the set of requirements is formulated:

- Soft/Flexible system: A flexible device is much more comfortable for the user and does not impose rigid motion limits onto the body. Flexible devices are generally lighter and easier to manufacture.
- Reversible/Repeatable Motion: The damper must be capable of withstanding repeated use without a drop in performance. This is to allow the patients to walk freely and for long durations without having to constantly replace or fix the damper.
- Complexity: The damper must be made of minimal parts so as to reduce the cost of manufacturing and maintenance. It must also be simple in functioning.
- Weight: The device must be as light as possible, so as to improve user comfort and reduce the metabolic cost the user expends to carry the device.
- Mechanical Constraints: The damper must be capable of withstanding the body weight of the user and the deformations associated with the knee range of motion. (See Appendix A)
- Adaptability: The damper must be capable of adapting to the variety of loads that the user will experience, and have the capacity to adjust accordingly.
- Passive Operation: Passive devices have lower cost, complexity, and maintenance. They are generally more robust, as they do not have fragile electric circuits in them.

2.4. Selection of an Energy Dissipation Mechanism for a Novel Flexible Damper

Based on the shortlisted requirements, the different mechanisms of energy dissipation are evaluated and compared in Table 2.1[1]. The criteria for evaluation are as follows:

- Positive: If a mechanism can address a criteria by means of its working principle, or could potentially do so with some small design interventions, it is given a ' ✓' and counts $+1$ to its total tally.
- Neutral: If a mechanism cannot address a criterion fully, requires considerable design interventions or requires compromise on another criterion in order to satisfy a criterion, it is considered neutral. It is given a 'O' mark and counts $+0$ to the total tally
- Negative: If a mechanism cannot address any one of the criteria by means of its working principle, it is given an 'X' and a score of -1 to its total tally

After all the criteria are rated, the total of each mode of dissipation is tallied. Based on this evaluation, the most prospective energy dissipation mechanism is viscous fluidic energy dissipation. It comes as no surprise that some of the most commonly used dampers involve hydraulic viscous damping. The mauch knee and the c-leg, two of the most popular prosthetic knee joints also use viscous dampers.
Viscous damping is versatile, controllable, can withstand large forces, and offers highly repeatable motion due to its dependence on fluids (solid damping elements are susceptible to wear and creep, but fluids have no such drawbacks). Hydraulic valve-based systems are also highly adaptable, as the magnitude of viscous damping depends on the magnitude of the velocity and the size of the valve diameter. This also allows for fine control of the dampers response, as seen in the C-leg.

[1] FR: Coloumb Friction, VC: Viscous, EM: Electromagnetic, HS: Hysteretic, PZ: Piezoelectric, VE: Viscoelastic, AD: Aerodynamic, TE: Thermoelastic

Table 2.1: Selection of Energy Dissipating Mechanisms for Assistive Device Use

Design Criteria	**Type of Damping**							
	FR	VC	EM	HS	PZ	VE	AD	TE
Soft/Flexible	**X**	✓	**O**	**O**	**X**	✓	✓	✓
Reusable/Repeatable	**O**	✓	✓	**X**	**O**	✓	✓	**O**
Complexity	✓	**O**	**X**	**O**	**O**	✓	**O**	✓
Weight	✓	**O**	**O**	✓	✓	✓	**O**	✓
Mechanical Constraints	**X**	✓	✓	✓	✓	**O**	**O**	**X**
Adaptable	**X**	✓	✓	**X**	✓	**X**	✓	**X**
Passive	✓	✓	**X**	✓	**O**	✓	**O**	✓
Number of **X** : (-1)	3	0	2	2	1	1	0	2
Number of **O** : (0)	1	2	2	2	3	1	0	1
Number of ✓ : (+1)	3	5	3	3	3	5	3	4
Total	0	5	1	1	2	4	3	2

2.5. Prelude to the Article

In Chapter 1, we established the need for a passive, cost-effective, and soft energy dissipating mechanism for assistive technology, particularly to help those without means in developing nations. Chapter 2 looked at the various energy-dissipating mechanisms and ultimately concluded that viscous damping was most conducive to the development of a soft, passive damper.

Such a flexible damper could be developed to provide a wide range of energy dissipation solutions, for instance, in the design of new seat-belts, whiplash protection, soft robotics, harnesses, and as bio-mimetic energy dissipators in assistive devices. The motivation of this thesis was to design a proof-of-concept damper that could be deployed to assist the quadriceps in the energy dissipation of knee joint torques. The purpose was to prevent the knee from buckling under body weight while providing minimal resistance to knee extension, and early swing flexion.

The following chapter presents a scientific article on the design and experimental characterization of a proof of concept flexible viscous damper capable of shear-rate adaptive passive energy dissipation. The novelty in this study is the development of a passive, flexible viscous damper. The damper is designed to act under tensile loading while providing minimal resistance to compressive and lateral loads.

3

Scientific Article

The Design Of a Flexible Shear-Rate Adaptive Viscous Damper For Passive Energy-Dissipation

Souri Venkata Shanmukha Sreeramagiri, Heike Vallery, and Gerwin Smit

***Abstract*—This article presents the design of a novel flexible viscous damper, capable of passive, shear-rate adaptive energy dissipation through the use of Shear Thickening Fluids (STF). The proposed design uses a braided mesh sleeve to squeeze an elastic pouch containing a working fluid, under tensile loading. The fluid is squeezed through a constriction, into a hollow relief chamber, where the elastic pouch is free to expand. Energy is dissipated to push the fluid through the constriction, against the viscous forces. A proof-of-concept prototype was assembled and experimentally studied with static, impact, and cyclic loading tests. When using STF as the working fluid, the prototype demonstrated an increased energy dissipation per cycle from 0.022J at 0.1Hz to 0.132J at 1.33Hz and delayed the deformation from impact loads by 1.1 seconds in comparison to static loads. The developed prototype is highly compliant in compression and bending and can withstand 13.3% elongation and 120N force in tension. The proposed idea is considered a flexible analog of conventional viscous dampers and is intended for use in assistive devices and soft robotics. With the rapid advancements in soft actuators and soft electronics, this work is a contribution to the development of soft passive viscous dampers.**

***Index Terms*—Viscous Damper, Soft Devices, Passive Energy Dissipation, Shear Thickening Fluids, Hysteresis**

I. Introduction

A. Background

Viscous dampers (VDs) are ubiquitous in a myriad of fields, including assistive devices [1], [2], automobiles [3] to structural engineering [4]. They protect structures from disturbances, improve stability, and mitigate noise and vibrations. They are preferred over other forms of energy dissipation due to their simplicity and reliability, offering sensor-free, adaptive energy dissipation [5]. Viscous energy dissipation is a consequence of the energy expended in overcoming viscous resistance when an object is displaced through a fluid medium. VDs exploit this phenomenon by employing pistons to move within a chamber filled with viscous fluids. The pistons force the fluid to flow through small constrictions, resulting in a large viscous resistance. The damping force generated is linearly proportional to the velocity of the piston within the casing. Ultimately the energy is dissipated as heat from the viscous fluid.

The authors declare that there are no financial interests or sponsorships that could have influenced the research, data analysis, or the content presented in this paper.

All authors are affiliated with the Delft Biorobotics Lab, under the Department of BioMechanical Engineering, Faculty of Mechanical, Maritime and Materials Engineering, Delft University of Technology, Mekelweg 5, 2628 CD Delft, The Netherlands.
Email:
sourisvs@gmail.com, H.Vallery@tudelft.nl, G.Smit@tudelft.nl

B. State of the Art

VDs have witnessed significant diversification, to address the energy dissipation and vibration control requirements in a variety of applications. Linear VDs exhibit damping forces that linearly vary with the relative velocity between the piston and cylinder [1], [5]. They are simple, passive devices that inherently adapt to the frequency of perturbations. To increase the magnitude of damping force for larger perturbations, dampers with a non-linear force-velocity displacement have been developed. They have been used in automobiles to improve rider comfort [3] and structural engineering to resist seismic perturbations without the need for active control [6]. Tuneable dampers, offer adjustable damping and have been designed for applications with diverse loading conditions [2], [7]. Finally, actively controlled dampers allow for precise modulation of energy dissipation through the use of sensors and the controlled action of valves. They are effective at stabilizing motion and adapting to various loading conditions in real-time. The C-leg is a microprocessor-controlled VD used in knee prosthetics to stabilize gait [8].

Some dampers regulate energy dissipation by varying the viscosity of the working fluids. Magnetorheological fluid dampers use magnetic fields to control the viscosity of magnetorheological working fluids [9]. These fluids contain suspended magnetic particles, which align to external magnetic fields, increasing the viscosity of the fluid. Similarly, electrorheological dampers use electric fields to control the rheology of the working fluid [10]. Some dampers achieve passive adaptive damping through the use of non-Newtonian fluids, whose viscosity varies with shear rate. The viscosity either increases (Shear thickening) [11], or decreases (shear Thinning) [12] with shear rate (excitation frequency) depending on the nature of the working fluid.

C. Research Motivation

There is a growing interest in flexible or compliant devices driven by rapid developments in material science and manufacturing techniques. They are versatile, lightweight, simple, and cost-effective [13]. Their flexibility allows them to adapt to changing environments and outperform conventional rigid devices. Moreover, the inherent compliance makes them safer for interaction with humans, driving increased efforts to deploy soft devices in the fields of biomedical and assistive technology [14]. Substantial progress has been made in the development of soft actuators, ranging from pneumatic muscles to electrically and magnetically controlled polymers [13]–[15]. Soft electronics are also evolving to drive the expansion of soft robotics and provide essential support to soft actuators [15]. However, a notable gap exists in the field of soft robotics:

soft energy dissipators. Energy dissipation forms a crucial aspect of control and stabilization in many assistive devices and robotic setups. Currently, viscoelastic dampers represent the only example of soft dissipators used in some soft robotics applications [16] and soft body armour [17]. However, they fail to offer the desired degree of control and reliability compared to other dampers. Furthermore, viscoelastic dampers are constrained by their limited deformation capacity and a sizeable component of elastic stiffness [18].
There is a lack of flexible dampers that can be reliably controlled, with repeatable, adequate deformation. The development of soft dissipators can bolster soft actuators and propel the advancement of entirely soft devices.

D. Research Objective

Viscous dampers seem most suited to the development of flexible dampers. The working principle relies on fluids, which are inherently compliant. They offer scope for passive, controllable operation with large displacements. A prior attempt to develop a flexible damping "ligament" employing the principle of viscous damping with shear-thickening fluids [19] showed promising results. The development of such simple, passive dissipators could pave the way for affordable, lightweight, flexible devices, without introducing unnecessary complexity. This study is an attempt to develop a novel way to achieve flexible viscous damping and create a flexible counterpart to conventional viscous dampers.

E. Article Structure

This article begins with an overview of viscous dissipation, and the rheology of various fluids in Section II. Section III presents the design and development of the proof of concept, along with a description of the experimental setups used in this study. Section IV delves into the results of the experiments, followed by a discussion of the key findings and comments on the future scope of the proposed damper in Section V. The study is finally concluded in Section VI.

II. Viscous Damping

A. Viscosity and Non-Newtonian Fluids

Viscosity is a measure of the resistance of a fluid to deformation and flow. It quantifies the internal friction between layers of fluid when there is relative motion between them [20]. It is typically measured in units of (Pa.s) or poise (P). Viscosity relates the shear stress of a fluid to the shear rate through the power law equation known as the Ostwald approximation and is as follows [21]:

$$\tau = K \left(\frac{dy}{dx} \right)^n \tag{1}$$

Here τ is the shear stress, $\frac{dy}{dx}$ is the velocity gradient or shear strain rate, n is the flow behaviour index and K is the flow consistency index.
Fluids can be categorized into two based on their viscosity: Newtonian fluids and non-Newtonian fluids. Newtonian fluids are those that show a linear relationship between shear stress and the shear strain rate or the velocity gradient. Here the flow behaviour index n is 1, and the consistency index K is the value of dynamic viscosity. This value is a constant, thermodynamic property for Newtonian fluids [20]. Water is an example of a Newtonian fluid with a viscosity of 1 centiPoise (cP) at room temperature.

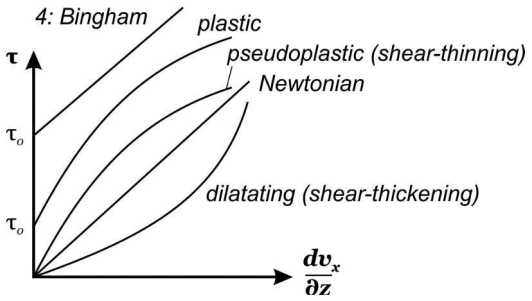

Fig. 1: Plot comparing the rheological behaviour of different fluids; Adapted from: 1. Fluids are either Newtonian (linear) or Non-Newtonian (non-linear) based on the shear-stress and strain-rate relationship.

Non-Newtonian fluids, however, have different values of the flow behaviour index n and exhibit a non-linear relationship between stress and strain. Fig.1 summarises the various types of fluids based on the relationship between the shear stress and strain rate.
Of particular interest to this study, are the Non-Newtonian fluids with n $>$ 1. They are known as shear thickening fluids (STF) or Dilatants. Their viscosity rapidly increases with shear rates. Suspensions of particles in liquids like cornstarch in water are examples of such fluids.

B. Rationale for STF in flexible dampers

VDs operate by pushing viscous fluids through narrow openings into relief chambers. Energy is dissipated in overcoming the viscous forces to push the working fluid through the narrow orifice. However emulating this principle in a flexible device can be challenging, as the high-pressure gradients required to pump the fluid through a narrow orifice can lead to high stresses and even tearing of the flexible pouches. Leveraging the shear-thickening effect of dilatant fluids could intensify the viscous resistance offered, without the need for high pressure gradients. This approach could potentially achieve effective damping in flexible devices without compromising the structural integrity of the flexible container. Studies implementing STF as working fluids in conventional VDs demonstrate an increase in damping force with the shear rate or excitation frequency [22]. This behaviour can be utilized to develop a shear-rate adaptive response in passive dampers [11], [22].

C. Expected Behaviour of a Flexible Viscous Damper

The response of the flexible VD to loading can be split into two components: the viscoelastic contribution of the flexible container (F_{VE_pouch}), and the viscous contribution of the damper (F_{V_damper}). The equation can be written as follows:

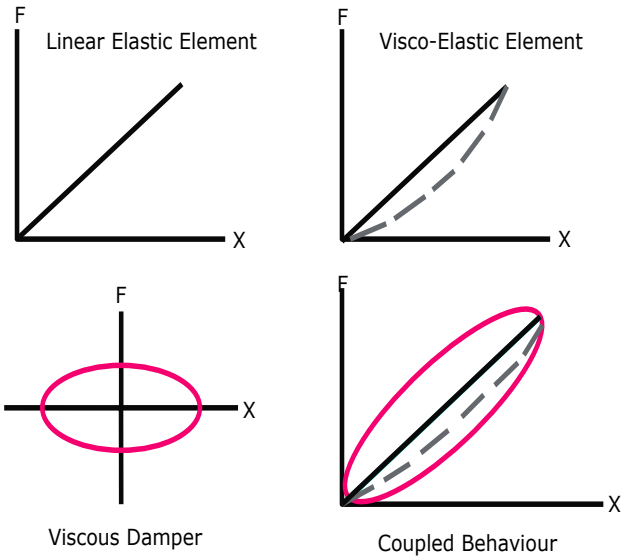

Fig. 2: Expected Force-Displacement Curves of the Combined Viscous-Viscoelastic Damper. The coupled behaviour functions as a spring-damper system, with improved energy dissipation

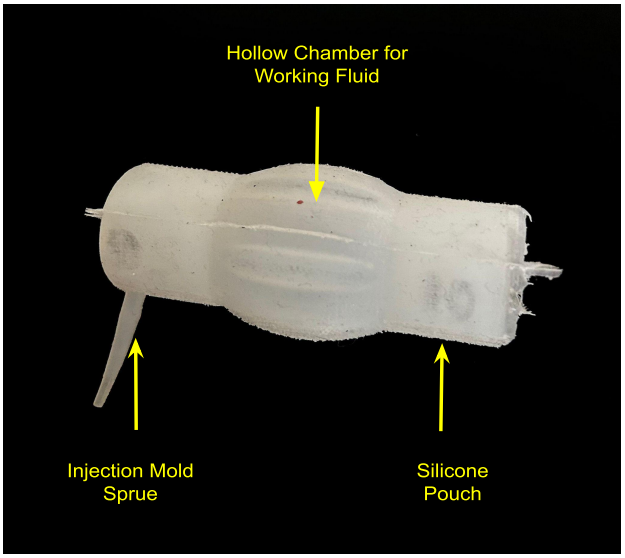

Fig. 3: Silicone Rubber (DragonSkin 10) Pouch with Working Fluid. The flexible pouch is designed to hold fluid within and apply radial pressure when stretched axially.

$$F_{external} = F_{VE\_pouch} + F_{V\_damper} \tag{2}$$

The general force-displacement behaviour of the individual elements viscoelastic pouch and viscous fluid and the expected behaviour of the combination is illustrated in Fig 2. The coupled behaviour is desirable, as it has a larger area leading to greater energy dissipation. The use of STF should generate larger hysteresis curves with increasing excitation frequency. In this study, the STF used is a slurry of cornstarch and water. The subsequent sections of the paper will elaborate on the development of a working prototype built to substantiate this hypothesis.

III. Methodology

A. Problem Decomposition

In light of the exploratory nature of the research question, the development of a working prototype, experimental verification of the energy-dissipating ability, and excitation-frequency dependant response are ascertained to be sufficient evidence for establishing a proof of concept.
With this objective in mind, the following design specifications are deemed relevant to the proof of concept:

- Power Input: The goal is to develop a fully passive system; therefore, the prototype must consume no power.
- Flexible/Soft: The device must comprise of flexible components, and operate through deformation rather than rigid body motion. To achieve this, we assign a metric of at least 10% longitudinal strain during operation, and a capacity to bend at least ≥ 45 °elastically.
- Dimensions: The prototype must be encompassed within a box of volume 20x10x10 cm length-breadth-height (lbh) so as to remain compact for potential applications.
- Total Displacement: The prototype must be capable of generating a displacement of 1 cm
- Complexity: To keep the prototype simple, and reduce maintenance, the number of parts must be limited to 5 total parts.
- Adaptability: The device must offer varying responses to different excitation frequencies. This change is quantified as at least a delay of 1 second between static and impact loading.

These specifications are arrived on based on preliminary analysis of loads and dimensions commonly produced in other proof of concept damper studies [11], [19], and for the convenience of rapid prototyping and testing. Since this is a pilot study, no specific force or energy dissipation requirements have been established beforehand. These metrics will be assessed during the experimental procedure, and their adequacy or potential areas for improvement will be addressed in the discussions. The design specifications are summarised in Table I.

TABLE I: Design Specification Table

Design Criteria	Desired Metric	Rationale
Power	0 W	Passive Device
Flexible	10 % Strain and ≥ 45 °bend	Compliance in Damper
Dimensions((lbh)	20x10x10 cm	Compact device
Total Displacement	$\sim$ 1cm	Meso-scale
Complexity	$<$ 5 parts	Simple assembly
Adaptability	$\geq$ 1 sec	delayed response for sudden load

The criteria are not representative of the desired finished product but are selected to provide insights into the expected behavior of such a device.

B. Design and Prototyping

When tensile loads are exerted on incompressible solids, they stretch along the direction of load (axial) and shrink in the

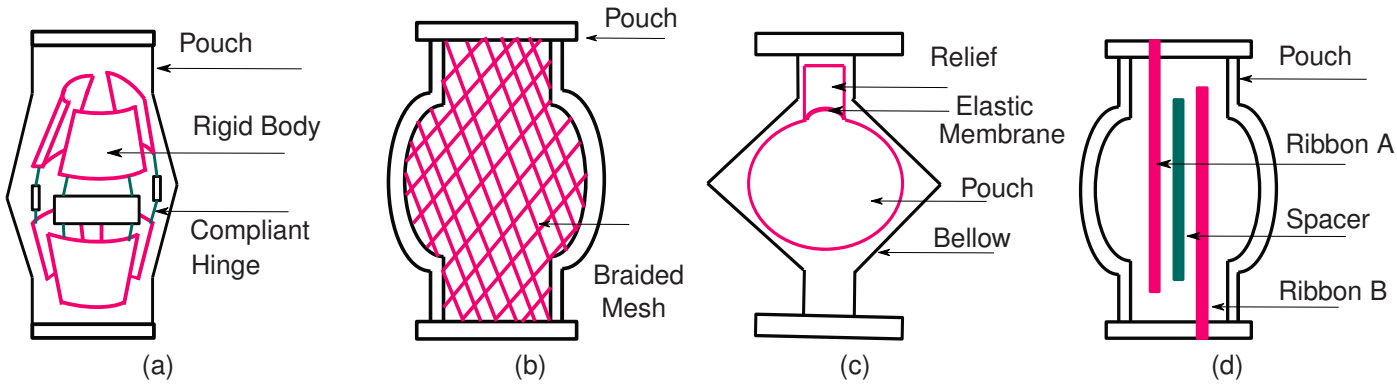

Fig. 4: Sketches of the Generated Concepts: (a): Compliant Scissor Mechanism. (b): Braided Mesh. (c): Bellow - Relief Valve. (d): Ribbon Stretch

other directions (radial) due to the conservation of volume. The preliminary hypothesis in designing a flexible viscous damper was that when a hollow pouch containing a fluid is subjected to axial tensile loads, it begins to contract radially and apply pressure on the fluid inside. The fluid resists this compression and consequently impedes axial elongation .

To test this hypothesis, a simple hollow pouch was molded from flexible Dragonskin-10 (DS10) Silicone [23]. DS10 was chosen as it is very easy to mold, and results in a strong, flexible, translucent rubber mold. Silicone Rubbers have a very high Poisson ratio, close to 0.5 [24], which results in considerable radial shrinkage for axial elongation.

The DS10 pouch was filled with a sample of cornstarch slurry and stretched axially after the ends were sealed off (Fig. 3). It was observed that the pouch indeed applied pressure onto the fluid and the shear-thickening effect was evident from the clumping of the working fluid. However, the resistance offered by the fluid to radial compression did not translate to impeding axial elongation. The flexible pouch stretched around the central portion rather than pushing the contained fluid, leading to a minimal effect on the motion of the endpoints. Therefore it became necessary to design a means to couple/link the axial elongation to radial constriction while maintaining the flexibility of the device.

1) Concept Generation: : To address the problem of coupling axial stretch to radial compression, the following concepts were developed Fig.4, based on principles taken from literature.

- *Compliant Scissor Mechanism Concept*: A scissor mechanism, found in car-jacks is a kinematic chain of rigid links that can contract laterally (radially) and lengthen longitudinally (axially). This concept has been applied to develop earthworm-mimicking compliant modular robots [25]. The concept in Fig. 4a involves a 3D radially symmetric scissor mechanism, with compliant hinge joints that close inward while extending in length. Such a mechanism can be incorporated as the ”skeleton” of the flexible pouch, to prevent the pouch from stretching around the fluid.
- *Braided Mesh Concept*: The Mckibben muscle is a pneumatic artificial muscle comprising an inflatable tube surrounded by a braided mesh [26]. The tube when pressurized tends to expand outward in all directions. The mesh can only expand outward radially while contracting in length. Therefore, the mesh restricts the tube to contract axially and expand radially when pressurized. This principle can be inverted and applied to the current design problem, where the braided mesh is initially in a contracted state Fig. 4b, and it can stretch axially while squeezing in radially. When this mesh is coupled with a flexible pouch containing the fluid, it can restrict the overall motion of the device as is desired.
- *Bellow Relief Valve Concept*: Bellows are flexible pouches commonly used to pump/blow out air. They compress axially, reducing the internal volume, thereby expelling the fluid contained. Pneumatic artificial muscles have been developed from bellows based on this behavior [27]. This principle can be applied to force fluid through a constriction into a relief chamber made of elastic material (Fig. 4c), analogous to a conventional mono-tube hydraulic damper. The fluid is sheared when being forced into the relief chamber, causing the elastic pouch to expand. This process requires energy. Once the external load is removed, the restoring force of the elastic chamber can squeeze the fluid back into the bellow.
- *Ribbon Stretch Concept*: As the working fluid is intended to be an STF, whose viscosity increases with shear stress, a concept is developed using two metal ribbons with rough surfaces encased inside a flexible tube, each attached to opposite ends of the tube (Fig. 4d). When the tube is stretched, the ribbons get pulled to opposite ends. To do so, they have to shear the working fluid, and thus offer resistance to axial stretching. Such a concept was developed as a rate-dependant tether [19]. This idea does not completely rely on the coupling of radial compression and lateral elongation but achieves the intended effect of shearing the working fluid, and is thus considered for the study.

2) Concept Selection: The four concepts were evaluated against the following criteria:

- *Effectiveness*: A metric to evaluate how effective the concept is in transmitting axial load to radial pressure,

or ultimately in shearing the working fluid to dissipate energy. It is determined by the pressure distribution capacity or extent of shearing each concept is capable of producing.
- *Flexibility*: The extent to which the proposed concept can be deformed in various directions.
- *Displacement*: The magnitude of axial stretch permitted by each concept, relative to its initial dimensions.
- *Complexity*: The number of components required and ease of manufacturing to realize the concept.
- *Dimensions*: The approximate design space required to realize the concept.

The first criteria compares the concepts on their ability to address the coupling problem, while the remaining are based on the design specifications: The designs were evaluated on a four-point scale of $[-2, -1, +1 + 2]$. The specifications for adaptability and power were not included in the comparison. All these concepts relate to a passive solution, and adaptability is a consequence of the working fluid. The results of the comparison are summarized in the following Harris profile:

TABLE II: Harris profile: Evaluating concepts against design criteria

Criteria	Weight	Concept			
	Total : 1	Scissor	Braid	Bellow	Ribbon
Effectiveness	30	-1	2	1	-1
Flexibility	30	1	2	-1	-2
Displacement	20	-1	-1	2	2
Complexity	10	-1	-1	-2	2
Dimensions	10	1	1	-1	2
Total		-0.2	1.0	0.1	-0.1

3) Concept Combination and Final Selection: Based on the evaluation, the braided mesh concept turns out to be the optimal solution. It boasts the most flexible design, with even pressure distribution and good coupling between lateral stretch and radial contraction. It has been used in a variety of artificial muscles for these properties. A prototype was made by made by molding the silicone pouch around a braided mesh.

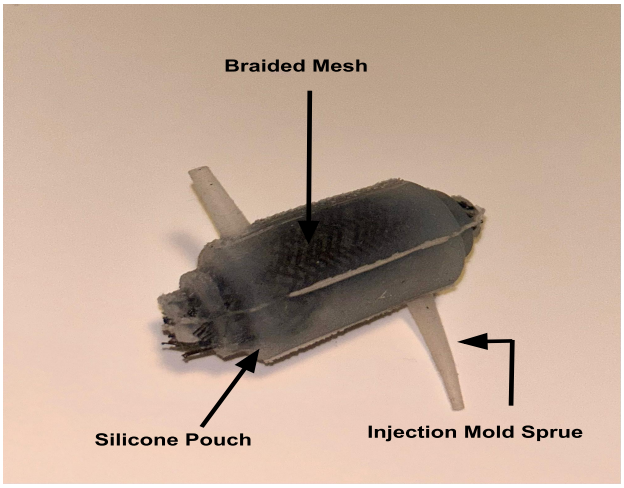

Fig. 5: Silicone Rubber (DragonSkin 10) Pouch with Embedded Braided Mesh. The mesh is fully integrated within the silicone pouch and provides structure to its stretching.

The prototype successfully yielded the desired coupling while maintaining flexibility. However, when tested with the cornstarch slurry, the prototype did not undergo any extension. The whole system behaved as a rigid unit on loading, ultimately resulting in rupture and leaks from the silicone membrane. It was deduced that the lack of axial stretch was because the volume of the cavity reduced on stretching, and the incompressible fluid had no relief to flow, which led to a very high pressure developing on the silicone pouch. This resulted in the leaking of fluid through the mesh pores and the rupturing of the pouch walls.

To obtain the desired motion, it was necessary to allow the fluid to move into another space when the mesh constricted the volume radially. Therefore the Bellow-Relief chamber concept was combined with the braided mesh idea to develop the final working principle. This idea incorporates the flexibility and even pressure distribution of the braided mesh while ensuring the fluid is pushed into a relief chamber, thereby mitigating the excessive pressure buildup.

C. Final Prototype

1) Prototype Design: The design consists of an elastic pouch that contains the working fluid, encapsulated within a braided mesh. The flexible pouch is clamped between two handles on one end. It is passed through a constriction, and housed within a hollow chamber on the other end. The braided mesh is clamped onto the handles and the outer surface, thereby fully encasing the elastic pouch (Fig. 6).

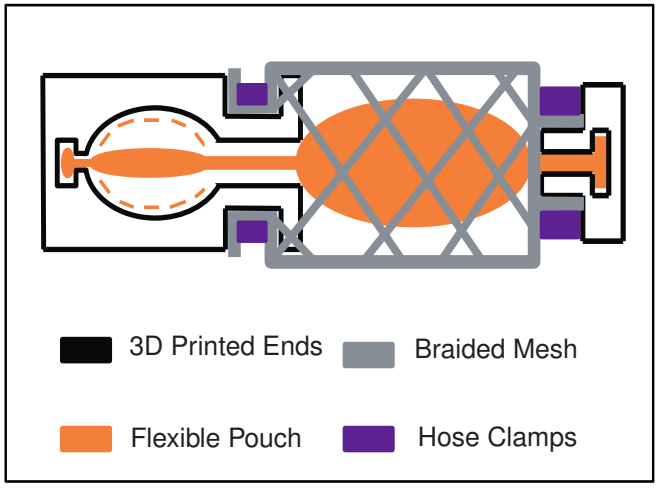

Fig. 6: Schematic of the Final Proposed Design. The braided mesh when stretched axially, squeezes the fluid within the pouch through the constriction.

2) Prototype Working: When the device is stretched axially, the braided mesh applies pressure onto the elastic pouch and contracts radially. This squeezes the fluid through the constriction into the portion of the tube inside the hollow chamber, where it is free to expand. Once the load is removed, the elastic stiffness of the balloon forces the fluid back through the constriction into the main body of the pouch. Work is dissipated in pumping the fluid through the constriction.

The design is analogous to a conventional monotube hydraulic

TABLE III: Test Specimen Description

Test Sample	Mass (g)	Vol (ml)	Comments
No Fluid Fill	53.5	3	Empty Pouch
Water	68.85	20	Newtonian Fluid
SAE 50 Oil	66.64	20	Viscous Newtonian Fluid
Cornstarch Slurry	74.3	21	Water:Cornstarch- 0.875:1 (53.3% Cornstarch)
Thick Cornstarch Slurry	73.3	20.5	Water:Cornstarch- 0.75:1 (57% Cornstarch)

damper. The braided mesh is comparable to the piston as it applies pressure on the working fluid, and the elastic pouch is comparable to the cylinder casing and the secondary chamber. Lastly, The constriction performs the role of the piston valve.

3) Prototype Fabrication: A Polyethylene Terephthalate (PET) sleeve, commonly used as a cable sleeve for electrical wires is selected for the braided mesh. For the elastic pouch, needle tail party balloons were selected, due to their inherent shape making it easier to incorporate the relief chamber. The hollow chamber and handle ends were designed on Solidworks and 3D printed using FDM printing with Tough PLA. The prototype was clamped with hose clamps as they can be equipped and removed with ease.

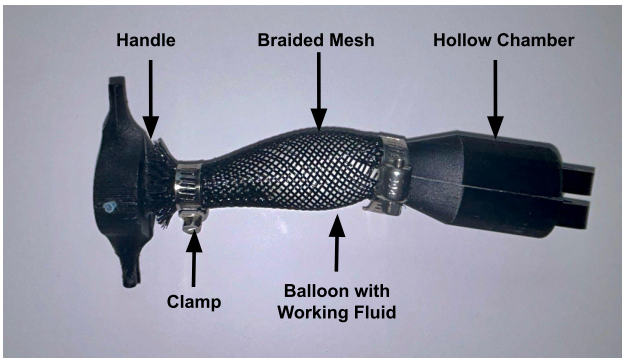

Fig. 7: The Final Assembled Prototype: A flexible viscous damper operating in tension.

D. Experimental Setup

To experimentally characterize the behavior of the damper, and quantify its shear rate adaptive properties, 5 specimens of the damper were tested with working fluids, as summarised in Table III. These specimens were selected to understand the behavior of a) the pouch and mesh alone, b) the behavior of the damper with Newtonian fluids, and c) the behavior of the damper with Non-Newtonian STFs of different mixing ratios. The following experimental setups were used for the tests:

1) Viscosity Measurement Setup: Rheological tests were conducted on the parallel plate AR-G2 Magnetic Bearing Rheometer: Fig. 8a. A linear sweep test, with the shear rate from 0.1 to 100 (1/sec), was performed with data collected from 15 to 20 points. All tests were conducted at a steady temperature of 25° C. The setup parameters are summarized in Table IV. Three trials were conducted for each fluid sample.

TABLE IV: Rheometer Test Parameters

Parameter	Value
Data Collected	Viscosity (cP) and Shear Stress (Mpa)
Data Points	15 - 20
Temperature (° C)	25
Soak time (sec)	15
Test Type	Linear Sweep
Shear Rate (1/sec)	0.1 to 100

2) Constant Force Loading Setup: The constant force loading tests were performed to quantify the response of the damper to static and impact loads of constant force. A custom setup was built using masses suspended by a tension cable, over a pulley applying loads on the damper (Fig. 8b). One end of the damper was fixed to rigid support via an S-type 100N FUTEK load cell to record the forces transmitted through the damper. A draw-wire displacement sensor (WPS MK30) of 150mm range from Micro-Epsilon is attached in parallel to the floating end of the damper to record linear stretch. The suspended masses are loaded onto a slider carriage to ensure motion is only along the vertical axis.

TABLE V: Constant Force Loading Test Parameters

Parameter	Value
Data collected	Displacement (mm) and Force (N)
Sampling Frequency (Hz)	20
Static Test Loads (kg)	3.25, 4.5 and 7
Impact Test Loads (kg)	4.5
Slider mass (Kg)	0.325
Height of drop (mm)	40 ± 5
Trials per sample	5

Static and impact tests were conducted by dropping the weights from a height of 40 ± 5mm. For static loading, the weights were lowered gently till maximum loading was reached and the tension cable was taught. For impact tests, the weights were dropped suddenly, ensuring the cable came under tension only after the drop height was crossed. Data was logged for at least 1 second after steady-state values of displacement and force were reached. Due to weak points in the setup, specifically the tension cable clamping and mass-damper attachment points, the impact tests could only be conducted for a mass of 4.5 Kg, while the static loading tests were conducted over three loads: 3.25 Kg, 4.5 Kg, and 7 Kg.

3) Cyclic Loading Setup: Cyclic loading tests were performed on the ProLine Z010 (ZwickRoell, NL), to assess the hysteretic behavior of the damper (Fig. 8c), and experimentally validate the shear-rate adaptive behavior of the damper with the STF working fluid.

TABLE VI: Cyclic Loading Test Parameters

Parameter	Value
Data collected	Displacement (mm) and Force (N)
Sampling Frequency (Hz)	10
Maximum Travel (mm)	12
Excitation rate (1/sec)	$0.1 - 1.33$
Return Stroke speed (mm/s)	3
Pretension (N)	5
Number of cycles per test	10

Displacement-controlled tests were performed, with a 500N Load cell, a forward stroke (Tensile loading) of 12 mm, at

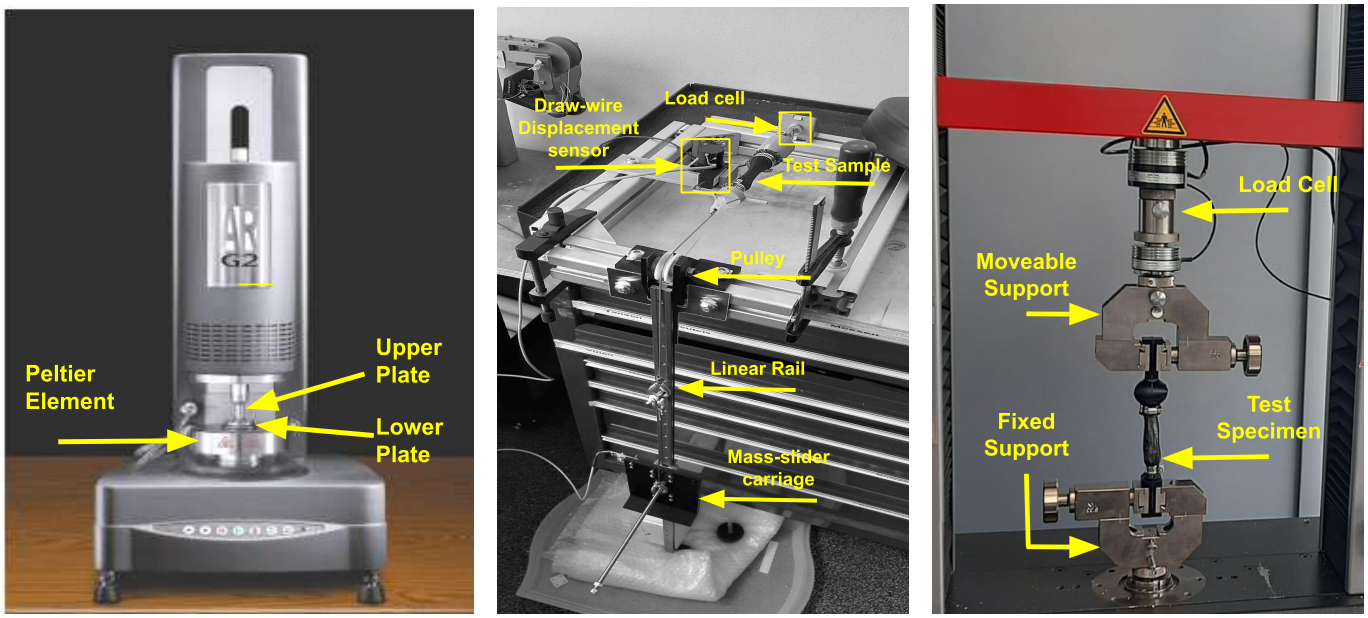

(a) (b) (c)

Fig. 8: Experimental Test Setup: (a): Parallel Plate Rheometer. (b): Constant Force Tests. (c): Cyclic Tests.

shear rates varying from 1.2 to 16 mm/s, and a return stroke of a constant 3 mm/s. The forward stroke length was set so that the damper was engaged effectively without reaching the end of its allowable motion. The shear rates [1] were selected to begin at 0.1 Hz and reach the maximum rate that the machine could perform 1.33 Hz, given the forward stroke travel.
The return stroke was kept constant to maintain uniformity amongst all the trials, as the more viscous samples required time to fall back into the primary chamber of the pouch. The damper was set with a pretension of 5 N, to prevent any slack at the beginning of the test. The tests were repeated for the five fluid samples, with 10 cycles for each shear rate.

IV. Results

A. Specimen Data

Five specimens (Table. III) were tested to establish the behavior of the damper. Three trials were performed for the viscosity measurements as it is regarded as a qualitative test to validate the Newtonian and Non-Newtonian nature of the samples. Five trials were performed for the loading tests to ensure the reliability of the data. The pouches were weighed with the fluid after fully assembling each prototype.

B. Viscosity Measurements

Fig. 9 shows the viscosity and shear stress behavior across varying shear rates. We observe that for Newtonian fluid samples: water and SAE 50 oil, the viscosity remains constant, with a value close to 1 cP and 456 cP respectively, which is in accordance with existing knowledge. Whereas, for the cornstarch slurry samples, we observe both the viscosity and shear stress increasing non-linearly with the shear rate. This behavior is indicative of STF or dilatant fluids. The best of three trials is plotted for each of the fluids.

[1]Shear rate (1/sec) in this article is regarded as analogous to excitation frequency (Hz)

C. Constant Force Response

Fig. 10 shows the displacement-time behavior for the static and impact tests. The displacement is represented by the elongation normalized by the maximum elongation, for better comparison of the samples. The static loading test with a 4.5 Kg load is displayed for comparison with the impact tests. Fig.12 illustrates the time taken reach to steady state elongation for each sample for the constant force loading test. Evidently, no significant change in the time taken is noted between the static loading tests. The plot displays the mean of five trials, with error bars for the range of measurements of the trials.
The velocity at the time of impact can be calculated with the following equation, ignoring the effect of air resistance and friction losses:

$$V = \sqrt{2 * g * H} \tag{3}$$

With g, the acceleration due to gravity is taken as 9.81ms^{-2}, and the height as 0.04m, the velocity at the time of impact comes to be 0.886ms^{-1}. The kinetic energy imparted to the damper on impact is 1.57J.
An additional delay of around 1.1 seconds is observed in the cornstarch slurry (53.3%) sample in the impact load case when compared to static loading.

D. Cycling Load Response

The hysteresis curves generated for each sample across the range of shear rates are presented in Fig. 11. The samples had an initial pretension of 5N to prevent any slack in the

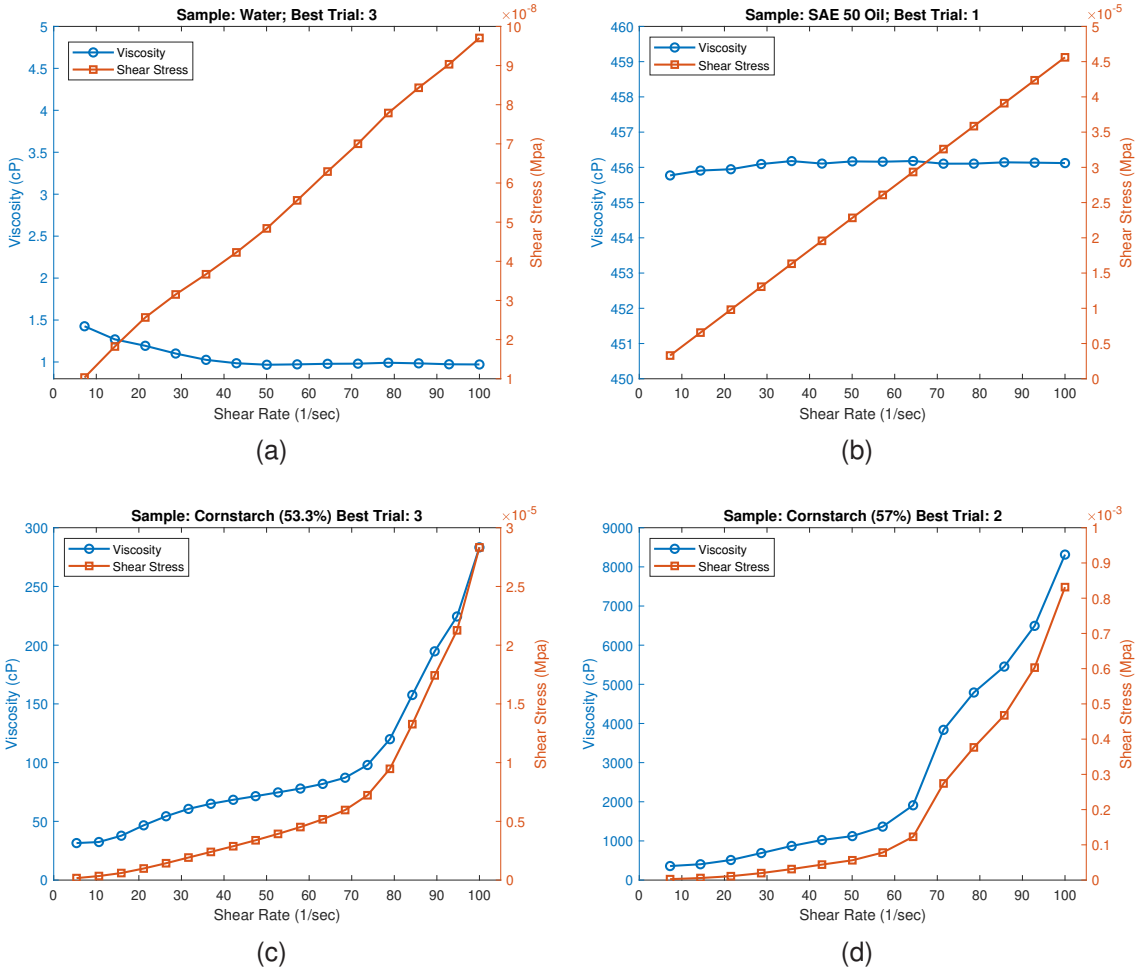

Fig. 9: Viscosity and Shear stress of fluids across different shear rates: Newtonian fluids (a) and (b) show a linear shear stress - shear rate relationship and constant viscosity. Non-Newtonian Fluids (Dilatants) (c) Cornstarch Slurry (53.3% wt cornstarch). (d) Thick Cornstarch Slurry (57% wt cornstarch) demonstrate a non-linear relationship between shear stress, viscosity and shear rate.

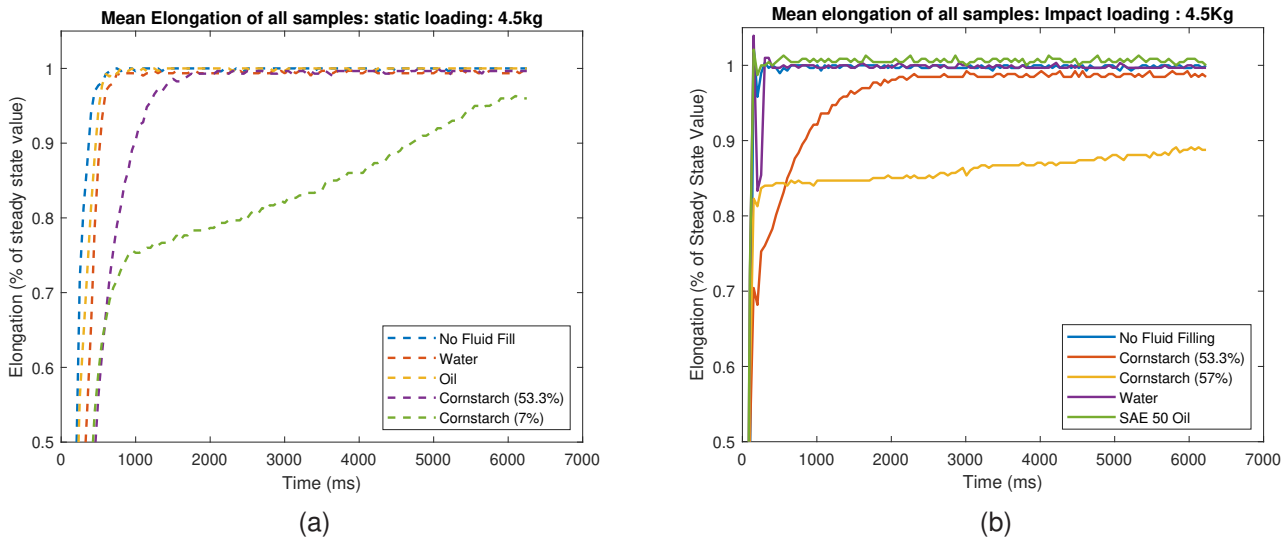

Fig. 10: Comparison of elongation vs. time of the viscous damper for (a) Static Load. (b) Impact Load of 4.5 kg each. The STF fluid samples delay the maximum elongation time in the impact case when compared to static loading.

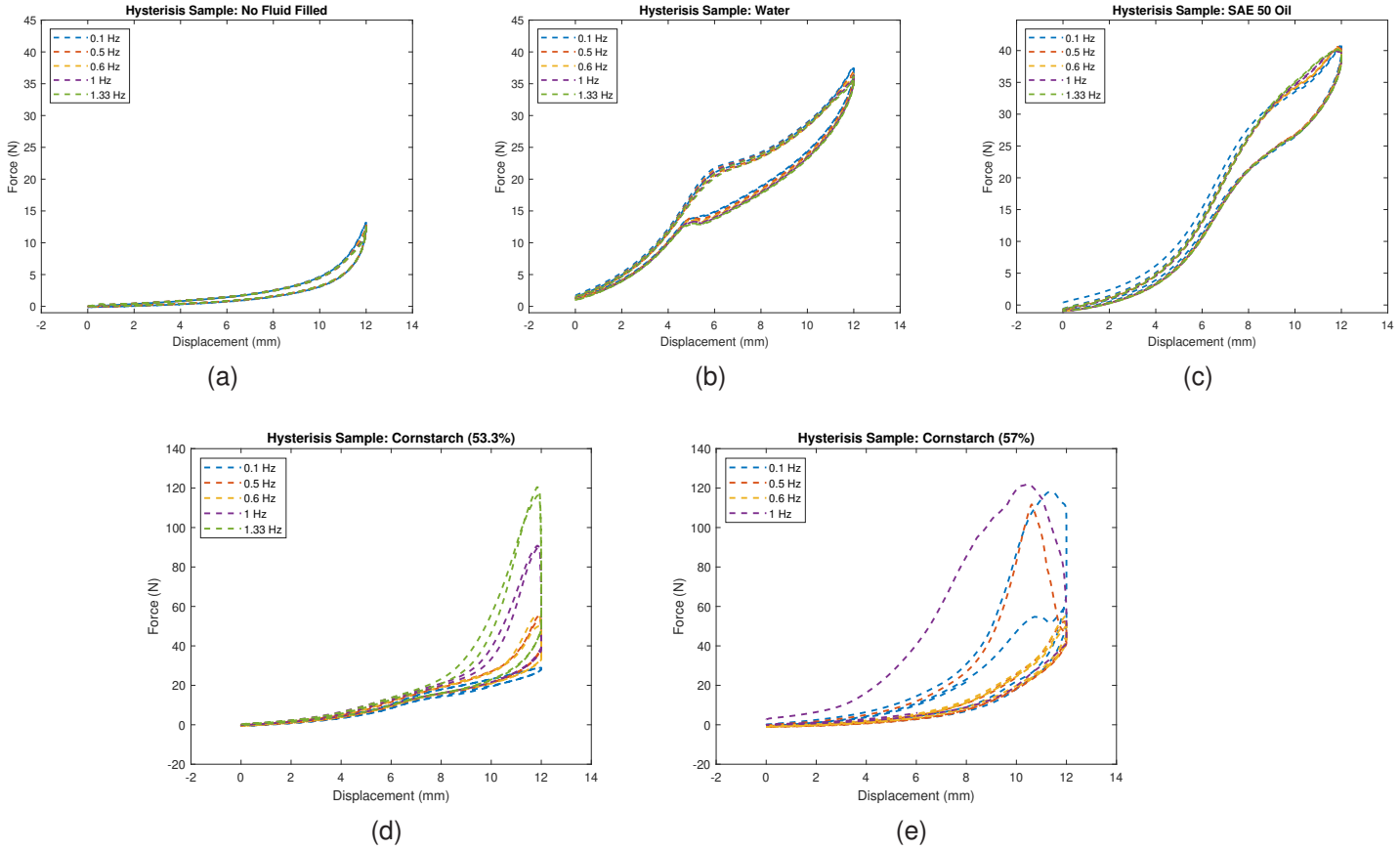

Fig. 11: Hysteresis curves of the damper with at various frequencies for (a) No Fluid Fill. (b) Water. (c) SAE 50 Oil. (d) Cornstarch Slurry. (e) Thick Cornstarch Slurry. The STF samples show an increase in dissipated energy (area under the hysteresis curve) with an increase in frequency. This demonstrates shear rate adaptive behavior.

damper before the test. The total travel was limited to 12mm to prevent the endpoint stiffness of the damper from affecting data, or even failure of the damper due to overloading.

The area under the hysteresis curve gives the total energy dissipated over the 10 cycles of the trial The Newtonian samples show constant energy dissipation, while the cornstarch sample increases with excitation frequency (Fig13). The thick cornstarch slurry could not return fully to the primary chamber during the tests leading to unreliable data. Thus it was not included in the analysis.

The thick cornstarch slurry sample encountered failure at frequencies beyond 1 Hz. This could be due to excess stiffening of the fluid under load. Failure was observed at the clamping, with the braided mesh coming lose.

V. Discussion

A. Experimental Analysis

1) Viscosity Measurements: The plots of the rheology tests for Newtonian fluids clearly show a constant viscosity value, and a linear relationship between shear stress and strain rate, whereas a non-linear increase in both viscosity and shear stress is observed for the cornstarch slurry samples. This behavior is a characteristic of dilatants.

Three trials were conducted for each fluid, but there was a significant deviation in the magnitude of viscosity in the STF samples. This deviation could be due to inconsistencies in the sample concentration, air bubbles or even overfilling of the fluid samples [28]. Therefore, this data was only considered as qualitative evidence for dilatant behavior.

2) Constant Force Loading: It is observed from Fig. 12 that the time taken for complete elongation decreases in the impact loading case when compared to the static tests, except for the STF samples. The cornstarch slurry shows an average of 1.1 second additional delay in stretch time for impact loading. The thicker cornstarch slurry offers considerable delay in both static $(5.7-7.3)$ seconds, and impact (12.5)seconds, and is not shown in the plot for better visualization of the other samples. These plots demonstrate adaptive behavior to slow and sudden loading, in the dampers with STF. This property of the damper can be exploited to develop passive, flexible, and lightweight impact-absorbing structures and stabilizing mechanisms.

The thick cornstarch slurry sample was deemed to be too viscous for the current setup. We infer that the response of the damper can be tuned by modulating the concentration of the STF samples.

3) Cyclic Loading: The hysteresis curves in Fig. 11 show a constant energy dissipation for the Newtonian fluid specimens, whereas, in the cornstarch slurry sample, a marked increase in

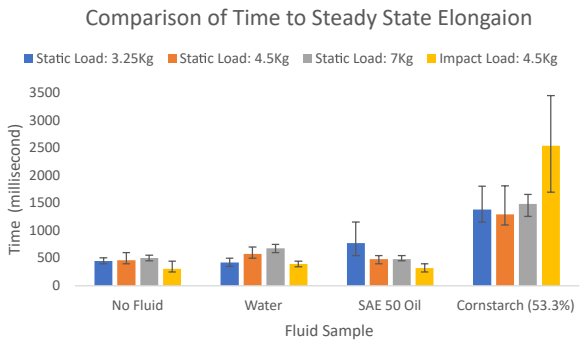

Fig. 12: Comparison of the mean time taken to steady state elongation amongst the various samples. In the STF sample, instead of having a smaller elongation time in impact loading, there is a delay, due to the increased damping from the STF effect.

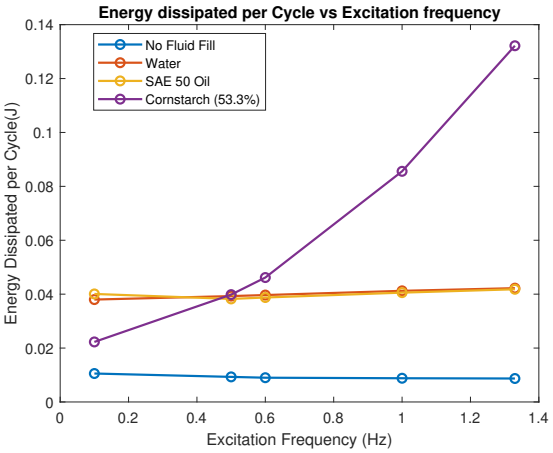

Fig. 13: Comparison of the energy dissipated per cycle across different Frequencies, Newtonian samples show constant damping, while the STF energy dissipation increases with shear rate.

the energy dissipation with excitation frequency is noted. This non-linear increase can be visualized in Fig. 13. The increased resistance in the damper is attributed to the shear thickening effect of the cornstarch slurry at higher shear rates. All fluid samples show increased energy dissipation when compared to the trials with no fluid-filled.

The Newtonian samples show no difference in response to varying shear rates. This can be because the diameter of the constriction is too large for the viscous effects of Newtonian fluids to play a role, and the damping stems from the energy required to overcome the elastic stiffness of the balloon and pump the fluid into the relief chamber.

The thick cornstarch slurry showed very high resistance to the first cycle, but then very low energy dissipation in subsequent cycles. It was observed that the high viscosity of the slurry prevented it from returning to the primary chamber in time for the subsequent cycles. Thus the specimen was considered a failure and excluded from the comparisons.

In all samples, the initial phase of the force-displacement curve shows very minimal damping. Since balloons demonstrate bistable behavior, the initial motion is of viscoelastic stretching (similar to the empty pouch case) till sufficient pressure is applied in the fluid to cause the sudden expansion of the relief chamber, allowing fluid to then be pumped into it. This hypothesis is corroborated by the visible kink (sudden change in slope) in the hysteresis plot of the water specimen Fig. 11b.

B. Equivalent Linear Model

As a preliminary step to characterizing the behavior of the flexible damper, the force-displacement behavior of the damper is approximated to that of a linear viscous damper [29].

$$F_{damper} = K_{eff}x + C_{eff}\dot{x} \tag{4}$$

The effective linear elastic stiffness and damping coefficient of the damper are calculated with the following equations [29], [30]:

$$K_{eff} = \frac{F_{max} - F_{min}}{\delta_{max} - \delta_{min}} \tag{5}$$

where F_{max}, F_{min} and δ_{max} δ_{min} are the maximum and minimum force and displacements respectively. K_{eff} is the slope of the peak-to-peak values of the force-displacement curve.

$$C_{eff} = \frac{E_{dissipated}}{\pi\omega A^2} \tag{6}$$

Where C_{eff} is the equivalent damping coefficient of a viscous damper, $E_{dissipated}$ is the energy dissipated per cycle at a given frequency, ω is the excitation frequency expressed as angular frequency, and A is the total amplitude of displacement. The

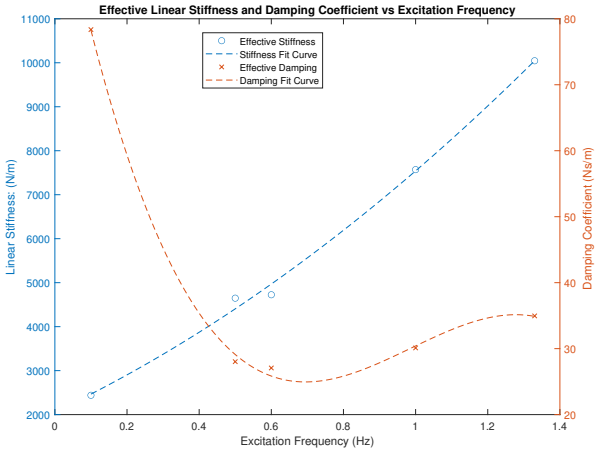

Fig. 14: Variation of Effective Linear Stiffness and Damping Coefficients with Excitation frequency: The stiffness and damping are approximated by a second-order polynomial (R^2 : 0.9966) and a third-order polynomial (R^2 : 0.9985) respectively.

variation of the effective linear stiffness and damping coefficients are illustrated in Fig. 14. It is observed that the Shear-Thickening Effect results in increased resistance to external forces, and subsequent increase in the perceived stiffness.

The effective damping coefficient decreases sharply in the beginning and then gradually increases with frequency. This could be due to the low frequency ($0.1Hz$) of the first trial, inflating the approximated value from Eq.6. Such a decrease in the effective damping in the shear thickening region is also observed in similar studies with conventional dampers [11], [29]. The linear effective model proved ineffective in replicating the provided cyclic curves, showing a tenfold decrease in energy dissipation. This discrepancy underscores the need for more rigorous exploration through nonlinear models in forthcoming investigations

C. Performance Analysis

The final prototype is a functional proof of concept shear-rate adaptive viscous damper employing STF as working fluids. The proposed design is evaluated against the initial design specifications to check whether it addresses the questions raised at the beginning of this study. The developed solution effectively addresses almost all the initial requirements of the design. The complexity arose due to the use of metal clamps, and split handles for the ease of assembly. Future designs must focus on incorporating these elements with fewer units. The braided mesh dimensions govern the displacement and strain in the final prototype, whereas the properties of the balloon determine the amount of energy absorbed and the speed at which the fluid is pumped back to the primary chamber. The volume of the hollow cavity functions as an additional end stop to the damper as it limits the amount of fluid that can be pumped by the mesh.

TABLE VII: Performance Analysis of the Final Prototype Against Design Requirements

Design Criteria	Desired Metric	Achieved Metric
Power	0 W (Passive)	0W (Passive Device)
Flexible	10 % Longitudinal Strain	10% Longitudinal strain
	$\geq$ 45 °bend	180 °bend
Dimensions((lbh)	20x10x10 cm	20x5x5 cm
Total Displacement	$\sim$ 1cm	$\sim$ 2cm
Complexity	$<$ 5 parts	9 parts
Adaptability	$\geq$ 1 sec	$\sim$ 1.1 sec

When compared with a similar "ligament "damper in [19], the energy dissipated per cycle ($\sim$ 0.4J for 30mm displacement) is comparable to the damper proposed in this study($\sim$ 0.19J for 14mm displacement) for the same frequency. The proposed damper demonstrates a larger force but has a smaller displacement. The proposed damper is also much heavier (74.3 g) in comparison to the ligament damper (4g) and thus has close to $\sim$ 20 times lower value of specific work. The clamps and rigid ends need to be redesigned to reduce the mass of the system. However, it is important to note that the proposed damper can provide damping even with Newtonian fluids, whereas the ligament damper can only provide damping with STF.

D. Limitations of This Study

This article provides insights into a new method of flexible viscous damping, however, the working principle is only verified with cornstarch as a representative of STF. Cornstarch slurry has a very low shelf life and begins to decompose within 24 hours of mixing, and therefore is not a viable long-term working fluid. The damper behavior with other STF working fluids, like a solution of Polyethylene glycol (PEG200) and silica Nanoparticles, must be experimentally studied.
During the experiments, it was observed that the total length of stretch in the damper is highly sensitive to the length of the mesh between the clamps. This led to variability in the total elongation lengths among specimens, and ultimately, data had to be normalized for comparison. The effect of this variation in length on the time taken for full stretch and energy dissipated was not studied in this work.
The prototype still incorporates rigid elements in the clamping and hollow chamber units which increase the damper mass. To realize a fully flexible or soft damper, further work is required to redesign these ends.
This study also did not look into the behavior of the damper over long cycles. Understanding the nature of fatigue, and creep on the viscoelastic elements and the STF of the damper is important to the ensure reliability of such a device time constraints

E. Future Work

The prototype developed in this study is a proof of concept flexible viscous damper. It's capacity for passive shear-rate based variable energy dissipation through the use of STF working fluids was experimentally demonstrated. However, the design needs to be refined further to make it a viable product. The following are some of the areas that could be improved upon:

- *Design Optimization:*The size of the balloons, the size of the mesh, the diameter of the constriction, and the relief volume can be tuned to improve performance.
- *Material Optimization:*The material composition of the elastic pouch (balloon) and the mesh can be investigated to improve durability and reduce the elastic stiffness, which is beneficial to a passive damper.
- *Working Fluid Study:* Cornstarch is not a viable long-term working fluid. The damper has to be tested with industrial STF like a suspension of silica nanoparticles in Polyethylene glycol 200.
- *Modelling and characterization:* Developing rigorous non-linear models will lead to a better understanding of the behavior and inform design optimization choices. The long-term behavior and effect of temperature change on damper functioning must also be studied to ascertain its viability.
- *Assembly:* Finally, the performance of the dampers can be compounded by stacking them in series or parallel arrangements, and the ends of the damper can be integrated into the body of a larger system it is part of, making it more compact.

VI. Conclusion

This article describes the design, prototyping, and experimental evaluation of a novel flexible, shear-rate adaptive

viscous damper capable of passive energy dissipation. The proposed design comprises an elastic pouch containing shear thickening fluid as the working fluid, clamped between a handle and a hollow expansion chamber. The body of the pouch is encased within a braided mesh sleeve.

The damper is designed to operate and dissipate energy under tensile loading while being highly compliant to compressive and lateral loads. The damper achieves this through the braided mesh, which transfers axial tension to the pouch and the contained fluid as radial pressure. The pressure forces the fluid through a constriction into the portion of the elastic pouch contained within the hollow chamber, where it can expand freely.

A prototype was developed and tested with static, impact, and cyclic loading. The damper is 15cm in length and can stretch 2cm longitudinally. It can withstand forces of 120N in tension and delay deformation under impact loading by 1.1 seconds when compared to static loading. The cyclic loading tests show an increase in energy dissipation from 0.22J at 0.1Hz to 0.132J at 1.33Hz, verifying the shear-rate adaptive response of the damper when using dilatant working fluids.

While the study developed a working proof-of-concept flexible viscous damper and successfully demonstrated shear-rate adaptive response, the specific energy dissipated by the damper was much smaller (20x) in comparison to a similar proposal and requires further development to establish its viability as an alternative. Further improvements are necessary to develop the idea to completion. The article discusses potential areas of future research, such as (a) design and material optimization, (b) development of accurate models to simulate the damper's behavior, and (c) understanding the damper's behavior with temperature and life-cycle tests.

The idea proposed in this study is an attempt to address the lack of flexible dampers, that can potentially be implemented in assistive technologies, harnesses, and soft robotics. With the development of soft actuators and soft sensors, similar ideas can be incorporated to develop a new class of soft, adaptive viscous dampers.

REFERENCES

[1] A. Naseri, M. M. Moghaddam, M. Grimmer, and M. A. Sharbafi, "Passive hydraulic prosthetic foot to improve the push-off during walking," *Mechanism and Machine Theory*, vol. 172, p. 104777, 2022.

[2] A. Naseri, M. Mohammadi Moghaddam, M. Gharini, and M. Ahmad Sharbafi, "A novel adjustable damper design for a hybrid passive ankle prosthesis," in *actuators*, vol. 9, no. 3. MDPI, 2020, p. 74.

[3] A. Kalyan Raj and C. Padmanabhan, "A new passive non-linear damper for automobiles," *Proceedings of the Institution of Mechanical Engineers, Part D: Journal of Automobile Engineering*, vol. 223, no. 11, pp. 1435–1443, 2009.

[4] M. Symans and M. Constantinou, "Passive fluid viscous damping systems for seismic energy dissipation," *ISET Journal of Earthquake Technology*, vol. 35, no. 4, pp. 185–206, 1998.

[5] A. Mo, F. Izzi, D. F. Haeufle, and A. Badri-Spröwitz, "Effective viscous damping enables morphological computation in legged locomotion," *Frontiers in Robotics and AI*, vol. 7, p. 110, 2020.

[6] W.-H. Lin and A. K. Chopra, "Earthquake response of elastic sdf systems with non-linear fluid viscous dampers," *Earthquake engineering & structural dynamics*, vol. 31, no. 9, pp. 1623–1642, 2002.

[7] L. P. Davis, D. Cunningham, A. S. Bicos, and M. Enright, "Adaptable passive viscous damper: an adaptable d-struttm," in *Smart Structures and Materials 1994: Passive Damping*, vol. 2193. SPIE, 1994, pp. 47–58.

[8] M. S. Orendurff, A. D. Segal, G. K. Klute, M. L. McDowell *et al.*, "Gait efficiency using the c-leg," *Journal of rehabilitation research and development*, vol. 43, no. 2, p. 239, 2006.

[9] F. Imaduddin, S. A. Mazlan, and H. Zamzuri, "A design and modelling review of rotary magnetorheological damper," *Materials & Design*, vol. 51, pp. 575–591, 2013.

[10] J. Li, D. Jin, X. Zhang, J. Zhang, and W. A. Gruver, "An electrorheological fluid damper for robots," in *Proceedings of 1995 IEEE International Conference on Robotics and Automation*, vol. 3. IEEE, 1995, pp. 2631–2636.

[11] H. Zhou, L. Yan, W. Jiang, S. Xuan, and X. Gong, "Shear thickening fluid–based energy-free damper: design and dynamic characteristics," *Journal of Intelligent Material Systems and Structures*, vol. 27, no. 2, pp. 208–220, 2016.

[12] A. Syrakos, Y. Dimakopoulos, and J. Tsamopoulos, "Theoretical study of the flow in a fluid damper containing high viscosity silicone oil: Effects of shear-thinning and viscoelasticity," *Physics of Fluids*, vol. 30, no. 3, 2018.

[13] O. Yasa, Y. Toshimitsu, M. Y. Michelis, L. S. Jones, M. Filippi, T. Buchner, and R. K. Katzschmann, "An overview of soft robotics," *Annual Review of Control, Robotics, and Autonomous Systems*, vol. 6, pp. 1–29, 2023.

[14] ——, "An overview of soft robotics," *Annual Review of Control, Robotics, and Autonomous Systems*, vol. 6, pp. 1–29, 2023.

[15] J. Wang, D. Gao, and P. S. Lee, "Recent progress in artificial muscles for interactive soft robotics," *Advanced Materials*, vol. 33, no. 19, p. 2003088, 2021.

[16] D. Accoto, N. L. Tagliamonte, G. Carpino, F. Sergi, M. Di Palo, and E. Guglielmelli, "pvej: A modular passive viscoelastic joint for assistive wearable robots," in *2012 IEEE International Conference on Robotics and Automation*. IEEE, 2012, pp. 3361–3366.

[17] U. Mawkhlieng and A. Majumdar, "Soft body armour," *Textile Progress*, vol. 51, no. 2, pp. 139–224, 2019.

[18] M. D. Titirla, "A state-of-the-art review of passive energy dissipation systems in steel braces," *Buildings*, vol. 13, no. 4, p. 851, 2023.

[19] P. T. Nenno and E. D. Wetzel, "Design and properties of a rate-dependent dynamic ligament containing shear thickening fluid," *Smart materials and structures*, vol. 23, no. 12, p. 125019, 2014.

[20] F. White, "Chapter 6: Viscous flow in ducts," *Fluid Mechanics*, pp. 314–339, 2011.

[21] B. E. Rapp, *Microfluidics: modeling, mechanics and mathematics*. Elsevier, 2022.

[22] M. Wei, K. Lin, Q. Guo, and H. Sun, "Characterization and performance analysis of a shear thickening fluid damper," *Measurement and Control*, vol. 52, no. 1-2, pp. 72–80, 2019.

[23] S. Park, K. Mondal, R. M. Treadway III, V. Kumar, S. Ma, J. D. Holbery, and M. D. Dickey, "Silicones for stretchable and durable soft devices: Beyond sylgard-184," *ACS applied materials & interfaces*, vol. 10, no. 13, pp. 11 261–11 268, 2018.

[24] S. Muslov, D. Polyakov, A. Lotkov, A. Stepanov, and S. Arutyunov, "Measurement and calculation of mechanical properties of silicone rubber," *Russian Physics Journal*, vol. 63, pp. 1525–1529, 2021.

[25] Y. Luo, N. Zhao, Y. Shen, and K. J. Kim, "Scissor mechanisms enabled compliant modular earthworm-like robot: Segmental muscle-mimetic design, prototyping and locomotion performance validation," in *2016 IEEE International Conference on Robotics and Biomimetics (ROBIO)*. IEEE, 2016, pp. 2020–2025.

[26] S. Kurumaya, H. Nabae, G. Endo, and K. Suzumori, "Design of thin mckibben muscle and multifilament structure," *Sensors and Actuators A: Physical*, vol. 261, pp. 66–74, 2017.

[27] G. Gregov, T. Ploh, and E. Kamenar, "Design, development and experimental assessment of a cost-effective bellow pneumatic actuator," in *Actuators*, vol. 11, no. 6. MDPI, 2022, p. 170.

[28] R. Cardinaels, N. K. Reddy, and C. Clasen, "Quantifying the errors due to overfilling for newtonian fluids in rotational rheometry," *Rheologica Acta*, vol. 58, pp. 525–538, 2019.

[29] X. Zhang, W. Li, and X. Gong, "The rheology of shear thickening fluid (stf) and the dynamic performance of an stf-filled damper," *Smart Materials and Structures*, vol. 17, no. 3, p. 035027, 2008.

[30] W. Li, G. Yao, G. Chen, S. Yeo, and F. Yap, "Testing and steady state modeling of a linear mr damper under sinusoidal loading," *Smart Materials and Structures*, vol. 9, no. 1, p. 95, 2000.

4

Reflection

4.1. Project Plan

This thesis project was my first experience in conducting long-term independent research. I developed a project plan to ensure a structured progression of my work, as illustrated in Fig. 4.1. This plan is formulated based on the basic product design process [42]. It incorporates an iterative style of design that takes advantage of rapid prototyping, facilitated by 3D printing technology and injection molding available at the department. This allowed me to quickly make models and physically check if the designs could address the issue at hand.

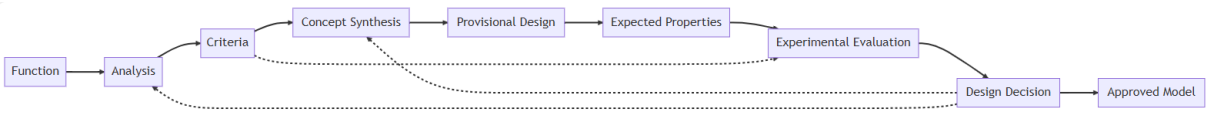

Figure 4.1: Basic Design cycle, with iterative structure. Adapted from: [42]

A project timeline was framed around this plan: Fig. 4.2. This timeline served as the road-map for the thesis project, providing direction to my work. Initially, the plan appeared well-structured and attainable, with clear milestones and deadlines. However, as is common with research, the timeline had to be adjusted and extended due to unforeseen challenges and complexities encountered during the research process. Delays occurred in selecting appropriate designs, developing functional prototypes, and placing orders for components. The most significant hurdle I faced arose during the detailed design phase, where replicating the observed behavior from the initial prototype became increasingly difficult. All attempted modifications failed to demonstrate the expected behavior. The delays are visualized as the orange bars in the Gantt Chart shown in Fig. 4.2. At this juncture, the extensive project planning I had undertaken and the flexibility to adjust the timeline were paramount in adapting to the uncertainty, which alleviated the stress of not achieving expected results. This adaptability allowed the project to conclude as originally anticipated.

4.2. Personal Reflection

This thesis project involved extensive research into energy dissipation, viscous damping, Shear-Thickening effect, and the behavior of confined fluids in flexible containers. In the beginning, I had a conceptual understanding of these topics and relied on my experience with product design to gain traction in the project. Over time, I deepened my understanding of these concepts through literature and practical experimentation with prototypes. Recognizing the complexity of the concept, I opted against time-consuming simulations which would ultimately result in approximate solutions. Instead, I employed rapid prototyping, leveraging the 3D printing and silicone molding facilities available in the lab to physically verify the behavior. I thoroughly enjoyed this hands-on approach to design. Due to delays in obtaining the safety permits for the desired working fluids, I had to compromise and proceed with cornstarch slurry as a substitute to demonstrate Shear Thickening behavior. While this is sufficient for demonstrating the working of the prototype, it is not viable for long-term application as it begins to decompose within 24Hr of mixing with water. Albeit far from a finished product, I successfully demonstrated a functional proof of concept. Further development is necessary to make this idea a viable product, including design optimization, rigorous testing with appropriate working fluids, and assessing the prototype's long-term behavior.

This project gave me a deeper understanding of how I work. I recognized the need to balance my inclination for swift action and design by taking a step back to critically assess the decisions I make. Additionally, I acknowledged the importance of allowing flexibility in project planning, as uncertainties are inherent in any undertaking. Collaborative projects depend not only on my schedule but also on others, reinforcing the need for adaptability. I found myself under pressure to meet the deadlines I had set and realized I needed to allow more time to account for delays and hurdles.

This endeavor pushed my problem-solving abilities to the limit, demanding creative thinking to manipulate the damper's design to achieve the desired behavior. Many of the problems that came up, were uncharted territory and required me to go back to the drawing board to come up with new solutions. Establishing reliable tests presented challenges, emphasizing the significance of experimental rigor, precise variable control, accurate measurements, and data interpretation. I have gained experience in using a variety of testing equipment, and in presenting large sets of data in a concise and coherent manner.

Overall, this project has spurred significant growth in my research capabilities, enabling me to identify both weaknesses and strengths in my approach. Armed with this newfound understanding, I am better equipped to make adjustments in future endeavors, striving for continuous improvement.

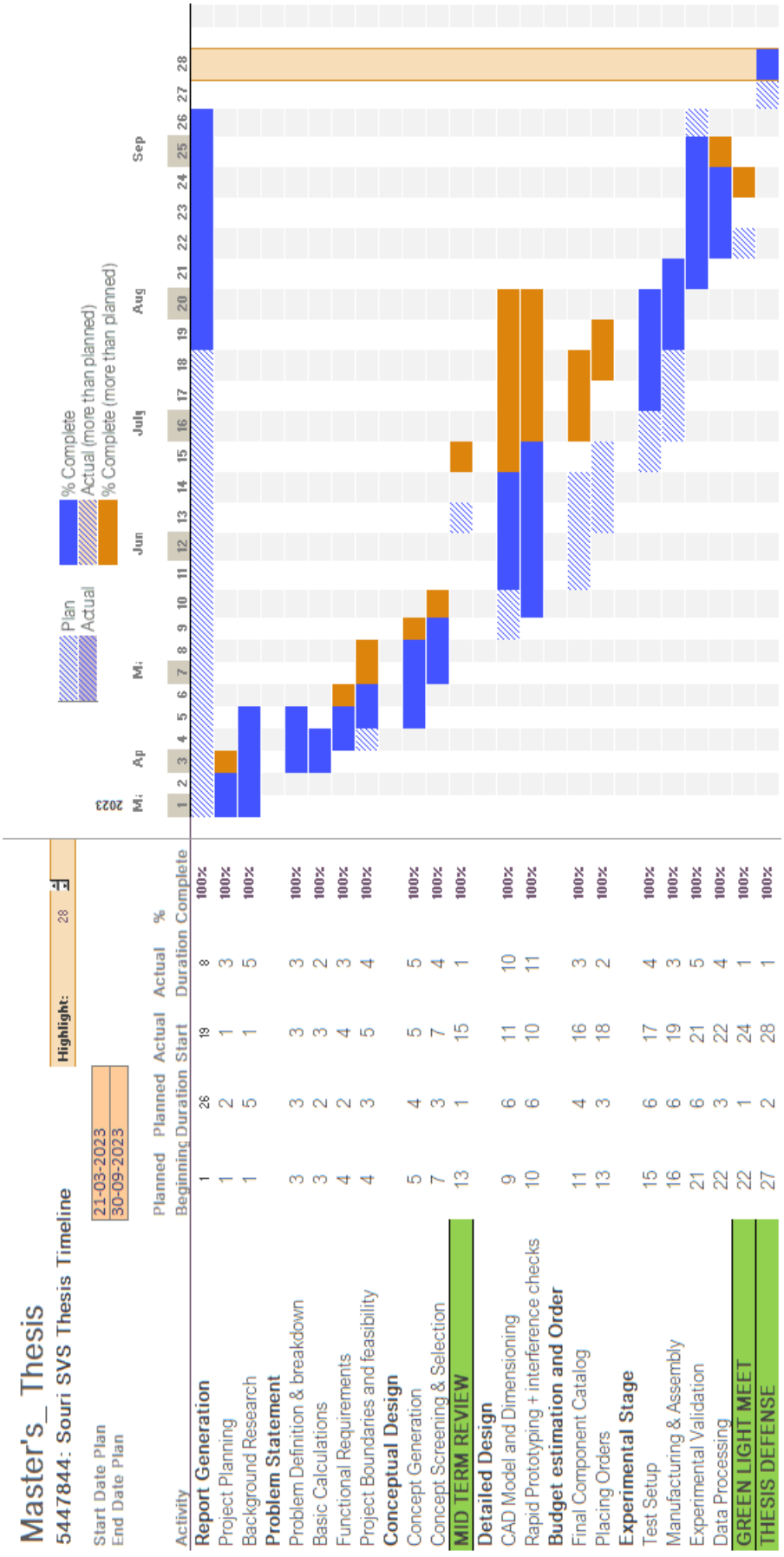

Figure 4.2: Gantt Chart showing the Project Timeline and Allocated Timw

5

Conclusion

This report marks the culmination of a master's thesis project that spanned 6 months, from March 2023 to September 2023. The thesis began with the goal of developing a novel soft damper for assistive devices. Initially, the project aimed at developing a potential implantable assistive device, however on conducting a feasibility study, this idea was deemed to be beyond the framework of the current undertaking. The scope of the project was revised to develop a proof of concept passive, soft damping system.

The primary objective of this study was to develop a functional prototype and experimentally validate its dissipative capabilities. Chapter 1 provides an overview of the existing energy dissipation mechanisms in assistive devices and establishes the need for a flexible passive damper to address the issues faced by them. Chapter 2 outlines the working principles of various energy dissipation mechanisms. The listed mechanisms are evaluated against selection criteria to determine the most suitable mode of energy dissipation for developing a flexible passive damper. It is concluded that viscous damping is the best choice.

Subsequently, Chapter 3 is a scientific article on the design, prototyping, and experimental validation of a flexible, passive viscous damper. The article covers the state of the art of viscous dampers, the conceptual designs of a flexible analog to viscous dampers, and the detailed design and prototyping of a proof-of-concept flexible viscous damper. The article also elaborates on the experimental methods implemented to test the prototype's behavior and the obtained results. Finally, Chapter 4 presents the project timeline and comments on the author's technical and personal growth over the course of the Masters BioMechanical Design course at TU Delft.

A successful proof-of-concept flexible viscous damper was demonstrated through the use of braided mesh sleeves to apply loads onto a flexible pouch containing working fluids. The mesh squeezes fluid contained within the pouch through a narrow constriction, into a relief chamber. Energy is dissipated to overcome viscous forces and pump the fluid through the constriction. Furthermore, the prototype demonstrated shear rate adaptive behavior through the use of cornstarch slurry (A shear-thickening fluid) as the working fluid.

While a proof of concept is established, considerable work is required to realize a market-ready device. Design optimization of the constriction and relief chamber; investigation of the balloon and mesh properties; modeling and numerical characterization of the behavior; study of long-term behavior; and rigorous testing with other working fluids are some of the suggested research areas that could be pursued to improve the proposed idea.

This thesis represents the inception of a novel class of soft viscous dampers with potential applications in assistive devices, seatbelts, safety harnesses, and ultimately as flexible shock absorbers in various domains.

References

[1] World Health Organization. "Global report on assistive technology". In: (2022).

[2] Disabled World. *Disability statistics: Information, charts, graphs and tables*. June 2023. url: https://www.disabled-world.com/disability/statistics/.

[3] Johan Borg et al. "Assistive technology in developing countries: a review from the perspective of the Convention on the Rights of Persons with Disabilities". In: *Prosthetics and orthotics international* 35.1 (2011), pp. 20–29.

[4] Jon Pearlman et al. "Lower-limb prostheses and wheelchairs in low-income countries [An Overview]". In: *IEEE Engineering in Medicine and Biology Magazine* 27.2 (2008), pp. 12–22. doi: 10.1109/EMB.2007.907372.

[5] CH Yeow. "Hamstrings and quadriceps muscle contributions to energy generation and dissipation at the knee joint during stance, swing and flight phases of level running". In: *The Knee* 20.2 (2013), pp. 100–105.

[6] Deborah Hebling Spinoso et al. "Quadriceps muscle weakness influences the gait pattern in women with knee osteoarthritis". In: *Advances in Rheumatology* 58 (2019).

[7] Parth Vyas et al. "Management options for extensor mechanism discontinuity in patients with total knee arthroplasty". In: *Cureus* 12.7 (2020).

[8] Joseph M Hart et al. "Quadriceps activation following knee injuries: a systematic review". In: *Journal of athletic training* 45.1 (2010), pp. 87–97.

[9] Sarah F Tyson et al. "Balance disability after stroke". In: *Physical therapy* 86.1 (2006), pp. 30–38.

[10] Ase Brandt et al. "Older people's use of powered wheelchairs for activity and participation". In: *Journal of rehabilitation medicine* 36.2 (2004), pp. 70–77.

[11] Michelle M Lusardi et al. *Orthotics and prosthetics in rehabilitation-e-book*. Elsevier Health Sciences, 2012.

[12] Eiji Kobayashi et al. "Efficacy of Knee–Ankle–Foot Orthosis on Functional Mobility and Activities of Daily Living in Patients with Stroke: A Systematic Review of Case Reports". In: *Journal of Rehabilitation Medicine* 54 (2022).

[13] TS Anand et al. "A method for performance comparison of polycentric knees and its application to the design of a knee for developing countries". In: *Prosthetics and Orthotics International* 41.4 (2017), pp. 402–411.

[14] John W Michael. "Modern prosthetic knee mechanisms". In: *Clinical Orthopaedics and Related Research®* 361 (1999), pp. 39–47.

[15] Wei Liang et al. "Mechanisms and component design of prosthetic knees: A review from a biomechanical function perspective". In: *Frontiers in Bioengineering and Biotechnology* 10 (2022), p. 950110.

[16] Hans A Mauch et al. "Stance control for above-knee artificial legs-design considerations in the SNS knee". In: *Bulletin of Prosthetics Research* 10.10 (1968), pp. 61–72.

[17] Agustín Barrera Sánchez et al. "State of the art review of active and passive knee orthoses". In: *Machines* 10.10 (2022), p. 865.

[18] Jorge Curiel Godoy et al. "Nonanthropomorphic exoskeleton with legs based on eight-bar linkages". In: *International Journal of Advanced Robotic Systems* 15.1 (2018), p. 1729881418755770.

[19] Ava D Segal et al. "Kinematic and kinetic comparisons of transfemoral amputee gait using C-Leg and Mauch SNS prosthetic knees." In: *Journal of Rehabilitation Research & Development* 43.7 (2006).

[20] Julius Thiele et al. "Designs and performance of three new microprocessor-controlled knee joints". In: *Biomedical Engineering/Biomedizinische Technik* 64.1 (2019), pp. 119–126.

[21] Malte Bellmann et al. In: *Biomedical Engineering / Biomedizinische Technik* 64.4 (2019), pp. 407–420. doi: doi:10.1515/bmt-2018-0026. url: https://doi.org/10.1515/bmt-2018-0026.

[22] Jung-Hwan Kim et al. "Therapeutic experience on stance control knee-ankle-foot orthosis with electromagnetically controlled knee joint system in poliomyelitis". In: *Annals of Rehabilitation Medicine* 40.2 (2016), p. 356.

[23] W. van Dijk et al. "Exobuddy - A Non-Anthropomorphic Quasi-Passive Exoskeleton for Load Carrying Assistance". In: *2018 7th IEEE International Conference on Biomedical Robotics and Biomechatronics (Biorob)*. 2018, pp. 336–341. doi: 10.1109/BIOROB.2018.8487794.

[24] Frank Sup et al. "Preliminary evaluations of a self-contained anthropomorphic transfemoral prosthesis". In: *IEEE/ASME Transactions on mechatronics* 14.6 (2009), pp. 667–676.

[25] Blair Hu et al. "Fusion of bilateral lower-limb neuromechanical signals improves prediction of locomotor activities". In: *Frontiers in Robotics and AI* 5 (2018), p. 78.

[26] Michael Goldfarb et al. "Design of a controlled-brake orthosis for FES-aided gait". In: *IEEE Transactions on Rehabilitation Engineering* 4.1 (1996), pp. 13–24.

[27] Güldal F Nakipoglu Yüzer et al. "The regularity of orthosis use and the reasons for disuse in stroke patients". In: *International Journal of Rehabilitation Research* 41.3 (2018), pp. 270–275.

[28] A. G. Dunning et al. "A review of assistive devices for arm balancing". In: *2013 IEEE 13th International Conference on Rehabilitation Robotics (ICORR)*. 2013, pp. 1–6. doi: 10.1109/ICORR.2013.6650485.

[29] Yong-Lae Park et al. "Design and control of a bio-inspired soft wearable robotic device for ankle–foot rehabilitation". In: *Bioinspiration & Biomimetics* 9.1 (Jan. 2014), p. 016007. doi: 10.1088/1748-3182/9/1/016007. url: https://dx.doi.org/10.1088/1748-3182/9/1/016007.

[30] Zhengyan Zhang et al. "The Effects of Unpowered Soft Exoskeletons on Preferred Gait Features and Resonant Walking". In: *Machines* 10.7 (2022), p. 585.

[31] Ali Sadeghi et al. "A Wearable Sensory Textile-Based Clutch with High Blocking Force". In: *Advanced engineering materials* 21.11 (2019), p. 1900886.

[32] Norman E Dowling et al. "Mechanical behavior of materials: engineering methods for deformation, fracture, and fatigue". In: *(No Title)* (1999).

[33] Temple H Fay. "Coulomb damping". In: *International Journal of Mathematical Education in Science and Technology* 43.7 (2012), pp. 923–936.

[34] David Lee et al. "Viscous damper development and future trends". In: *The structural design of tall buildings* 10.5 (2001), pp. 311–320.

[35] Henry A Sodano et al. "Eddy current damping in structures". In: *Shock and Vibration Digest* 36.6 (2004), p. 469.

[36] John Magliaro et al. "A review of advanced materials, structures and deformation modes for adaptive energy dissipation and structural crashworthiness". In: *Thin-Walled Structures* 180 (2022), p. 109808.

[37] RS Paranjpe. "Dynamic analysis of a valve spring with a coulomb-friction damper". In: (1990).

[38] SO Reza Moheimani. "A survey of recent innovations in vibration damping and control using shunted piezoelectric transducers". In: *IEEE transactions on control systems technology* 11.4 (2003), pp. 482–494.

[39] Roderic S Lakes. *Viscoelastic materials*. Cambridge university press, 2009.

[40] Willy Armand Fongue. "Air spring air damper: modelling and dynamic performance in case of small excitations". In: *SAE International Journal of Passenger Cars-Mechanical Systems* 6.2013-01-1922 (2013), pp. 1196–1208.

[41] Ron Lifshitz et al. "Thermoelastic damping in micro-and nanomechanical systems". In: *Physical review B* 61.8 (2000), p. 5600.

[42] Annemiek Van Boeijen et al. *Delft design guide: Design strategies and methods*. 2014.

[43] David A Winter. "Energy generation and absorption at the ankle and knee during fast, natural, and slow cadences". In: *Clinical Orthopaedics and Related Research®* 175 (1983), pp. 147–154.

[44] Dominik Simon Pieringer et al. "Review of the actuators of active knee prostheses and their target design outputs for activities of daily living". In: *2017 International Conference on Rehabilitation Robotics (ICORR)*. IEEE. 2017, pp. 1246–1253.

[45] Robert Riener et al. "Stair ascent and descent at different inclinations". In: *Gait & posture* 15.1 (2002), pp. 32–44.

[46] MI Awad et al. "Estimation of actuation system parameters for lower limb prostheses". In: *2016 11th France-Japan & 9th Europe-Asia Congress on Mechatronics (MECATRONICS)/17th International Conference on Research and Education in Mechatronics (REM)*. IEEE. 2016, pp. 354–359.

[47] David A Winter. *Biomechanics and motor control of human movement*. John wiley & sons, 2009.

[48] Janet L Krevolin et al. "Moment arm of the patellar tendon in the human knee". In: *Journal of biomechanics* 37.5 (2004), pp. 785–788.

[49] Amir M Navali et al. "Is there any correlation between patient height and patellar tendon length?" In: *Archives of Bone and Joint Surgery* 3.2 (2015), p. 99.

[50] Dane C Todd et al. "Height, weight, and age predict quadriceps tendon length and thickness in skeletally immature patients". In: *The American Journal of Sports Medicine* 43.4 (2015), pp. 945–952.

[51] Tom Håggmark et al. "Cross-sectional area of the thigh muscle in man measured by computed tomography". In: *Scandinavian journal of clinical and laboratory investigation* 38.4 (1978), pp. 355–360.

[52] Paul T Nenno et al. "Design and properties of a rate-dependent 'dynamic ligament'containing shear thickening fluid". In: *Smart materials and structures* 23.12 (2014), p. 125019.

[53] CH Hwang et al. "Changes in specific heat of corn starch due to gelatinization". In: *Journal of food science* 64.1 (1999), pp. 141–144.

A

Problem Analysis: Knee Joint

Research Problem Decomposition

The objective of this work is to develop a proof-of-concept of a novel passive, flexible energy dissipation system that can be used in assistive devices to aid in balance and prevent knee buckling. The project workflow can be outlined as the following sub-problems:

- The estimation of the forces and geometric dimensions involved in lower limb "above knee" or transfemoral assistive devices.
- The comparison and selection of the most suitable energy dissipation mechanism.
- The generation of a design incorporating the selected dissipation mechanism in a "soft" or "flexible" manner.
- The construction of a functional prototype from the selected design.
- The design and assembly of an experimental setup to evaluate the behavior of the prototype.

In addition to these sub-problems, an attempt was made to assess the feasibility of such a device as an implanted long-term solution. Accordingly, the following sub-problems were introduced to the initial research question:

- The selection of energy dissipation mechanisms and materials that promote or inherently demonstrate biocompatibility.
- The implementation of fail-safe measures in the design.
- The design of the appropriate mechano-biological coupling (attachment of the device to the musculoskeletal system)

Geometric And Load Analysis

The device must be capable of withstanding the typical loads of the knee joint to function effectively. A study on the dynamics of the ankle and knee during different walking speeds [43] demonstrated that the knees primarily function as energy absorbers (In other words energy dissipators) and reported a maximum knee torque of approximately $150Nm$, which resulted in a mean peak power of $218W$ and a corresponding $13.2J$ of dissipated energy. When addressing anthropometric measurements, owing to the inherent variability in human physiques, values are typically normalized to body weight to ensure consistency. Studies on lower limb knee prostheses report a maximum extension torque of $1.35Nm/kg$ corresponding to a power dissipation of $4.46W/kg$ while descending stairs, and around $0.49Nm/kg$ torque during the stance phase of walking with a power dissipation of $1.25W/kg$ resulting in a total of $0.148J/kg$ energy dissipated. [44, 45, 46].

Preliminary calculations

As preliminary validation of this data, elementary calculations were performed assuming the body to be an inverted pendulum, pivoted on the knee joint with the lower leg fixed.

A.0.1. Torque on the knee joint

The body is approximated to be an inverted pendulum, pivoted on the knee joint with the lower leg fixed (Fig. A.1). Assuming the mass of the upper body to be concentrated at the pelvis and the thigh mass to be

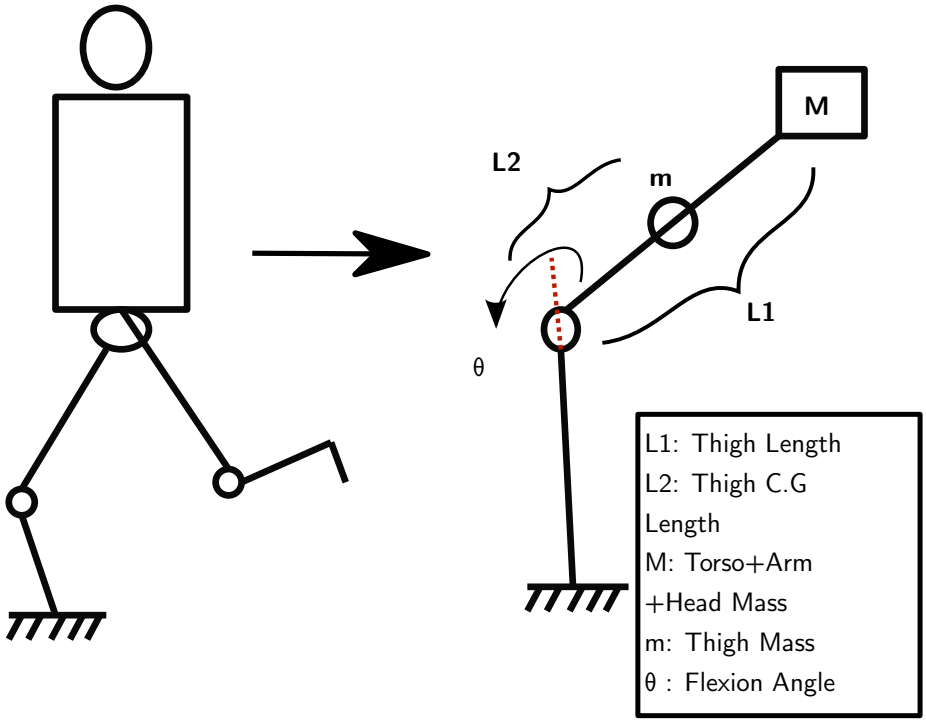

Figure A.1: Inverted Pendulum Approximation for Knee-Torque Calculations

located at its center of gravity, the following equation is obtained for the balance of moments around the knee:

$$M = F_1 * L_1 * cos(90 - \theta) + F_2 * L_2 * cos(90 - \theta) \tag{A.1}$$

Where F_1 is the weight of the upper body, F_2 is the weight of the thigh, L_1 is the total length of the thigh, L_2 is the distance of the thigh center of gravity from the knee joint and θ is the angle between the femur (thigh-bone) and the Tibia (shinbone).
Assuming the mass of the body to be 75 kg and a height of 1.75m, the corresponding lengths and masses were taken from the anthropometric data [47].
This results in a maximum knee torque of $229.6Nm$ and a specific torque of $3.06Nm/kg$, which is a larger estimate than the literature, but is within reasonable limits.

A.0.2. Tendon stretch from patellar motion

Based on the variation of the patella moment arm [48], the maximum and minimum values were taken to be $20mm$ and $55mm$ respectively. The minimum moment arm is assumed to correspond to the leg being completely straight. The change in length of the tendon, and consequently the passive damper, can be calculated from trigonometric relations of right angles triangles as per Fig. A.2.

Change in length (l) during stretching (Deformation):

$$\delta l = (p + q) - (a + b) \tag{A.2}$$

Where,

$$p^2 = (55)^2 + x^2$$
$$q^2 = (55)^2 + y^2$$
$$a^2 = (20^2) + x^2$$
$$b^2 = (20)^2 + y^2$$

The values of x and y correspond to the lengths of the patellar [49] and quadriceps tendon [50] respectively. The maximum change in length of the damper comes out to be $3.6cm$ based on this calculation.

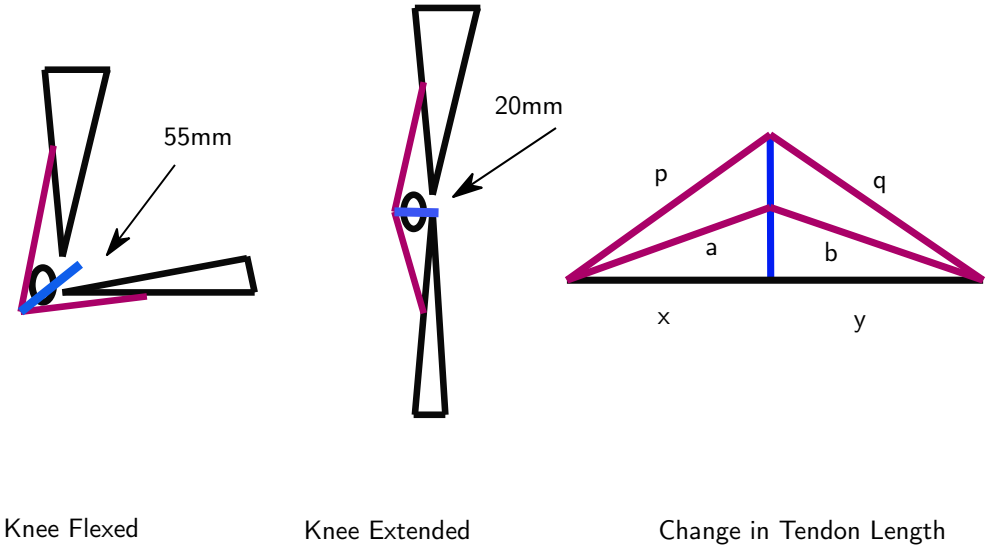

Figure A.2: Trigonometric Approximation of Tendon Stretch During Benging

The patella (knee cap) serves as the moment arm for the quadriceps tendon, and due to its sliding movement during knee rotation, the effective moment arm varies from $20mm \sim 55mm$ [48]. This variation translates to a maximum stretch of up to $3.6cm$ as per the calculations.
As for the spatial constraints regarding the implanted application, the average cross-sectional area of the thigh is $203.56cm^2$, with the muscle taking up close to 85% of the area of the thigh in healthy individuals [51]. This leaves a cross-sectional area of around $20cm^2$ and a calculated length of $42cm$ for a human of height $1.75m$[47] that can be used for the implanted actuator.

A.0.3. Maximum Velocity of Tendon Stretch

In addition to the total stretch, the maximum velocity of the tendon stretch is important to establish the working limits of the assistive energy dissipator being designed. A study on the system parameters involved in lower limb prosthetic design [46] found that the maximum speed of knee flexion occurs just before toe-off at the end of the stance phase. The maximum angular flexion velocity of the knee is found to be around 52.05 RPM.
From the moment arm calculations of the previous section, we find that the maximum possible stretch velocity of the tendon is related to the flexion velocity by the following equation:

$$V_{stretch} = \omega_{flex,max} * M_{max} \tag{A.3}$$

Where, $V_{stretch}$ is the stretch velocity, $\omega_{flex,max}$ is the maximum knee flexion angular velocity expressed in RPM, and M_{max} is the maximum moment arm of the patella, found to be 55mm. We obtain a maximum possible stretch velocity of 4.77 cm/s. The instantaneous shear rate corresponding to the angular velocity of 52.05 RPM is 0.8675 Hz. The damper behavior can be tuned around this value as required.

B

Case Study: Feasibility of an Implantable Assistive Device

The appeal of developing an implantable actuator arises from the potential to mitigate skin irritation, discomfort, social stigma, exposure to external contaminants, and physical damage often associated with conventional assistive devices. If safely implanted, the device could work in synchrony with the musculoskeletal system, instead of imposing motion on the body externally. This would allow the patients to avoid the inconvenience of equipping and maintaining the device. The clinical and market acceptance of implanted devices like pacemakers, ventricular assistive devices, and sphincter cuffs indicates a positive trend in favor of the adoption of other similar implanted assistive devices.

Functional Requirements

In order to approach the design in a systematic manner, a functional analysis was conducted on the problem statement. Based on the sub-problems formulated, the following functions were deemed critical to the development of the implanted passive energy dissipator prototype:

- Energy Dissipation: The device must be capable of dissipating the energy of heel strike and resisting knee buckling under gravitational forces.
- State Detection (Sensing): The device must be capable of identifying when energy is required to be dissipated (for instance, no energy dissipation is desired during knee extension, but is required in the stance phase during flexion).
- Switching between states: When the desired state is detected, the device must have mechanisms to switch between resisting (dissipating) or allowing free motion of the knee joint.
- Coupling: The device must be mechanically connected to the musculoskeletal system within the body in order to exert its influence on the knee joint.
- Safety: The device must incorporate fail-safe measures to prevent unwanted damage to the internal tissues of the user in case of failure

Non-Functional Requirements

In addition to these requirements, a few general guidelines to be targeted in the design were classified as nonfunctional requirements.

- Biocompatibility: The device must be manufactured from materials that elicit minimal immune response, not cause adverse reactions from the host, and remain 'bio-inert' at the very least.
- Position: The device should be wholly encompassed within the body or have no physical connection to an object external to the body.
- Size and weight: The device should be designed to be as small and lightweight as possible, to minimize its impact on the user's mobility and comfort.
- Life: The device must have a minimum lifetime of at least 10^7 cycles, without considerable change in performance. This is to minimize the need for revision or replacement surgeries.

- Power: If a passive device is infeasible, the system should be designed to have a portable source with a long life or incorporate energy harvesting mechanisms.

Morphological Table

A morphological table is a method to channel creativity and generate conceptual ideas [42]. Starting from the functional analysis, various embodiments (ideas that can solve a function) are listed, to address each of the sub-functions. New concepts can then be generated by combining different embodiments of each function. This process is useful for generating a large number of concepts spanning a diverse set of working principles in a systematic manner. However, the feasibility of each generated concept must be evaluated independently; this tool is limited to generating potential ideas. The practicality and realization of these ideas are not considered at this stage. From the functional requirements listed above, the following morphological table is developed:

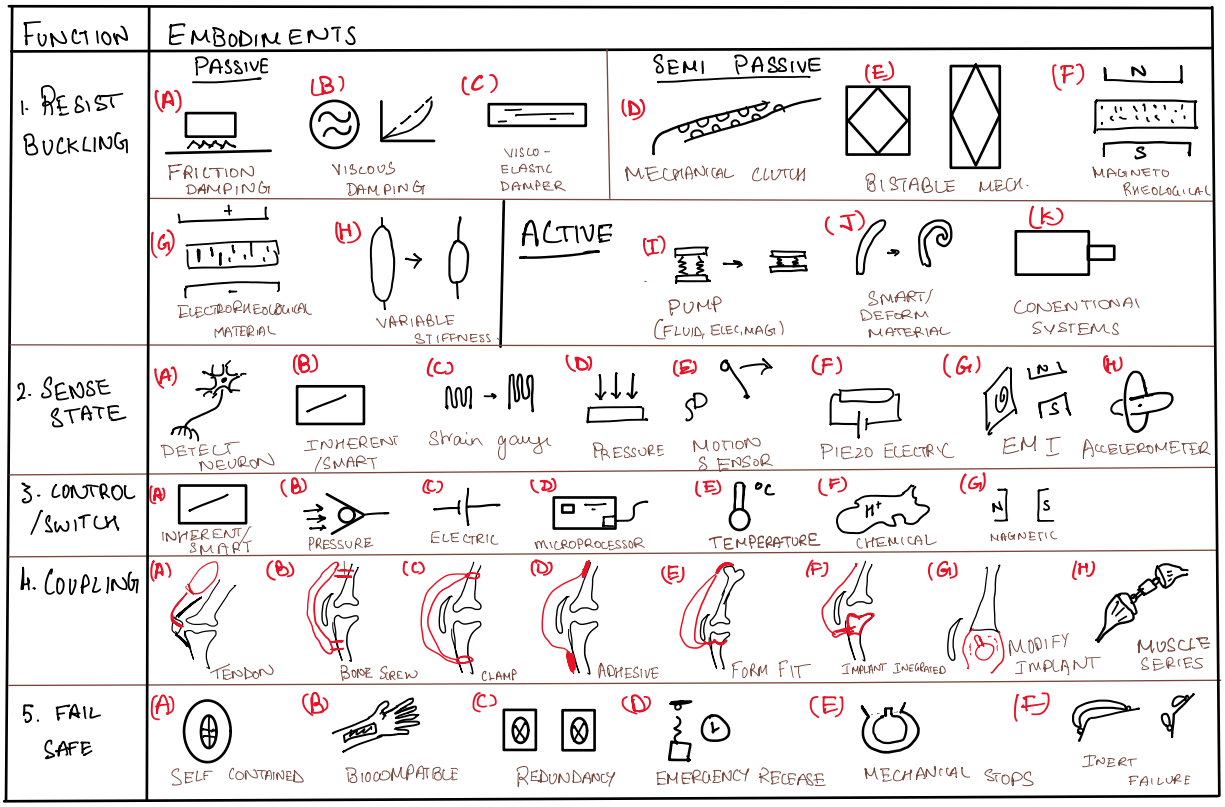

Figure B.1: Morphological Table to address the functional requirements

Concept Generation

By combining various embodiments of each sub-function Fig. B.1, different concept designs were developed to address the issue of implanted energy dissipation. A few of the outcomes are presented here Fig. B.2:

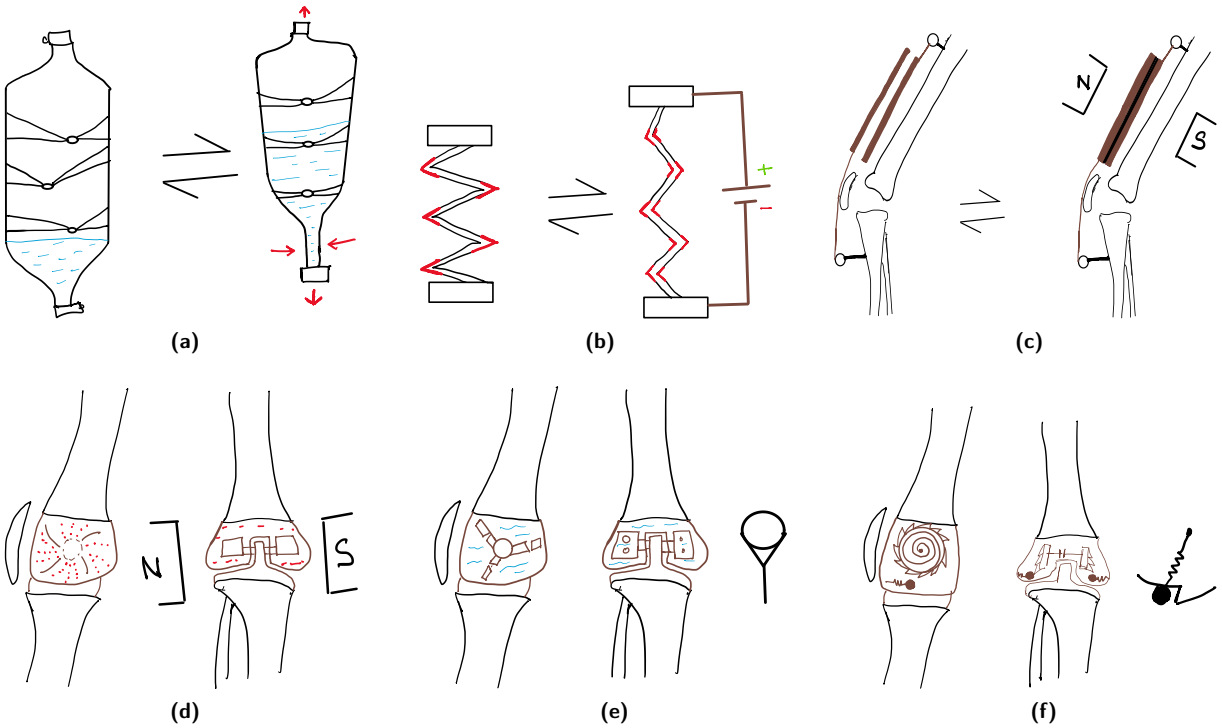

Figure B.2: Concepts Generated from the Morphological Table: (a) Flexible Viscous Damper Pouch.(b) Cascading Bi-stable Mechanism. (c)Flexible Magnetic Linear Clutch. (d) Magnetorheological Knee Joint. (e) Viscous Damping Knee Joint. (f) Clutch-Spring-Based Knee Joint.

B.0.1. Concept 1: Flexible Viscous Damper Pouch

Obtained by combining the embodiments: 1B-2D-3A-4C-5A, a principle solution that is based on squeezing viscous fluids through small openings or orifices within a flexible pouch is generated: Fig. B.2a. The knee joint torque is used to overcome viscous resistance and squeeze the fluid through the orifices within the pouch. This results in the rotational kinetic energy being converted to pressure and ultimately heat. During stance, when the body weight is on the leg, there is a large pressure on the walls of the pouch, which serves as state detection. During the swing phase, when body weight is not on the pouch, the fluid is not squeezed. Viscous dampers are inherently rate-sensitive, leading to greater resistance for faster excitations. The whole pouch can be contained within another safety pouch to prevent the working fluid from coming into contact with body tissue.

B.0.2. Concept 2: Cascading Bi-stable Mechanism

Obtained by combining the embodiments: 1E-2A-3C-4B-5C. The solution is based on multiple bistable joints attached in series to make a longitudinal member: Fig. B.2b. The bistable joints are made with piezoelectric material and can switch between contracted and stretched states by applying an electric field. When the joints are contracted, there is extra resistance offered to knee flexion. When nerve signals are detected for knee flexion, the bistable joints can be activated, allowing free joint motion. The individual units can be stacked to amplify the resistance, and screwed to the bones. The whole system is designed to be redundant, with multiple bistable joints attached in both series and parallel. The individual contribution of each joint is small when compared to the overall system.

B.0.3. Concept 3: Flexible Magnetic Linear Clutch

Obtained by combining the embodiments: 1D-2E-3D-4D-5B. The generated solution is based on using magnetic polymers made from touch elastomers to behave as clutches: Fig. B.2c. When external magnetic fields are applied, the magnetic polymers attach to one another and form a single unit. This prevents the knee from flexing. Using a motion sensor to detect when the knee is required to be stiff (stance phase or when the person is about to fall), a microprocessor can control the operation of an electromagnetic coil attached outside the leg. The magnetic polymers can be attached to the femur and shank, respectively, to provide selective stiffness of the knee joint. The magnetic polymers can be made of a material like PDMS: poly-dimethyl Siloxane, which is

a known biocompatible polymer, to ensure device safety.

B.0.4. Concept 4: Magnetorheological Knee Joint

Obtained by combining the embodiments: 1F-2G-3G-4G-5E. The generated solution involves incorporating a rotational magnetorheological brake: Fig. B.2d, similar to the ones used in prosthetic feet (Rheo-knee), inside the body of an artificial knee joint. The treatment involves replacing the knee joint through total knee replacement surgery. Electromagnetic induction sensors can be used to detect when there is a sudden change in the knee motion, or when stability is required. Through the action of external magnetic fields, the viscosity of the rheological fluid can be varied. This leads to variable energy dissipation and resistance to knee flexion. While the system is fully self-contained, as a fail-safe, mechanical stops are added to limit the motion of the joint.

B.0.5. Concept 5: Viscous Damping Knee Joint

Obtained by combining the embodiments: 1B-2D-3A-4G-5E. This solution also involves using an artificial knee joint but as a rotational viscous damper: Fig. B.2e. Valves can be incorporated into the design to ensure knee rotation is only possible by forcing fluid through constrictions within the joint. In this manner, the artificial knee joint inherently dampens motion and offers velocity-dependent resistance. While the system is fully self-contained, as a fail-safe, mechanical stops are added to limit the motion of the joint.

B.0.6. Concept 6: Clutch-Spring-Based Knee Joint

Obtained by combining the embodiments: 1A-2B-3A-4G-5E. This solution takes inspiration from car seatbelts and incorporates a spring clutch system within an artificial knee joint: Fig. B.2f. When sudden knee rotation occurs, a small ball inside the joint is forced out of its socket due to centrifugal force, jamming a ratchet gear mechanism. This ratchet gear is attached to the knee joint and therefore stops its motion. When slow rotations happen, the ball stays in its position, and the ratchet gear is allowed to rotate freely. In this manner, the joint can resist sudden knee rotation. The ratchet gear can be mounted on a torsion spring, which will allow some compliance preventing sudden stopping of motion. The system is self-contained and inert when it breaks down, but mechanical end stops are added as safety measures.

Feasibility Study

Once sufficient conceptual designs were created, a discussion was held with medical specialists in Orthopedics and implant surgery. The conversation focused on the viability of the idea, the solutions generated, and their scope of implementation. During this discussion, it was concluded that successful mechano-biological coupling of such a device within the confines of the thigh is currently unfeasible.

A consensus was reached that the lack of appropriate soft-to-hard tissue interface technology and means to mitigate foreign body response meant that the long-term effectiveness of the idea was highly uncertain. The notion of using the moment arm of the patella from within the body was seen as particularly challenging, owing to the lack of physical space, the chances of inducing patellofemoral pain, and disturbing the balance of equilibrium in the patella motion. In addition, the successful incorporation of a deformable component that actively applies variable forces to the musculoskeletal system requires substantial interconnection with bone and connective tissue. There are currently no methods to achieve this integration, thereby limiting the possibility further.

The final conclusion was that, at this conjecture, patients would benefit more from external assistive devices, until this issue of mechano-biological integration can be addressed.

In light of the duration of this thesis, and the lack of technical means to address these concerns effectively, the idea of developing this implantable assistive device for quadriceps assistance, was deemed to be out of the purview of this current study. Therefore, the scope of this work was limited to developing a proof-of-concept passive, soft damper that is intended for assistive devices. It is expected that, with the resolution of the mechano-biological integration problem, this proof of concept can be developed further into the complete implanted assistive device solution as initially envisioned.

C

Methodology: Supplementary Figures

Concept Phase

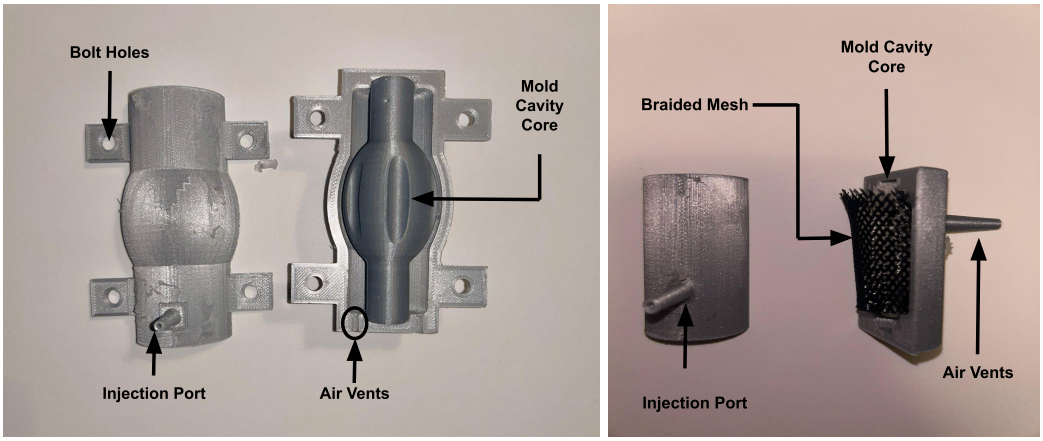

(a) (b)

Figure C.1: Injection Mold Casing for Silicone Pouch: (a) First Prototype (b) Braided Mesh prototype. Silicone polymer is injected and allowed to cure. Once cured, the core is removed to obtain the hollow pouch.

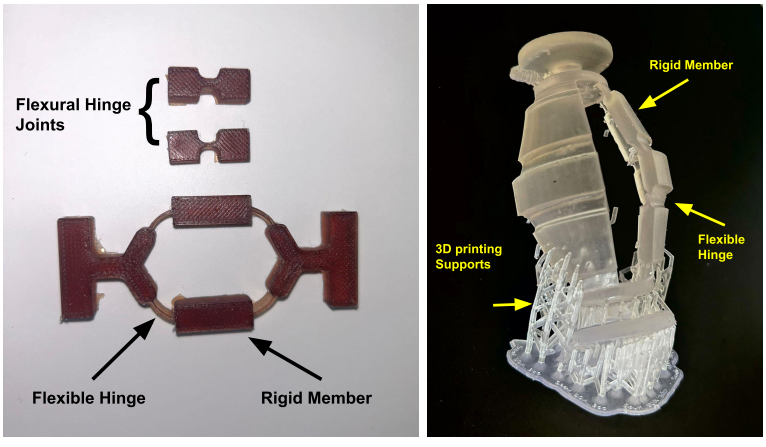

(a) (b)

Figure C.2: Compliant Scissor Mechanism: (a) Compliant Planar 4 Bar (b) 3D Scissor mechanism. A compliant version of a scissor mechanism is developed in 3D based on flexure hinges and a 4-bar mechanism.

Final Prototype

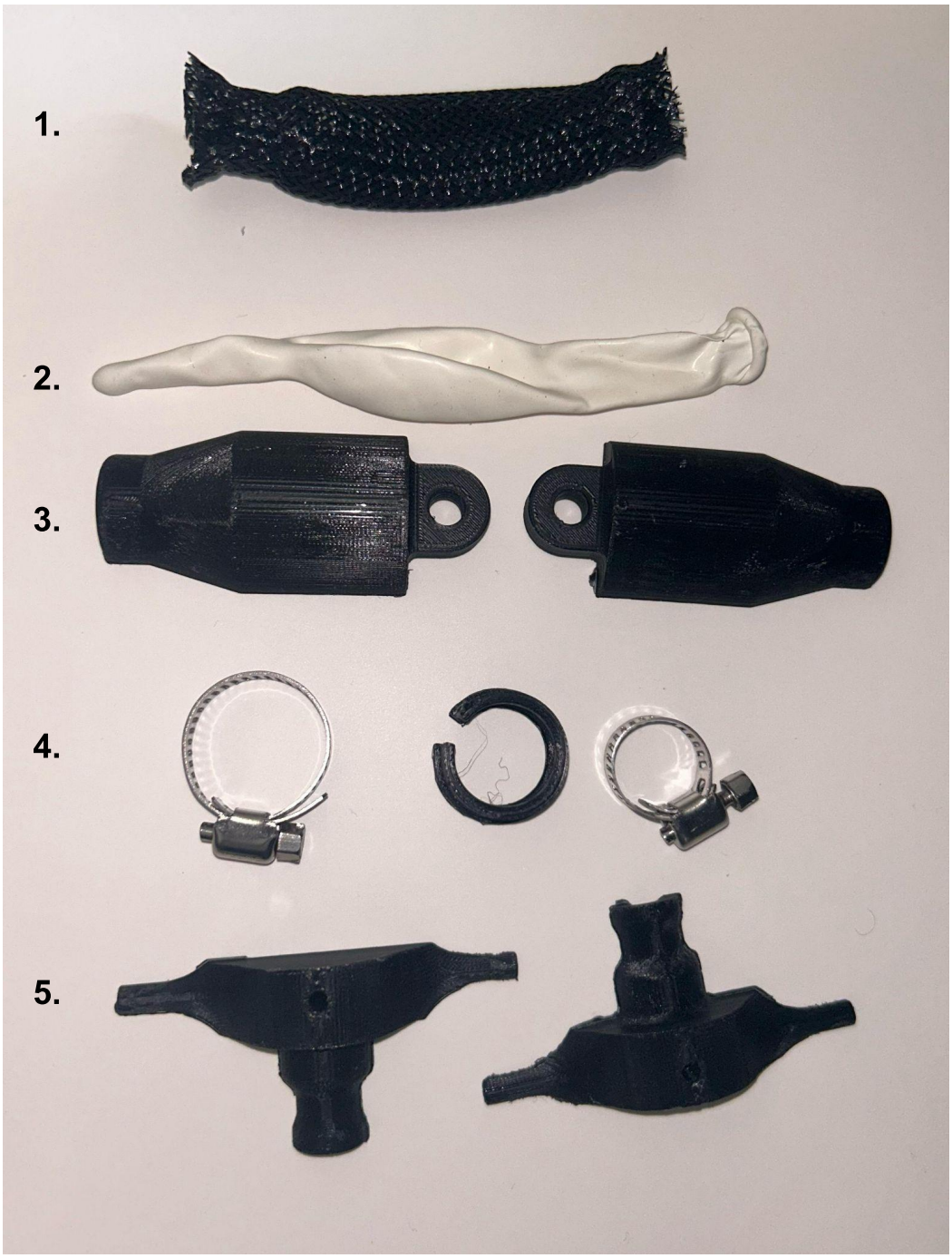

Figure C.3: Components of Final Prototype: First the pouch (2) is filled with fluid and tied/sealed. The mesh (1) is placed around the balloon. The tied end is clamped between (5), with the help of (4). The other end is lodged in (3), and (1) is clamped around both (3) and (5). Spacer(4) ensures mesh is secure in place. The dimensions are provided in Table C.1

Table C.1: Description of Components

Nr	Component	Quantity	Comments
1	Braided mesh	1	Length: 10cm, Diameter: 2cm, PET Mesh Sleeve
2	Elastic pouch	1	Length: 12cm, Volume: 20ml, Needle Tail Balloon
3	Hollow chamber	2	Empty Chamber 15.35ml, Tough PLA 3D printed
4	Clamps, Spacer	2,1	Steel Hose Clamps, 3D printed form fit Spacer
5	Clamped handle	2	Clamped Together, holds balloon, Tough PLA 3D printed

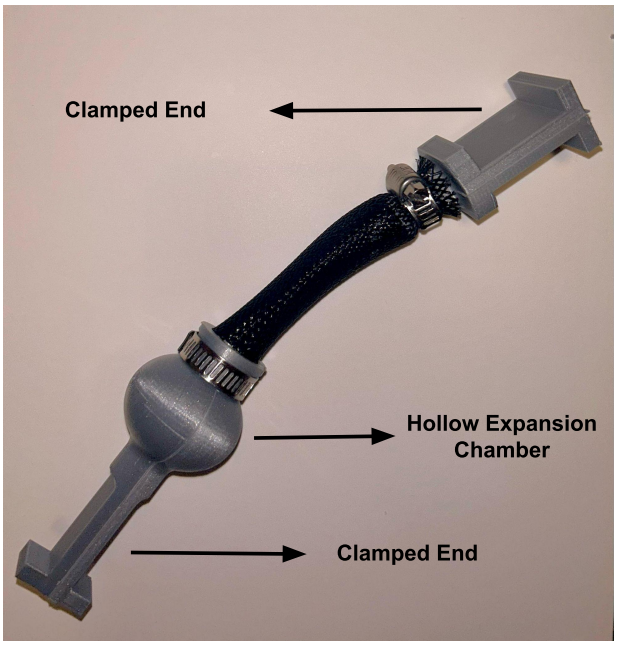

Figure C.4: Assembled prototype Used for Cyclic Tests

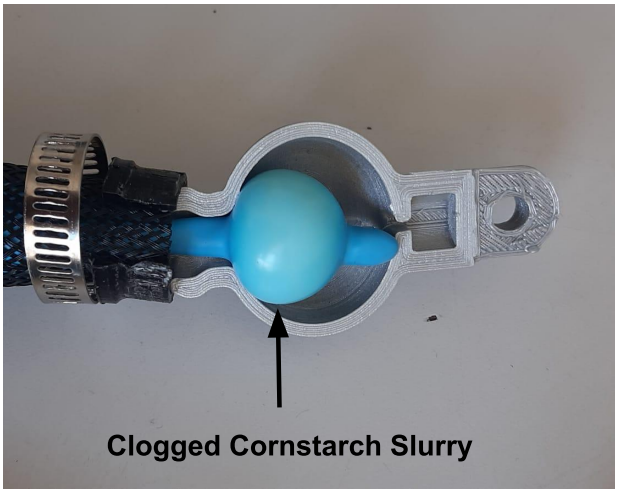

Figure C.5: Clogged Relief chamber with Thick Cornstarch After Cyclic Tests

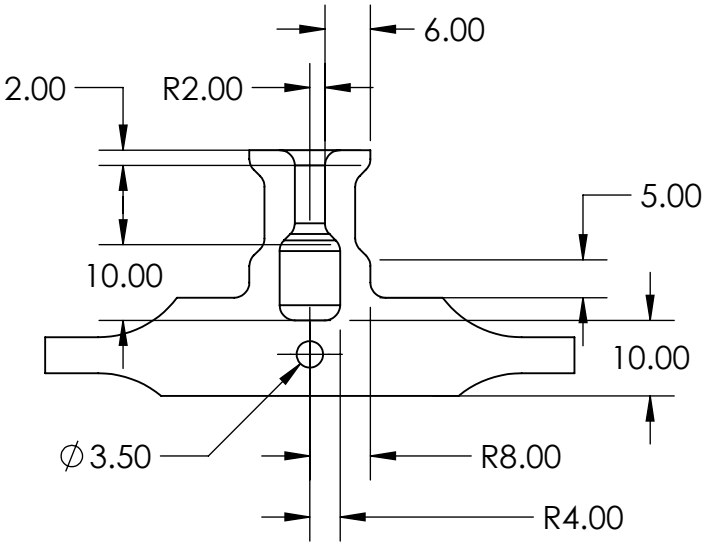

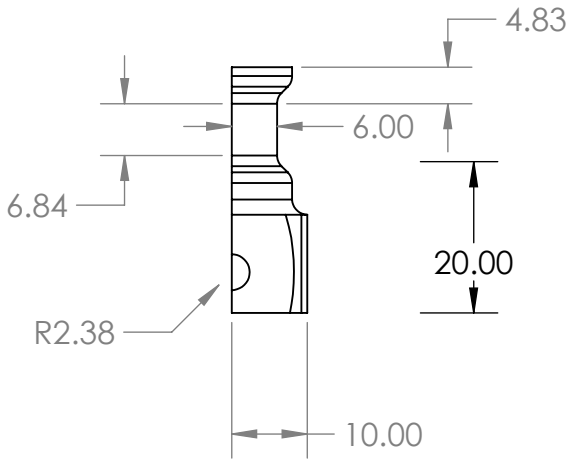

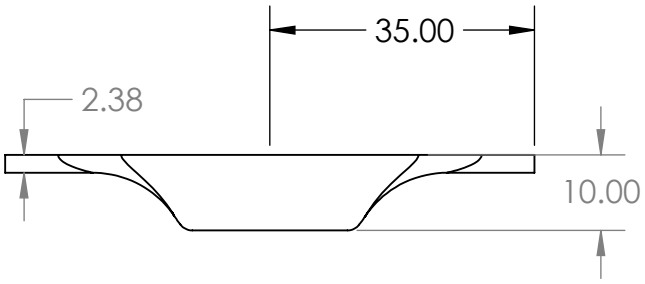

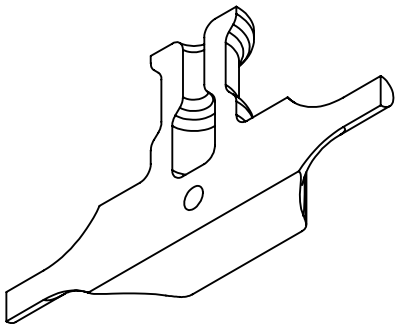

VIEW -

UNLESS OTHERWISE SPECIFIED: DIMENSIONS ARE IN MILLIMETERS SURFACE FINISH: TOLERANCES: LINEAR: ANGULAR:		FINISH:		DEBURR AND BREAK SHARP EDGES		DO NOT SCALE DRAWING	REVISION
	NAME	SIGNATURE	DATE			TITLE:	
DRAWN						Clamp Handle	
CHK'D							
APPV'D							
MFG							
Q.A				MATERIAL:		DWG NO.	A4
						DW1 : 1:1	
				WEIGHT:		SCALE:1:1	SHEET 1 OF 1

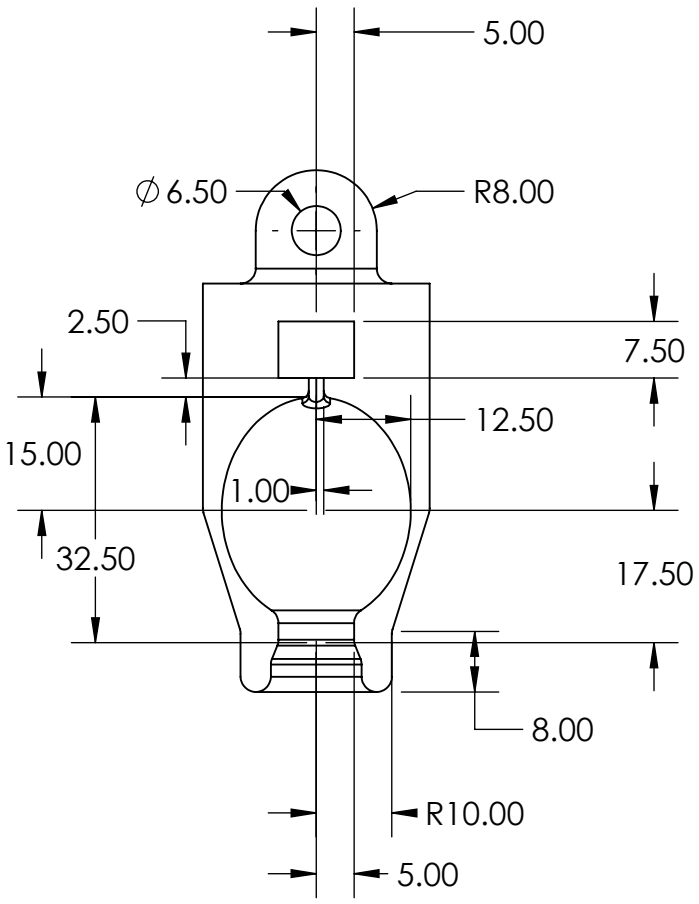

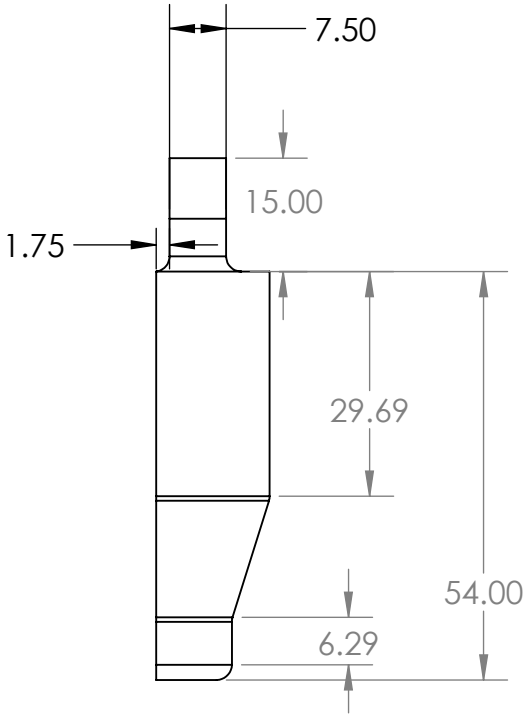

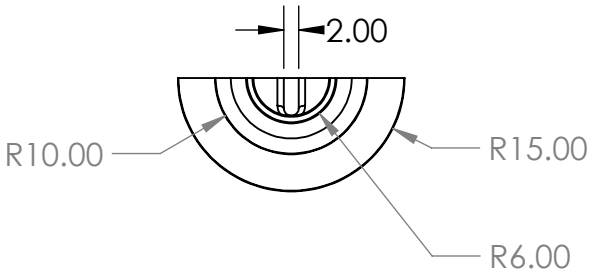

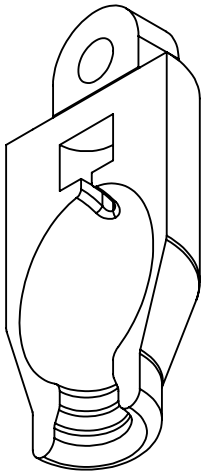

UNLESS OTHERWISE SPECIFIED: DIMENSIONS ARE IN MILLIMETERS SURFACE FINISH: TOLERANCES: LINEAR: ANGULAR:		FINISH:			DEBURR AND BREAK SHARP EDGES	DO NOT SCALE DRAWING	REVISION
	NAME	SIGNATURE	DATE			TITLE:	
DRAWN						Hollow Expansion Chamber	
CHK'D							
APPV'D							
MFG							
Q.A				MATERIAL:		DWG NO.	A4
						DW2 1:1	
				WEIGHT:		SCALE:1:1	SHEET 1 OF 1

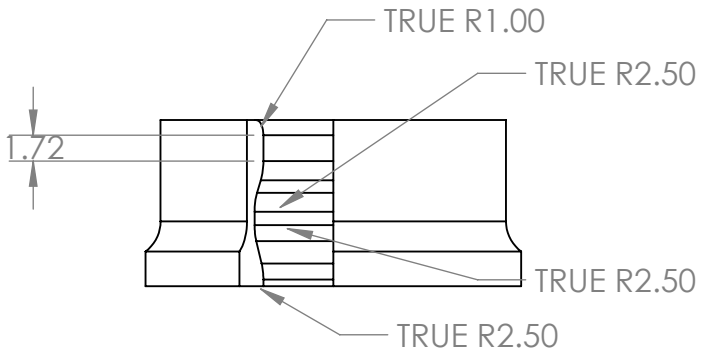

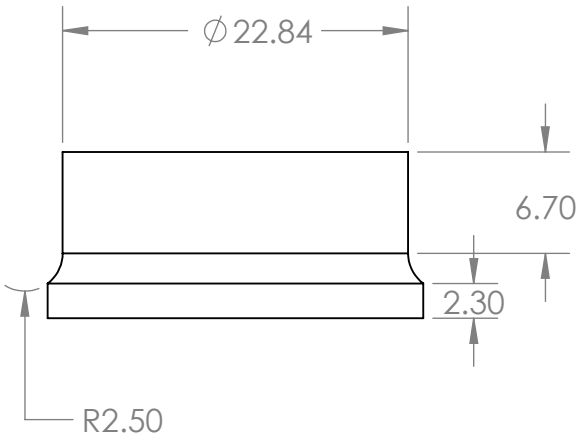

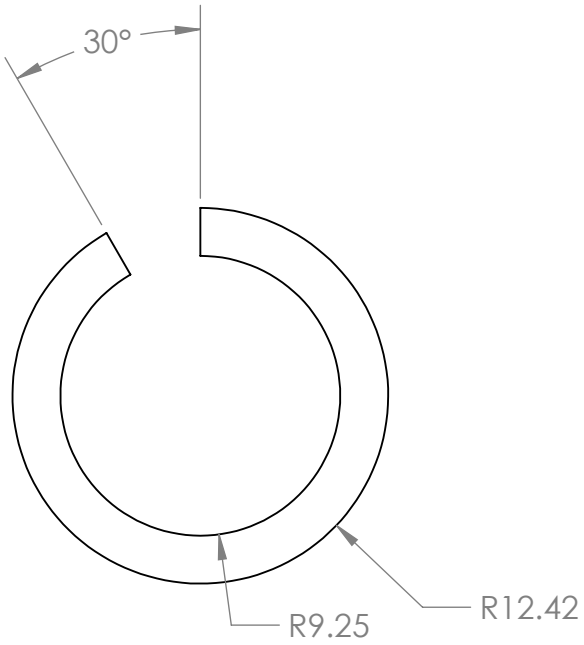

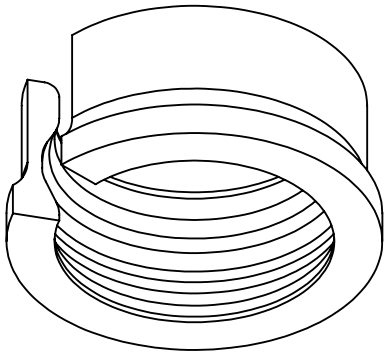

UNLESS OTHERWISE SPECIFIED: DIMENSIONS ARE IN MILLIMETERS SURFACE FINISH: TOLERANCES: LINEAR: ANGULAR:		FINISH:			DEBURR AND BREAK SHARP EDGES	DO NOT SCALE DRAWING	REVISION
	NAME	SIGNATURE	DATE			TITLE: Clamp Interface	
DRAWN							
CHK'D							
APPV'D							
MFG							
Q.A				MATERIAL:		DWG NO. DW3 2:1	A4
				WEIGHT:		SCALE:2:1	SHEET 1 OF 1

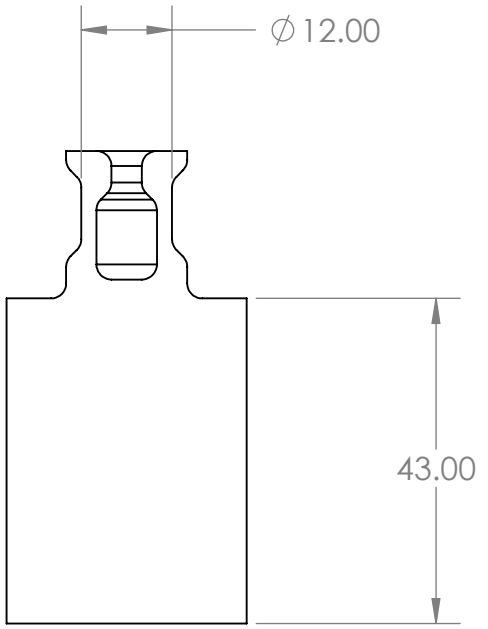

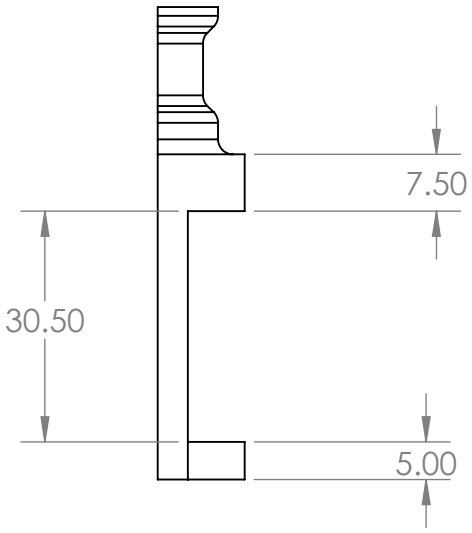

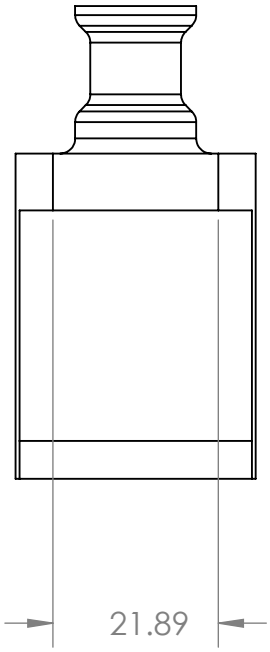

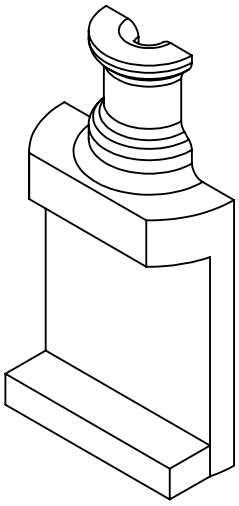

UNLESS OTHERWISE SPECIFIED: DIMENSIONS ARE IN MILLIMETERS SURFACE FINISH: TOLERANCES: LINEAR: ANGULAR:		FINISH:		DEBURR AND BREAK SHARP EDGES		DO NOT SCALE DRAWING	REVISION
	NAME	SIGNATURE	DATE			TITLE:	
DRAWN						Cyclic Test Clamp Handle	
CHK'D							
APPV'D							
MFG							
Q.A				MATERIAL:		DWG NO.	A4
						DW4 1:1	
				WEIGHT:		SCALE:2:1	SHEET 1 OF 1

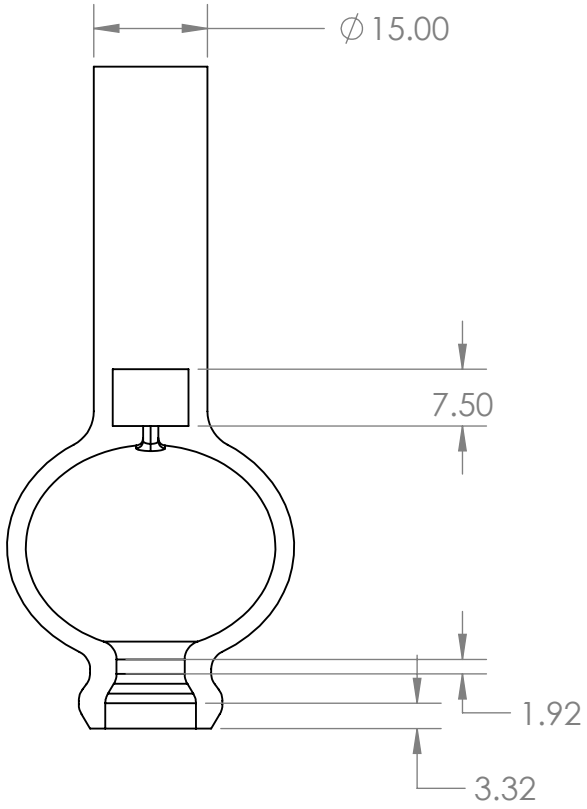

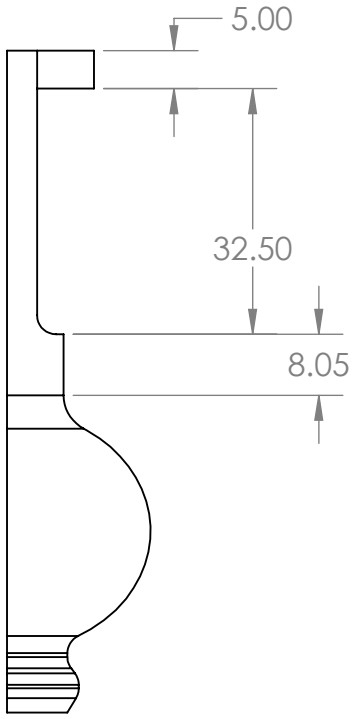

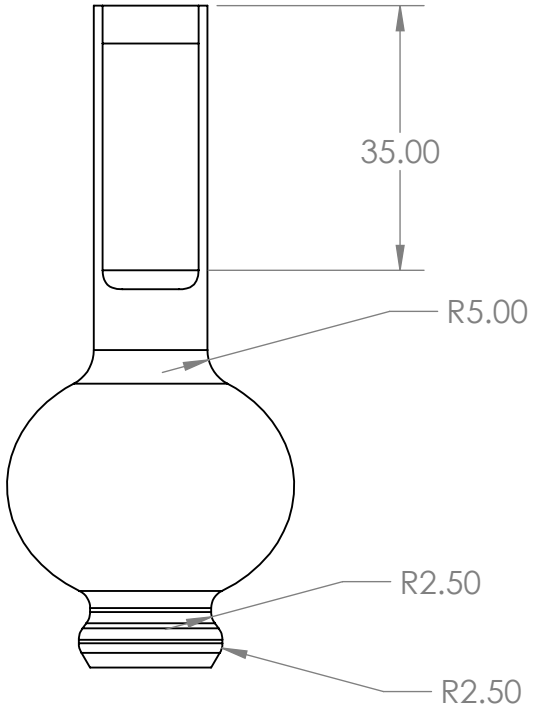

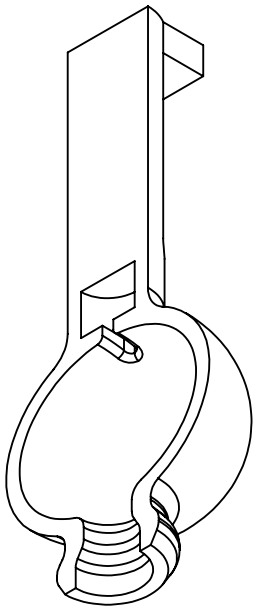

UNLESS OTHERWISE SPECIFIED: DIMENSIONS ARE IN MILLIMETERS SURFACE FINISH: TOLERANCES: LINEAR: ANGULAR:		FINISH:			DEBURR AND BREAK SHARP EDGES	DO NOT SCALE DRAWING	REVISION
	NAME	SIGNATURE	DATE			TITLE:	
DRAWN						Cyclic Test Hollow Chamber	
CHK'D							
APPV'D							
MFG							
Q.A				MATERIAL:		DWG NO.	A4
						DW5 1:1	
				WEIGHT:		SCALE:1:1	SHEET 1 OF 1

D

Experiments: Protocols

Viscosity Measurements

This test involved measuring the viscosity and shear stress of the working fluid samples using a parallel plate rheometer. The test is a Linear Sweep test that increases the shear rate imparted to the fluid between linearly two fixed values. (In this case 0.1 to 100 1/sec). The complete setup is described in the methods section of the scientific article (Chapter 3).

1. Check the air supply, ensure it is 2.1 bar. Switch on the controller, wait till the screen shows 'System test Ok'. (If it doesn't show, check the error code in the manual), Switch on the water cooler.
2. Open the software (ARG2 @ TU Delft) on the computer.
3. Set the experiment name and parameters: Temperature, Soak Time, Test Type, Test Range, and Data Points (See Method).
4. Set the Zero Gap, and once it's done raise the head to the loading gap.
5. Load 1 to 2ml of the sample fluid using a pipette (not possible for shear thickening fluids, use syringe and let 2 to 3 drops drip down)
6. Click on the trim gap option. Once the trim gap is reached, lock the head.
7. Wipe away any excess fluid with cardboard and tissue.
8. Start experiment, log readings of shear stress and viscosity.
9. Turn the top screw to loosen the plate, Raise the clamp with the button on the front panel of the instrument, Remove the plate and clean the setup.
10. Repeat steps 4-9 to take 3 trials for each sample fluid.

Constant Force Measurements

This test involved measuring the response of the damper to static and impact loads. A custom setup was made involving masses suspended from a pulley, applying their weight onto the damper. The force and displacements are measured through a Load cell in series, and a displacement sensor in parallel to the damper. The setup uses a linear rail and slider to restrict the masses to vertical motion. The parameters of the test setup are described in the methods section of the scientific article (Chapter 3).

1. Connect the Data Acquisition System to the computer. Connect the terminals to the voltage regulator and ensure 3.3V is applied, at a low current.
2. Turn on the LabView Software. Open the setup file $Constant_Force_Tests.vi$. In the front panel, Select the appropriate physical channels as per the schematic in Appendix C.
3. Run the program, now observe the steady state readings of the sensors without any load.
4. Stop the program, and add the values of the steady state readings taken previously as the offsets under each sensor tab.
5. Now select the save button and type in the trial name. The software is ready to test.
6. Load the damper onto the setup by bolting it to the load cell and attaching the displacement sensor wire to the clamp handle of the prototype.

7. Attach the tension cable through the hole in the clamp handle and use the screw fasteners to secure the cable in its loop.
8. On the other end, attach the hook of the cable to the slider by looping it around the mounting screw provided.
9. Now raise the slider to the desired height. Load the masses as per the trial.
10. Run the program, after 1 second : (A) Static Tests: Gently lower the weights till steady state force is reached and let go. Wait for around 3 seconds and stop the program. (B): Impact Tests: Let the weights go suddenly from the desired height, allow steady-state force to be reached after 3 seconds stop the program.
11. Check for any damages or loose screws. If any, fix the issue, then remove the masses, and raise the slider to the desired height.
12. Repeat steps 7-11 for all loading cases, for each sample fluid, with 5 trials for each test.
13. Once tests are completed, remove the tension cable from the slider, release the displacement sensor from the damper, and unload the damper from the setup.

Cyclic Tests

This test involved measuring the response of the damper to cyclic loads. The test setup used was a universal test bench setup with a 500 N load cell. The dampers with various working fluids were excited at different shear rates, and the force-displacement data was noted down. The parameters of the test setup are described in the methods section of the scientific article (Chapter 3).

1. Login to the machine, and open the setup program. Turn on the machine with the button.
2. Set force zero. Place the damper specimen between the grips and tighten them.
3. In the configure test tab, define the test parameters, the data to be read, and the pre and post-test settings.
4. Using the arrow buttons, stretch the damper until the force reads 5N. (This is the pretension value).
5. Set this position as the start position.
6. Once the test parameters are defined (number of cycles, speed, travel) and the setup is done, place the transparent safety shield in front of the setup.
7. Start the test, log the test. In case of any failure terminate the trial.
8. Once the test is done, export the results as an Excel file.
9. Repeat steps 2 to 8 for all the samples for each of the selected shear rates
10. Loosen the grips and unmount the damper.

E

Experiments: Supporting Results

Viscosity Measurements

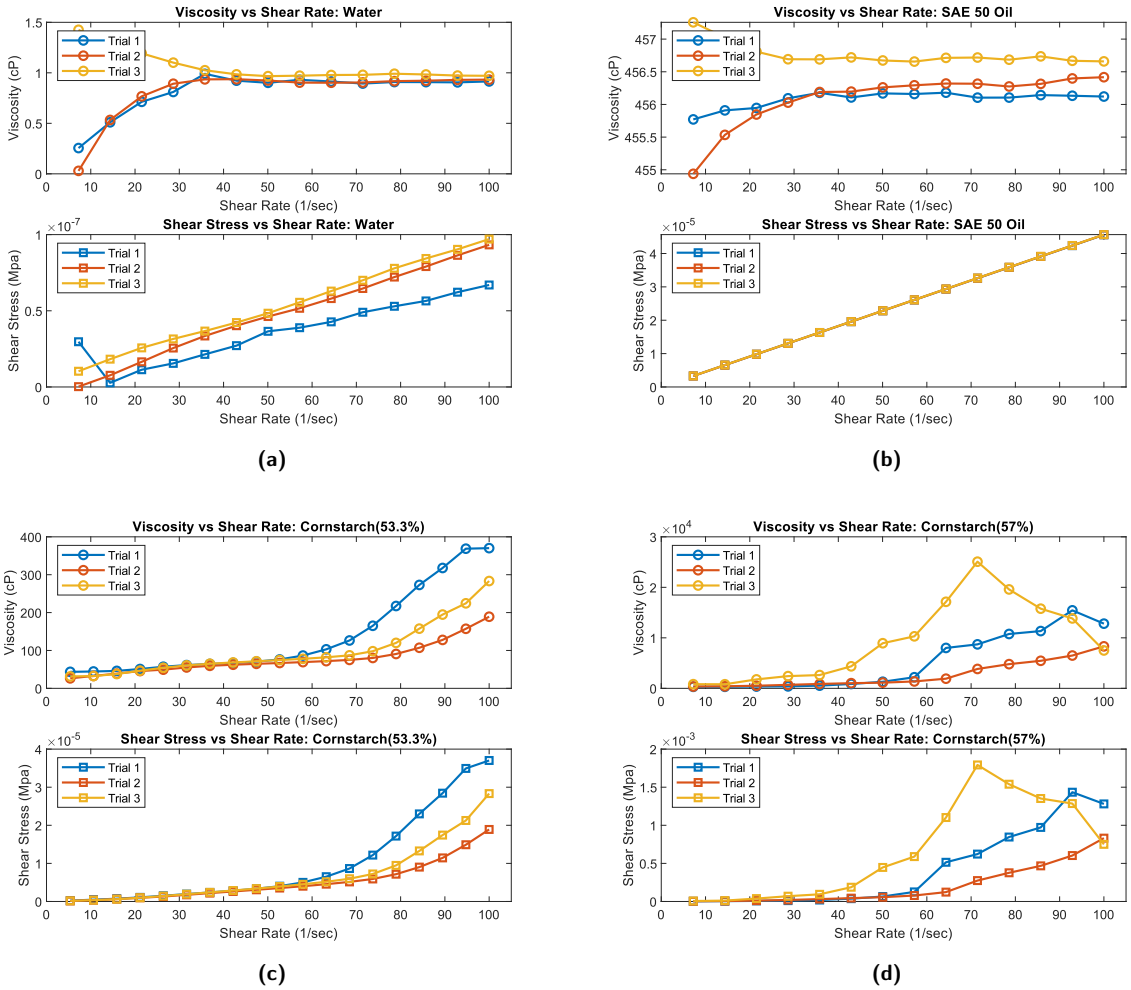

Figure E.1: Variation of Viscosity and Shear Stress with Shear Rate, 3 Trials: (a) Water. (b) SAE 50 Oil. (c) Cornstarch Slurry (53.3%). (d) Thick Cornstarch Slurry (57%). The best trial (most representative) of each sample is presented for the qualitative analysis.

Constant Force Tests

E.0.1. Static Load, Sample: No Fluid (Empty Pouch)

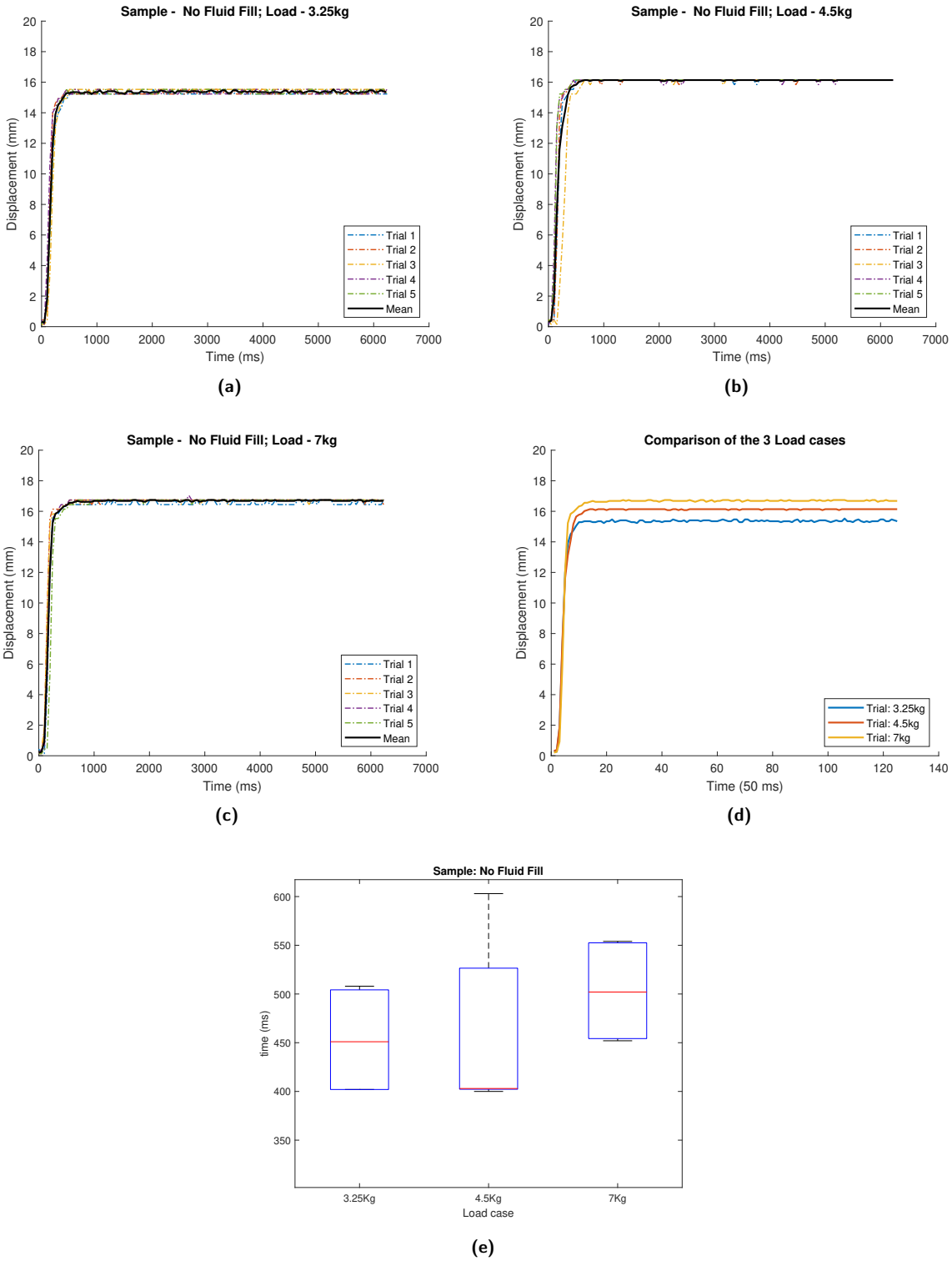

Figure E.2: Constant Force Measurement: No Fluid Static Plots: (a)-(c) Mean loading plots. (d) Comparison of mean across loading cases. (e) Box plot of time taken to steady state stretch

E.0.2. Static Load, Sample: Water

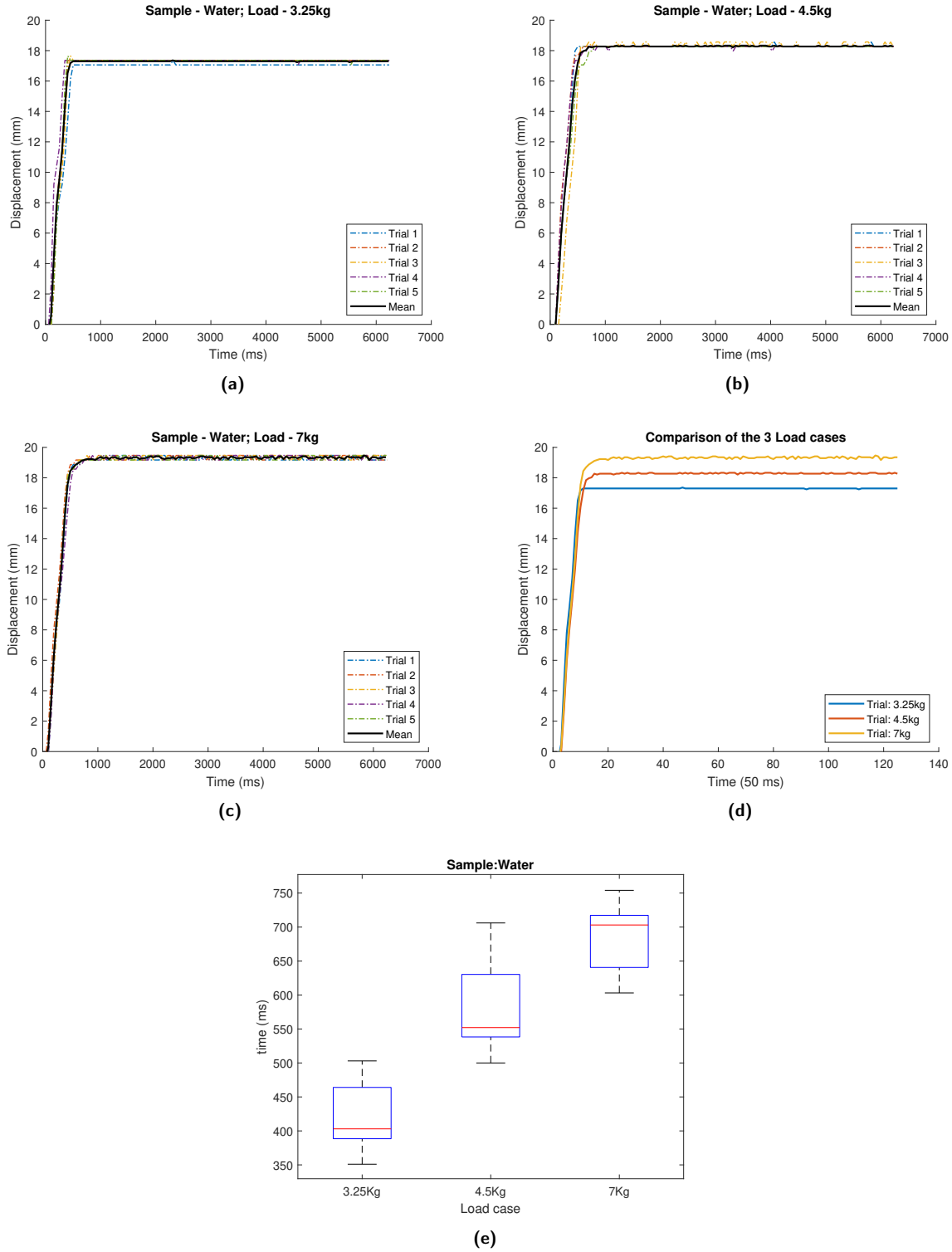

Figure E.3: Constant Force Measurement: Water Static Plots: (a)-(c) Mean loading plots. (d) Comparison of mean across loading cases. (e) Box plot of time taken to steady state stretch

E.0.3. Static Load, Sample: SAE 50 Oil

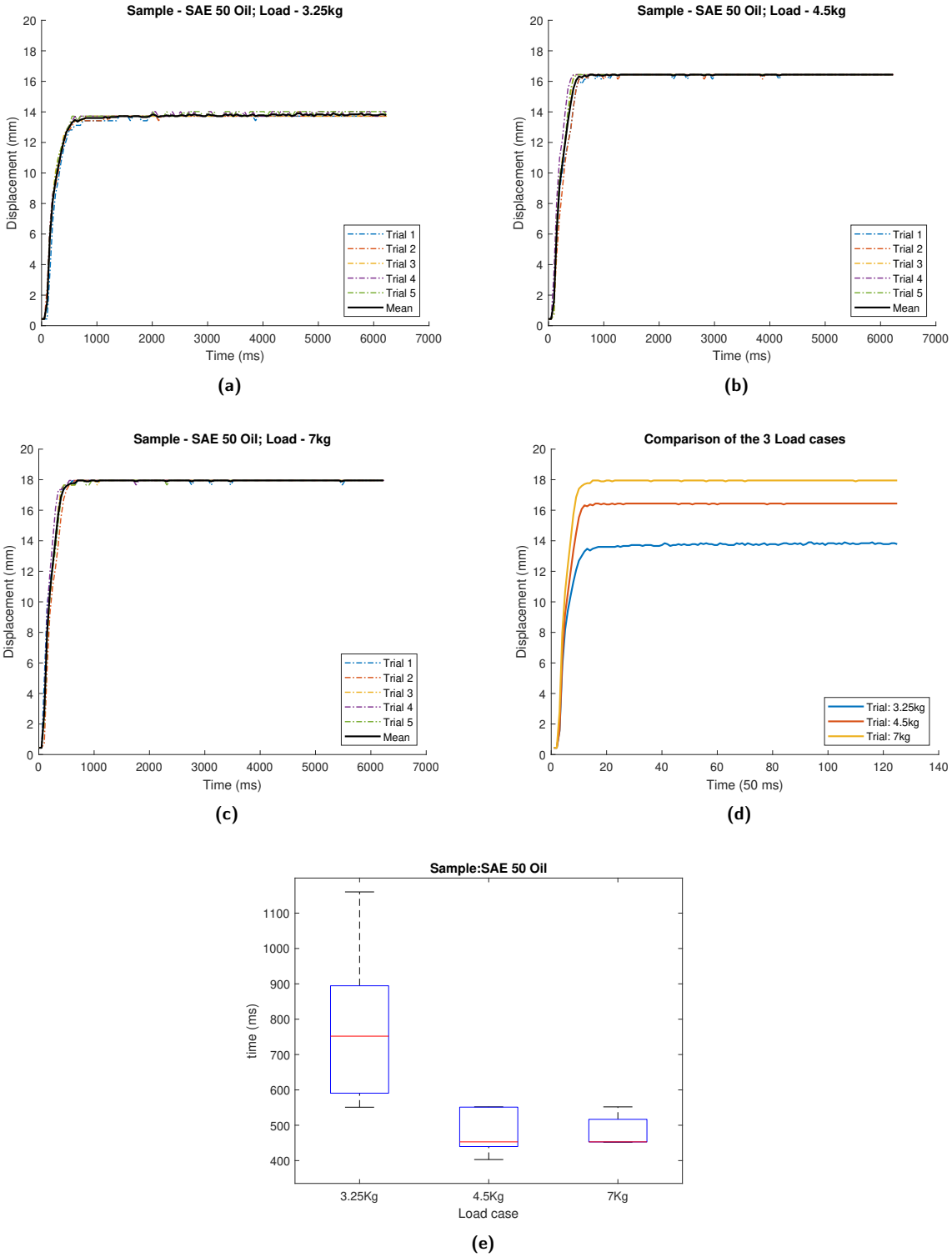

Figure E.4: Constant Force Measurement: SAE 50 Oil, Static Plots: (a)-(c) Mean loading plots. (d) Comparison of mean across loading cases. (e) Box plot of time taken to steady state stretch

E.0.4. Static Load, Sample: Cornstarch Slurry (53.3%)

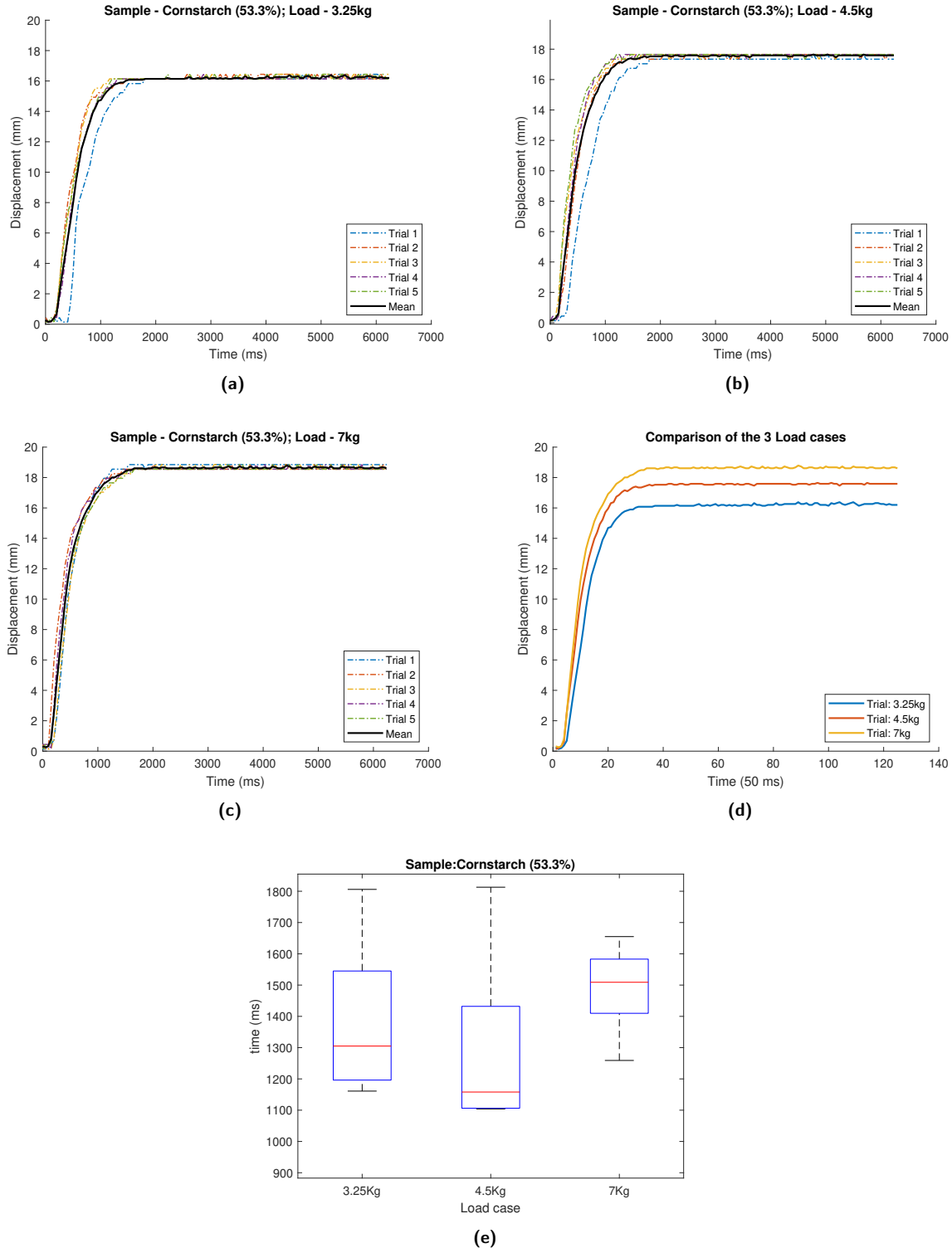

Figure E.5: Constant Force Measurement: Cornstarch (53.3%), Static Plots: (a)-(c) Mean loading plots. (d) Comparison of mean across loading cases. (e) Box plot of time taken to steady state stretch

E.0.5. Static Load, Sample: Thick Cornstarch Slurry (57%)

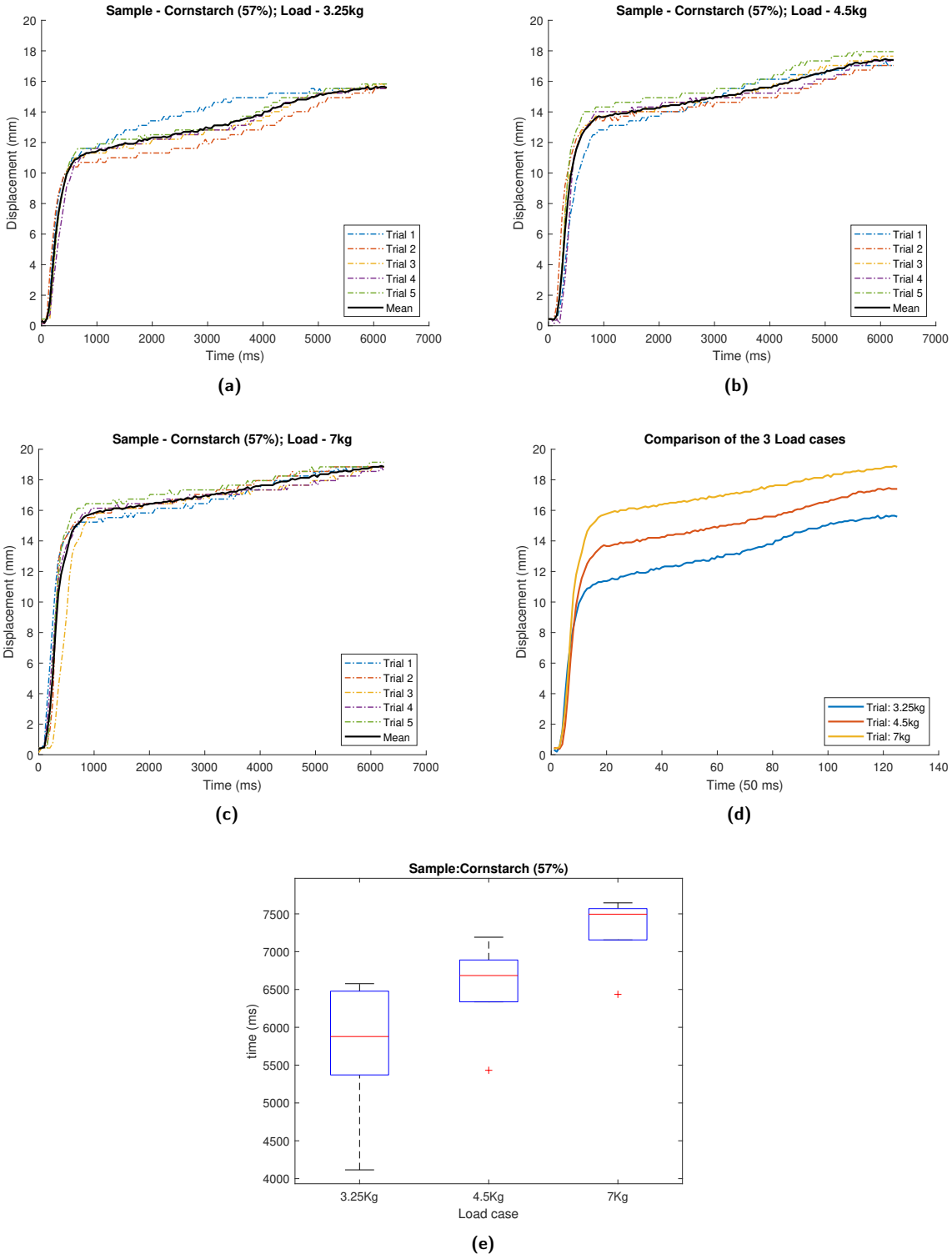

Figure E.6: Constant Force Measurement: Cornstarch (57%), Static Plots: (a)-(c) Mean loading plots. (d) Comparison of mean across loading cases. (e) Box plot of time taken to steady state stretch

E.0.6. Impact Load, Displacement-Time Plots

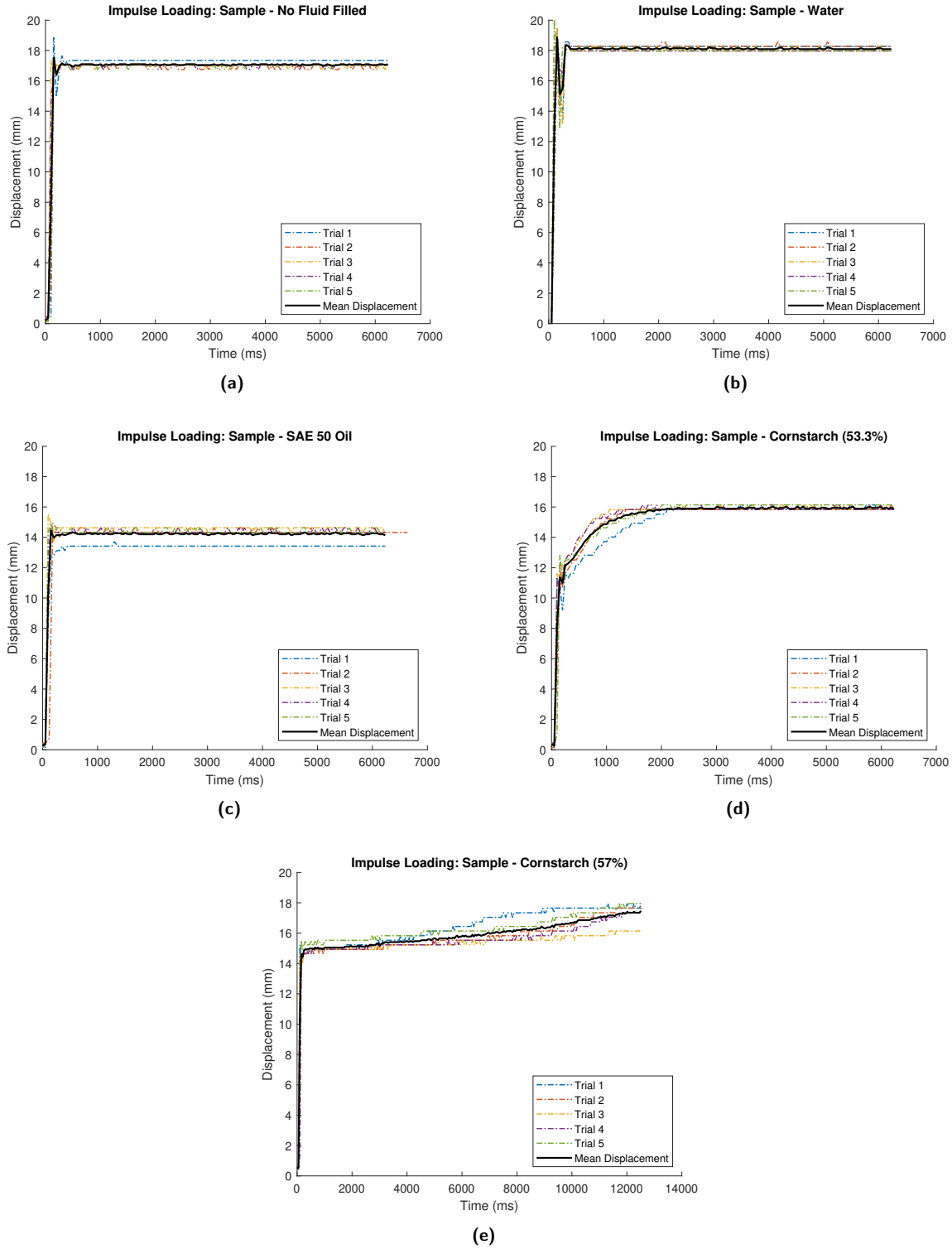

Figure E.7: Constant Force Measurement: Impact test Displacement Time Plots: (a) No Fluid Fill. (b) Water. (c) SAE 50 Oil. (d) Cornstarch Slurry (53.3%). (e) Thick Cornstarch Slurry (57%) Mean loading plots.

E.0.7. Impact Load, Time to full Displacement

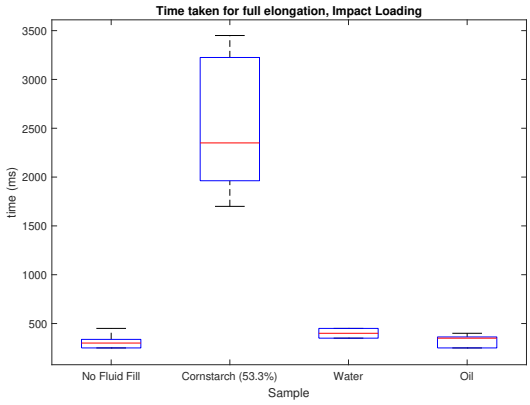

Figure E.8: Impact Test: Time box Plot Without Thick Cornstarch Slurry Sample

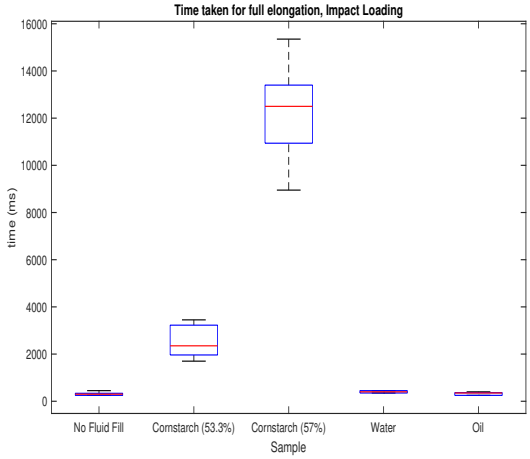

Figure E.9: Impact Test: Time box Plot Without Thick Cornstarch Slurry Sample

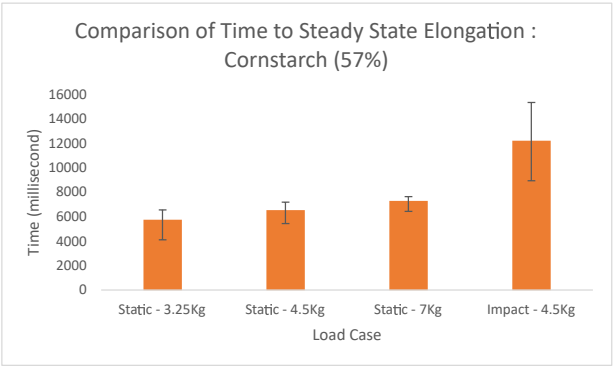

Figure E.10: Elongation Time for Thick Cornstarch Slurry, All Constant Force Tests

Cyclic Tests

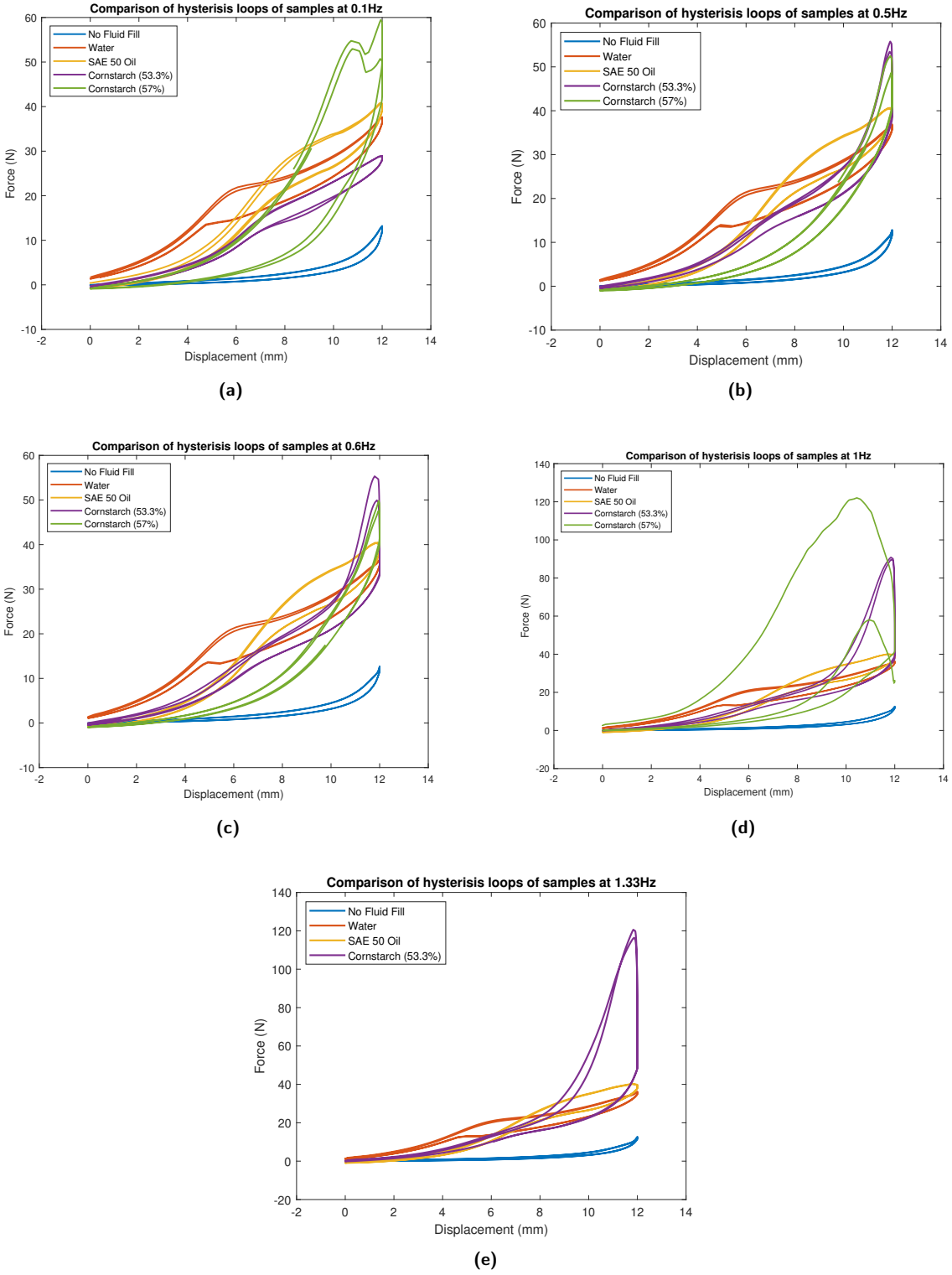

Figure E.11: Comparison of Sample Response to Different Frequencies: (a) 0.1Hz. (b) 0.5Hz. (c) 0.6Hz. (d) 1Hz. (e) 1.33Hz

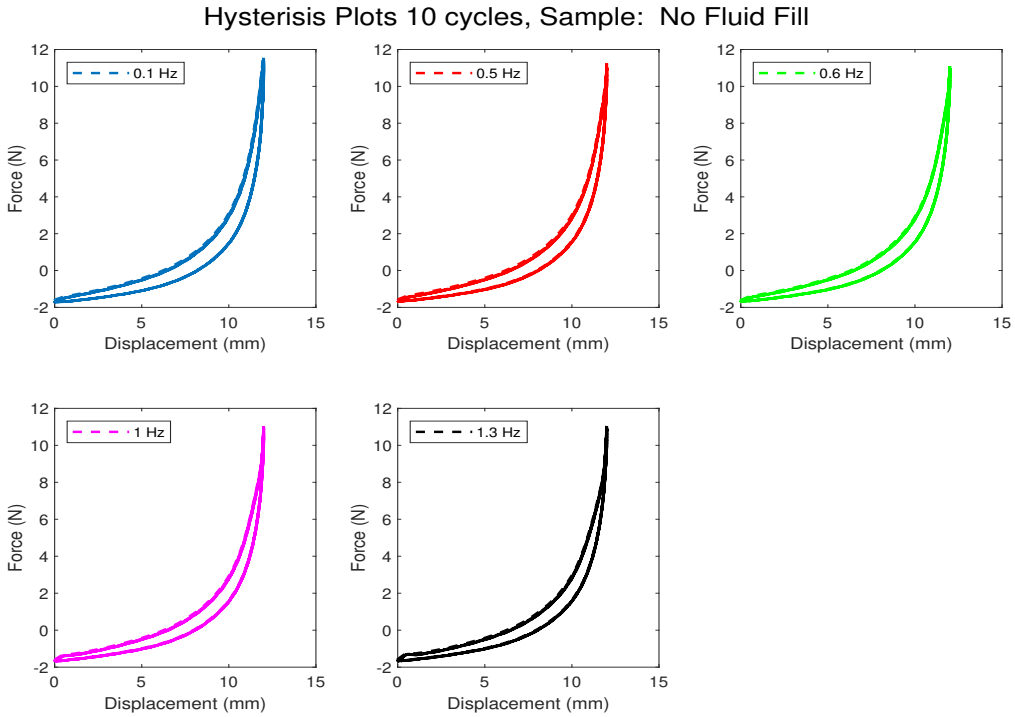

Figure E.12: Cyclic Loading plot for various frequencies: No Fluid Filled

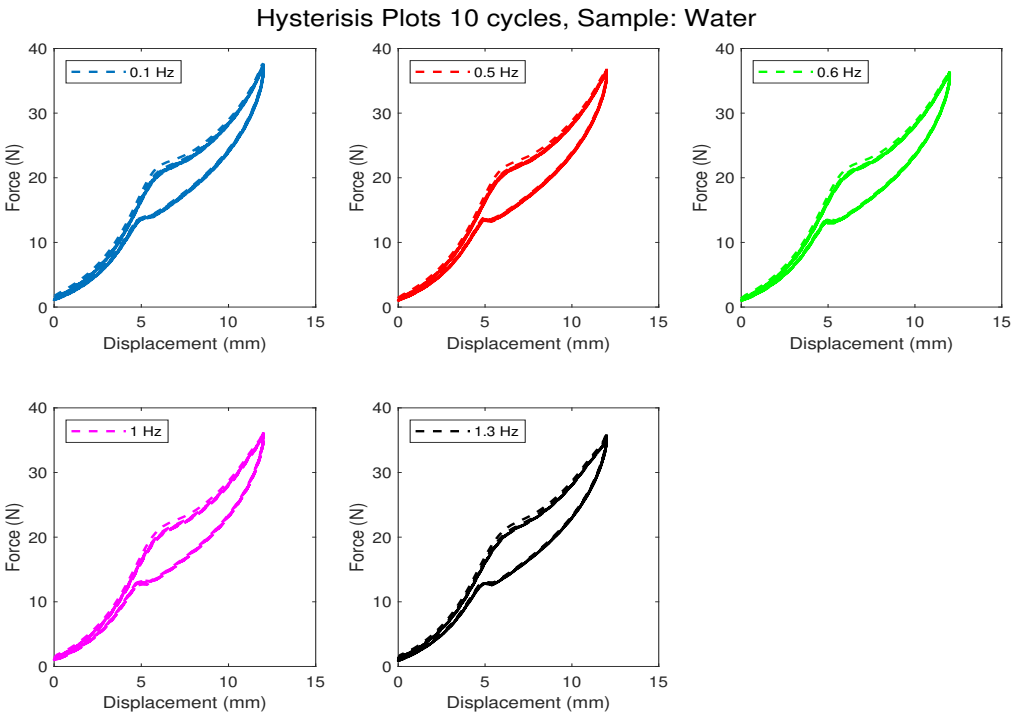

Figure E.13: Cyclic Loading plot for various frequencies: Water

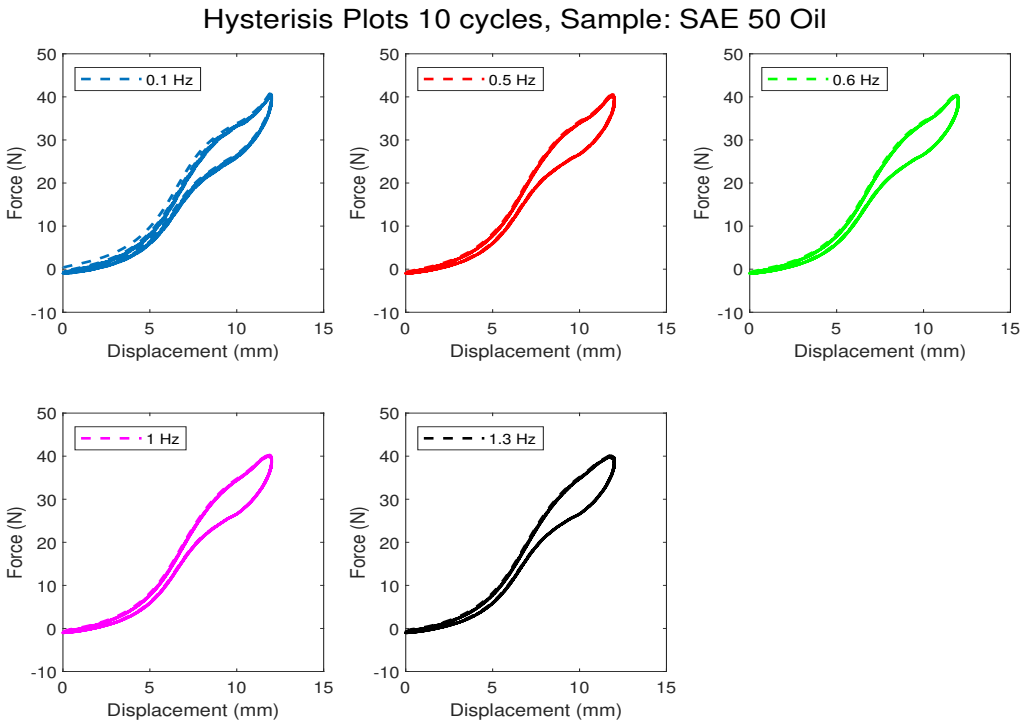

Figure E.14: Cyclic Loading plot for various frequencies: Oil

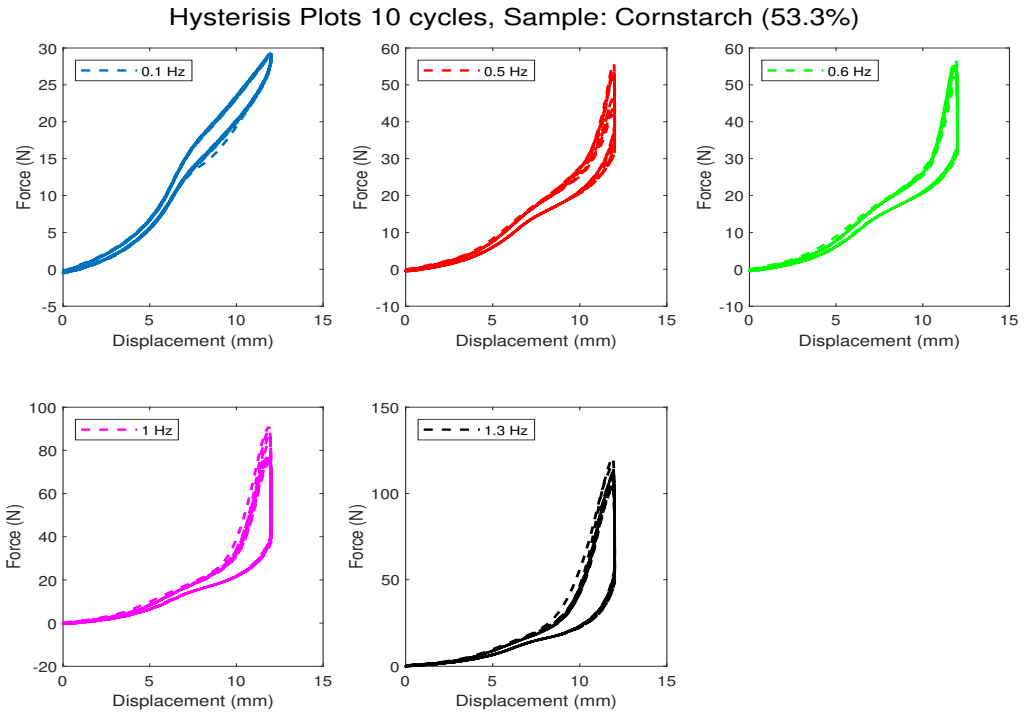

Figure E.15: Cyclic Loading plot for various frequencies: Cornstarch (53.3%)

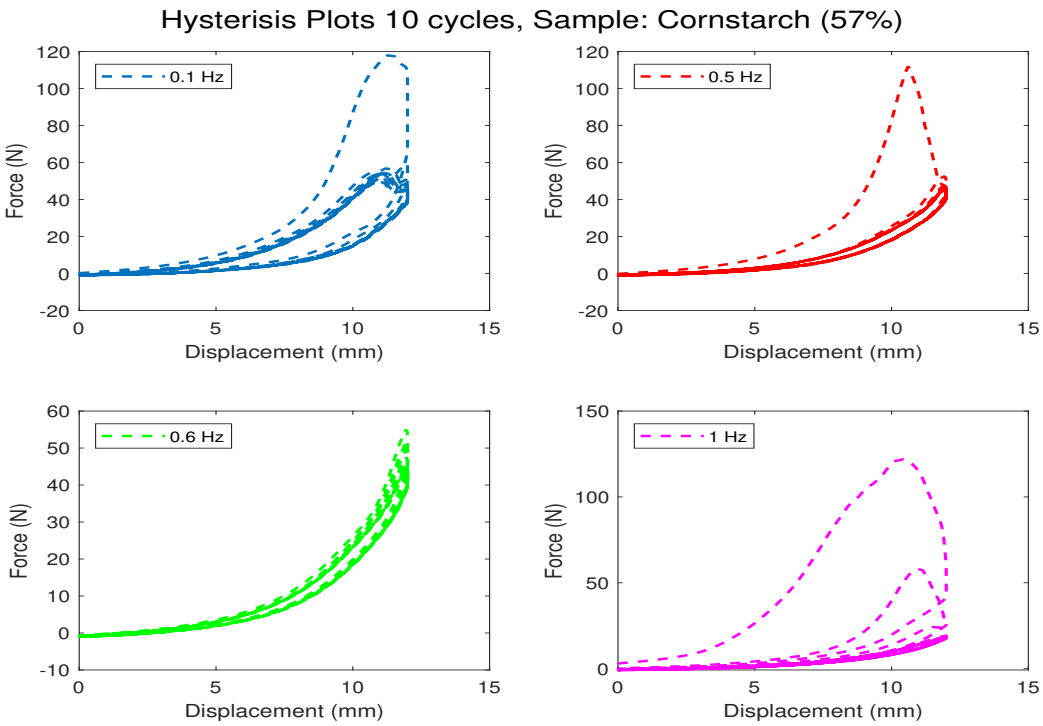

Figure E.16: Cyclic Loading plot for various frequencies: Cornstarch (57%)

F

Additional Calculations

Energy Dissipation Comparison

The study in [52], with a flexible pouch and STF-based fluid demonstrated an energy absorption of $3-4$ J over a displacement of 30mm and at a shear rate of 167mm/s. The prototype ("ligament damper") had a mass of 8g, leading to a maximum energy density of 0.5J/g. The paper states that at a shear rate of 16.7mm/s, the energy dissipated is around 0.3J, corresponding to a specific work of 0.05J/g.

The largest value for the energy dissipated in our work was obtained in a force-controlled test with the Cornstarch sample. The highest force and loading rate that could be reliably conducted on the given setup was a load of 70N, at a rate of 50N/s (16.77 mm/s maximum rate possible by the machine). It resulted in a travel

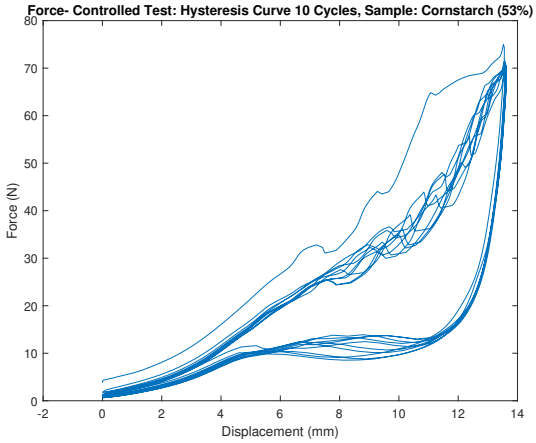

Figure F.1: Hysteresis Curve of Force Controlled Cyclic Loading: Cornstarch Slurry Sample

of 14mm in the damper and a subsequent 0.1915 J of work, or 0.0026J/g specific energy dissipated per cycle. When comparing the performance of the damper introduced in this paper (referred to as the "braid") to the "ligament" damper proposed in [52] for similar shear rates, it is evident that the braid damper can generate higher forces at the same shear rate, highlighting a more pronounced shear-thickening effect. However, due to the smaller displacement in the braid damper, the work done per cycle was nearly half that of the ligament damper. It's worth noting that the ligament damper provides almost twice the displacement of the current model. Consequently, if the braid damper is designed to allow a 30mm displacement, we anticipate comparable energy dissipation performance in both dampers.

Furthermore, the ligament damper can only perform with shear-thickening fluids, whereas the proposed braid damper can work even with Newtonian fluids. The adaptive behavior is only seen with shear-thickening fluids, but the experimental results show energy dissipation capacity even for Newtonian fluid samples. Nonetheless, the ligament damper stands out in terms of specific work capacity, primarily due to its exceptionally lightweight design. The current braid prototype, which utilizes metal clamps and rigid ends, has a mass of 75.3 grams, significantly higher than the ligament's 8-gram mass. This results in nearly a 20-fold smaller specific work capacity when

compared to the ligament damper. Further research is imperative to enhance the total displacement and reduce the mass of the braid damper, improving its overall performance.

Heat Generated

The energy absorbed by the viscous fluid is ultimately dissipated as heat energy. This leads to a rise in the temperature of the working fluid. It is important to verify the magnitude of temperature change, to assess whether the temperature change can affect the rheological behavior of the working fluid. The equation for the change in temperature for an isolated substance is as follows:

$$\delta T = \frac{Energy}{mass * HeatCapacity} \tag{F.1}$$

. Based on the results of the previous section, the maximum energy dissipated per cycle for the damper is found to be 0.1915J. The specific heat capacity of cornstarch slurry is taken to be 3.25 KJ/KgC [53], and the experimentally calculated cornstarch slurry mass of the damper is 24.3g.

Assuming no heat transfer takes place from the fluid to the surroundings, the calculated rise in temperature of the fluid comes out to be 0.00242 °C. This is a really small value, and when extrapolated to 1000 cycles, it comes out to be 2.42 °C. In reality, the fluid sample is in contact with the pouch, and heat transfer occurs between them. It can be concluded that this rise in temperature will have no significant effect on the rheology of the fluid and thus have no effect on damper performance.

Linear Approximation - Curve Fitting

Based on the Linear model developed, the Effective Linear stiffness and Damping Coefficients are obtained. These coefficients are then parameterized as functions of the shear rate, to obtain an equation that quantifies the shear thickening effect.

The process of establishing this parametric relationship involves employing polynomial curve-fitting on the damping and stiffness vs. excitation frequency data.

Table F.1: Polynomial fitting parameters for stiffness and damping

Parameter	f^3 coefficient	f^2 coefficient	f coefficient	f^0 coefficient	Rsquare value
Stiffness K (N/m)	-	1585	3896	2061	0.9966
Damping C (Ns/m)	-102.6542	303.7257	-273.3383	102.6767	0.9985

The proposed fit has a 3rd-order polynomial approximation for the damping coefficient and a 2nd-order polynomial relation for the effective stiffness.

However, it is evident that the proposed linear model falls short of accurately replicating the hysteresis data. The calculated energy dissipation per cycle, derived from the linear model, deviates significantly from the experimental results, falling short by a factor of 10. While the model effectively captures the stiffness of the system, as evidenced by its ability to reproduce the maximum force, it underestimates the damping term in comparison to the experimental findings. Therefore, a nonlinear estimation of the effective damping coefficient is imperative to achieve a precise prediction of the system's behavior.

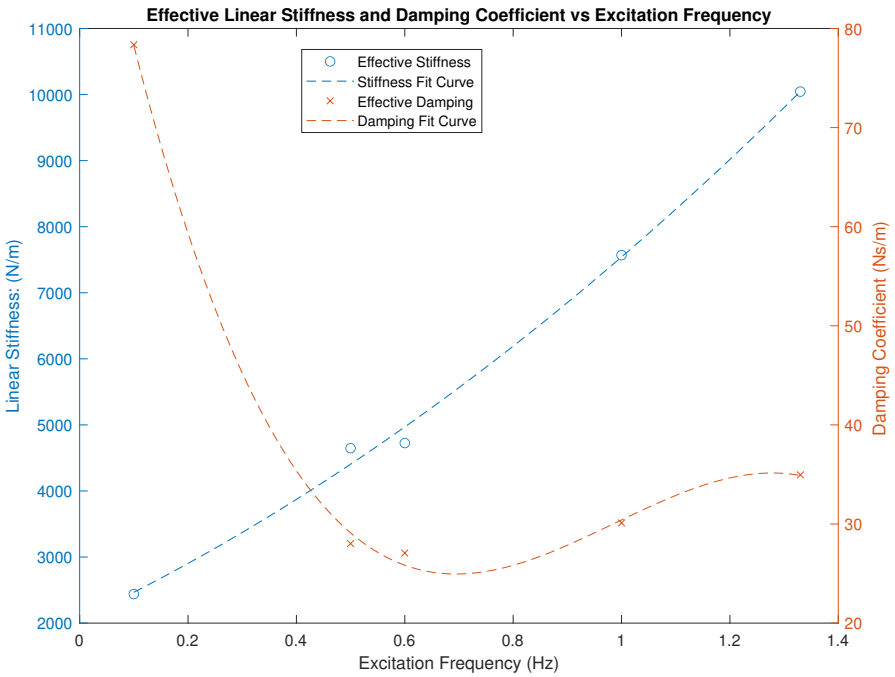

Figure F.2: Equivalent Polynomial Fit curves for Stiffness and Damping